CEFET/RJ
DIRETORIA DE PESQUISA E PÓS-GRADUAÇÃO

DEVELOPMENT, MECHANICAL CHARACTERIZATION AND JOINING OF NEW ADDITIVE MANUFACTURED POLYMERIC MATERIALS

DANIEL KIOSHI KAWASAKI CAVALCANTI

Tese apresentada ao Programa/Curso de Pós-Graduação em Engenharia Mecânica e Tecnologia dos Materiais - PPEMM, do Centro Federal de Educação Tecnológica Celso Suckow da Fonseca, CEFET/RJ, como parte dos requisitos necessários à obtenção do título/certificado de Doutor em Engenharia Mecânica e Tecnologia dos Materiais.

Orientadora: Doina Mariana Banea

Rio de Janeiro
Junho/2023

DocuSign Envelope ID: DFA9F5CC-3665-408C-B7E2-6F78910264FF

DEVELOPMENT, MECHANICAL CHARACTERIZATION AND JOINING OF NEW ADDITIVE MANUFACTURED POLYMERIC MATERIALS

Tese apresentada ao Programa/Curso de Pós-Graduação em Engenharia Mecânica e Tecnologia dos Materiais - PPEMM, do Centro Federal de Educação Tecnológica Celso Suckow da Fonseca, CEFET/RJ, como parte dos requisitos necessários à obtenção do título/certificado de Doutorado em Engenharia Mecânica e Tecnologia dos Materiais.

DANIEL KIOSHI KAWASAKI CAVALCANTI

Banca Examinadora:

Mariana Doina Banea
Assinado de forma digital por Mariana Doina Banea
Dados: 2023.06.26 12:34:55 -03'00'

Presidente, Professora Dra. Doina Mariana Banea (CEFET/RJ) (orientadora)

Hector Reynaldo Meneses Costa 92600514791
Assinado de forma digital por Hector Reynaldo Meneses Costa 92600514791
Dados: 2023.06.27 19:44:59 -03'00'

Professor Dr. Hector Revnaldo Meneses Costa (CEFET/RJ)

gov.br
Documento assinado digitalmente
DANIEL CARLOS TAISSUM CARDOSO
Data: 28/06/2023 20:32:43-0300
Verifique em https://validar.iti.gov.br

Professor Dr. Daniel Carlos Taissum Cardoso (PUC)

DocuSigned by:
Marcelo Leite Ribeiro
60BD6ADB1C9447C...

Professor Dr. Marcelo Leite Ribeiro (USP)

Professor Dr. João Marciano Laredo dos Reis (UFF)

Rio de Janeiro

Junho/2023

Ficha catalográfica elaborada pela Biblioteca Central do CEFET/RJ

C377 Cavalcanti, Daniel Kioshi Kawasaki
Development, mechanical characterization and joining of new additive manufactured polymeric materials / Daniel Kioshi Kawasaki Cavalcanti. — 2023.
112f. : il. color. , enc.

Tese (Doutorado) Centro Federal de Educação Tecnológica Celso Suckow da Fonseca, 2023.
Bibliografia : f. 104-109
Orientadora: Doina Mariana Banea

1. Impressão tri-dimenssional. 2. Ensaios mecânicos. 3. Fibras naturais. 4. Resistências de materiais. 5.Tecnologia de materiais. I. Banea, Doina Mariana (Orient.). II. Título.

CDD 620.11292

Elaborada pela bibliotecária Tania Mello – CRB/7 nº 5507/04

AGRADECIMENTOS

Primeiramente,

Agradeço aos meus pais pelo apoio durante todo o meu percurso acadêmico.

Aos professores, que me proporcionaram a base de conhecimento necessária para o cumprimento dos meus estudos.

À minha orientadora, Ph.D. Doina Mariana Banea, pela amizade, orientação, ensinamentos e paciência que me nortearam durante toda a pesquisa.

Ao grupo de pesquisa do LADES/CEFET, composto por Henrique Queiroz, Jorge Neto e Rosemere Lima, assim como Brenno Duarte do LASEI/CEFET, Hiron Akira do LAMAT e o técnico Leonardo da Silva, pelo suporte e utilização de equipamentos. Além disso, gostaria de agradecer também ao grupo de pesquisa da Universidade de Aveiro, em especial ao Professor Victor Neto e seus alunos Tiago Gomes, Carlos Correia, Mylene Cadete, Yiyun Wu e Laura Prior, e ao corpo técnico do laboratório Centre for Mechanical Technology and Automation (TEMA/UA) pelo suporte durante a minha estadia em Portugal.

Ao técnico de assuntos acadêmicos Fernando Berçot, pelo apoio e ajuda durante o curso.

Ao Centro Federal de Educação Tecnológica Celso Suckow da Fonseca (CEFET/RJ), pela oportunidade de obtenção dos graus de Engenheiro, Mestre e Doutor.

À Coordenação de Aperfeiçoamento de Pessoal de Nível Superior (CAPES) e ao Programa de Doutorado-sanduíche no Exterior (PDSE) pelo financiamento das pesquisas nacionais e internacionais, bolsas de estudo e auxílio financeiro durante todo o período do doutorado.

Ao Centro de Caracterização em Nanotecnologia em Catálise e Materiais (CENANO) no Instituto Nacional de Tecnologia (INT) pelo auxílio nas pesquisas, em especial ao Luiz da Cunha Ferro, Alan Nascimento e à Fernanda dos Santos pelo apoio e excelente trabalho.

RESUMO

DEVELOPMENT, MECHANICAL CHARACTERIZATION AND JOINING OF NEW ADDITIVE MANUFACTURED POLYMERIC MATERIALS

O desenvolvimento de novos materiais poliméricos fabricados por manufatura aditiva (AM) tem despertado considerável interesse devido às suas promissoras aplicações em diversas indústrias. Esse domínio de pesquisa abrange várias facetas, incluindo a caracterização mecânica abrangente e técnicas avançadas de união, visando otimizar o desempenho e a funcionalidade desses materiais. Ao explorar as propriedades mecânicas e os métodos inovadores de união, valiosas percepções podem ser obtidas para o avanço e utilização de materiais poliméricos AM em componentes estruturais de alto desempenho e outras aplicações industriais críticas. Esta tese explora as propriedades mecânicas e o desempenho de peças poliméricas fabricadas por manufatura aditiva (AM) reforçadas com diferentes tipos de fibras. A pesquisa concentra-se em quatro áreas-chave: (a) exploração do impacto que o tipo de filamento e os parâmetros de impressão têm sobre as propriedades mecânicas de termoplásticos utilizados na impressão 3D, (b) caracterização do comportamento mecânico de peças AM feitas de Ácido Poliláctico (PLA) e Estireno-Acrilonitrila-Butadieno (ABS) reforçadas com fibras naturais (juta e curauá) e sintéticas (vidro), (c) avaliação do desempenho mecânico de uniões adesivas utilizando diferentes reforços de fibras para peças poliméricas AM, e (d) desenvolvimento de compósitos de PLA reforçados com fibras curtas de curauá através da modelagem por deposição fundida. Ensaios de tração e flexão foram realizados para avaliar os parâmetros de impressão, propriedades mecânicas das peças AM e das uniões adesivas. Os resultados destacam melhorias significativas nas propriedades mecânicas com a adição de reforços de fibras nas peças AM. Além disso, a incorporação de diferentes reforços de fibras aprimora o desempenho mecânico das uniões adesivas. O estudo também se concentra no desenvolvimento de compósitos de PLA reforçados com fibras curtas de curauá, variando os comprimentos e concentrações das fibras. Através de análises abrangentes de tração, flexão e térmicas, a estabilidade mecânica e térmica desses compósitos foi avaliada. Os resultados enfatizam a influência significativa da fração de peso das fibras

nas propriedades mecânicas, enquanto o efeito do comprimento das fibras nas propriedades foi mínimo. Em resumo, essa pesquisa forneceu uma base solida sobre o comportamento mecânico de peças poliméricas AM que utilizam diversos reforços de fibras. A incorporação de fibras resulta em aprimoramentos notáveis tanto no desempenho individual das peças quanto na resistência das uniões adesivas. Além disso, a tese demonstra o potencial dos compósitos de PLA reforçados com fibras de curauá como uma promissora via para a manufatura aditiva, abrindo novas possibilidades para sua aplicação em várias aplicações.

Palavras-chave: Impressão 3D, Caracterização mecânica, Reforços de fibra natural;

ABSTRACT

Development, Mechanical Characterization and Joining of New Additive Manufactured Polymeric Materials

The development of novel additive manufactured (AM) polymeric materials has garnered considerable interest owing to their promising applications across diverse industries. This research domain encompasses various facets, including comprehensive mechanical characterization and advanced joining techniques, aimed at optimizing the performance and functionality of these materials. By exploring the mechanical properties and innovative joining methods, valuable insights can be gained for the advancement and utilization of AM polymeric materials in high-performance structural components and other critical industrial applications. This thesis explores the mechanical properties and performance of additive manufactured (AM) polymeric parts reinforced with different types of fibres. The research focuses on four key areas: (a) exploration of the impact that filament type and printing parameters had on the mechanical properties of thermoplastics used in 3D printing, (b)characterizing the mechanical behaviour of AM parts made from Polylactic Acid (PLA) and Acrylonitrile Butadiene Styrene (ABS) reinforced with natural (jute and curauá) and synthetic (glass) fibres, (c) evaluating the mechanical performance of adhesive joints using various fiber reinforcements for AM polymeric parts, and (d) developing short curauá fiber-reinforced PLA composites through fused deposition modelling. Tensile and flexural tests were conducted to assess printing parameters, mechanical properties of the AM parts and adhesive joints. The findings highlight substantial improvements in mechanical properties with the addition of fiber reinforcements to the AM parts. Moreover, incorporating different fiber reinforcements enhances the mechanical performance of the adhesive joints. The study also focuses on the development of curauá fiber-reinforced PLA composites with varying fiber lengths and concentrations. Through comprehensive tensile, flexural, and thermal analyses, the mechanical and thermal stability of these composites were evaluated. The results emphasize the

significant influence of the fiber weight fraction on the mechanical properties, while the effect of fiber length on the properties was minimal. In summary, this research provides valuable insights into the mechanical behaviour of AM polymeric parts utilizing diverse fiber reinforcements. The incorporation of fibres leads to remarkable enhancements in both the individual performance of the parts and the strength of adhesive joints. Furthermore, the thesis demonstrates the potential of curauá fiber-reinforced PLA composites as a promising avenue for additive manufacturing, opening up new possibilities for their application in various applications.

Keywords: 3D printing, Mechanical characterization, Natural fibre reinforcements;

Table of contents

CHAPTER 1 ..... **1**

1. INTRODUCTION 1

1.1. MOTIVATION 2

1.2. OBJECTIVES 3

1.3. THESIS STRUCTURE 4

REFERENCES **8**

CHAPTER 2 ..... **11**

2.1. INTRODUCTION 12

2.2. MATERIALS AND METHODS 13

2.2.1. Materials 13

2.2.2. Specimens' fabrication 14

2.2.3. Test method 17

2.2.4. Preliminary parametric study 18

2.3. RESULTS AND DISCUSSION 20

2.3.1. Tensile tests 20

2.3.2. Flexural tests 23

2.3.3 Comparative analysis 26

2.4. CONCLUSIONS 27

CHAPTER 3 ..... **31**

3.1. INTRODUCTION 32

3.2. Materials And Methods 34

3.2.1. Materials 34

3.2.2. Specimen fabrication 35

3.2.2.1. 3D printed part fabrication 35
3.2.2.2. Composite specimens' fabrication 37
3.2.3. Test method 38
3.3. RESULTS AND DISCUSSION 39
3.3.1. Tensile tests 39
3.3.2. Flexural tests 45
3.3.3. Fracture analysis 49
3.4. Conclusions 52
CHAPTER 4 58
4.1. INTRODUCTION 59
4.2. MATERIALS AND METHODS 62
4.2.1. Materials 62
4.2.2 Substrate specimen fabrication 62
4.2.3 SLJ specimen fabrication 66
4.2.4 Test method 66
4.3. RESULTS AND DISCUSSION 67
4.3.1. Effect of reinforcement type on the bonded joint performance 67
4.3.1.1. PLA core specimens 67
4.3.1.2. ABS core specimens 71
4.3.2 Effect of number of the fibre layers on the bonded joint performance 75
4.4. CONCLUSIONS 77
CHAPTER 5 82
5.1. INTRODUCTION 83
5.2. MATERIALS AND METHODS 85
5.2.1. Materials 85
5.2.2. Filament and 3D part specimens' fabrication 86

5.2.3. Tensile and flexural tests 89
5.2.4. Thermal analysis 90
5.2.4.1. Thermogravimetric analysis (TGA) 90
5.2.4.2. Differential Exploratory Calorimetry (DSC) 90
5.3. RESULTS AND DISCUSSION 90
5.3.1. Effect of curauá fibre weight fraction 92
5.3.1.1. Effect of curauá fibre length 93
5.3.2. Flexural tests 95
5.3.3. Fracture analysis 97
5.4. THERMAL PROPERTIES 98
5.4.1. TGA analysis 98
5.4.2. DSC analysis 101
5.5. CONCLUSIONS 103
CHAPTER 6 110
6. CONCLUSION 110
6.1 FUTURE WORKS 111

CHAPTER 1

1. INTRODUCTION

Additive manufacturing (AM), also known as 3D printing, is a technology that has rapidly gained space in both industrial and civil sectors and is becoming a main stay in all areas of production. This process consists in the joining of materials to make objects and parts from a 3D model through the staking of layers, therefore, unlike traditional manufacturing methods, material is added rather than subtracted [1]. AM has provided unprecedented freedom in design and manufacture of complex and on-demand parts at a low cost, when compared to more traditional manufacturing methods [2, 3].

Originally, this technology was limited to the production of aesthetic focused parts and rapid prototyping. In recent years this use has increased in scope, being used in medical, aeronautical, and civil industries. This versatility is due to the wide range of AM processes and the material it employs, such as polymers, ceramics, alloys, and concrete to cite a few. The most common material used are thermoplastics like, polylactic acid (PLA) and acrylonitrile butadiene styrene (ABS) due to their low cost, ease of processability and wide availability [4]. However, the technology has its limitations. The finished 3D printed part is still highly susceptible to the feedstock material properties, printing parameter. Therefore part properties are still low when compared to more traditional production methods and high anisotropy is common [4]. Therefore, to obtain useful parts it is necessary to take into account these factors.

As stated before, the most common materials used are the PLA and ABS plastics. These materials have been the focus of many studies, mainly due to the wide availability of the AM technology they use [5-18]. The Fused deposition fabrication (FFF) or fused deposition modelling (FDM), at the time of writing, are the most common and low-cost AM machines in the market, making them ubiquitous in both industrial and household use.

Withing the relevant literature many studies have been dedicated to investigating the optimal printing parameters for 3D printed components, aiming to enhance their

mechanical properties [6, 8]. Moreover, appropriate materials selection for the printing process is crucial, as it acts as a constraining factor when attempting to enhance the mechanical properties of the parts. This can be achieved by reinforcing either the feedstock material or the final part.

Another limitation to this process is the printing area size. Although, new 3D printers can produce large scale parts, there is still a necessity to understand how to join said part to a variety of other materials, this is especially interesting to the transport industry. In this regard, the utilization of adhesive joining holds particular interest. Adhesive joining offers the advantage of providing a robust bond while distributing loads across the joint at a reduced weight compared to traditional joining methods. Additionally, it presents the possibility of joining dissimilar materials with minimal drawbacks. Therefore, the study in the adhesive joining of 3D printed parts is relevant.

The literature is rife with studies in tailoring the mechanical properties of FFF manufactured parts trough printing parameters and geometry[3, 19-26]. However, these studies do not provide a clear answer to the optimum printing parameters. Also of note, at the time of writing, there is a clear lack of studies on the adhesion of 3D printed parts with non-planar bond geometry. Furthermore, many studies focused on the reinforcing of 3D printed parts using carbon fibre reinforced filaments and highly specialized machinery [11-14, 16, 27, 28], which limit their use in more common 3D printers, increasing costs and complexity. Therefore, this thesis is focused on these areas with the objective of expanding the use of 3D printed parts maintaining the advantages provided by low-cost, available feedstock and machinery.

1.1. MOTIVATION

Additive manufacturing has earned itself a growing market in both household and industrial settings. The wide range of application and scalability of the technology made possible the manufacture of customizable parts with high complexity at a relatively low cost, when compared to traditional manufacturing methods. However, the technology still has many limitations, especially when taking into consideration the FDM or FFF printing. The mechanical properties of 3D printed parts is directly related to the feedstock's mechanical properties, of which the most common is thermoplastics.

Thermoplastics such as PLA and ABS are among the most used in both household and industrial use. They present a cost-effective alternative to produce prototypes for the industry and, in some cases, a tailored final product. Nevertheless, in most cases, they are limited to non-structural applications. Therefore, to expand the use of FFF printed parts it is necessary to study means to increase their overall mechanical properties, whilst maintaining their inherent advantages. The mechanical characteristics can be improved using either natural or synthetic fibre reinforcements.

Hence, this research is focused on the development, mechanical characterization, and adhesive bonding of novel 3D printed materials.

1.2. OBJECTIVES

The primary focus of this thesis centres around the development, mechanical characterization and joining of new additive manufactured polymeric materials.

The specific objectives are as follow:

1. Evaluate and study the influence of the material and the 3D-printing parameters on the mechanical properties of additive manufactured thermoplastic parts. Three different filaments that were commercially available, Polylactic acid (PLA), acrylonitrile butadiene styrene (ABS) and Tritan were used.
2. Investigate the mechanical properties of additive manufactured (AM) polymeric parts (Polylactic Acid (PLA) and Acrylonitrile Butadiene Styrene (ABS)) reinforced by different types of fibres (i.e. Jute, Curauá and Glass fibre).
3. Explore experimentally the mechanical performance of adhesive joints made of additive manufactured (AM) polymeric parts reinforced with different types of fibres.
4. Develop a short curauá fibre reinforced PLA composites made via fused deposition modelling. Three different fibre lengths (3, 6 and 8 mm), and three concentrations in weight percentage (2%, 3.5% and 5% wt.%) were used to fabricate reinforced PLA filaments.

1.3. THESIS STRUCTURE

The thesis is organized in 6 chapters. The first chapter consists of an Introduction where the background of the thesis is presented. Furthermore, the main and specific objectives are stated. The thesis structure is also shown. The following chapters, from 2 to 5, consists in the published works. Each section is independent, consisting of introduction, methodology, results, discussion, and conclusions. They are as follows:

The second chapter named "**Effect of material on the mechanical properties of additive manufactured thermoplastic parts.**" consists in the additive manufacturing of reinforced thermoplastics, specifically the mechanical characterization of ABS and PLA. These thermoplastics are widely utilized in 3D printing applications. Subsequent sections of the study will explore methods to enhance the mechanical properties of these thermoplastics. To optimize the mechanical characteristics of 3D printed components, it is crucial to conduct meticulous mechanical characterization. Furthermore, the feasibility of Tritan thermoplastic as a viable substitute for food packaging materials was investigated in this study. The assessment of mechanical properties involved the careful selection of 3D printing parameters, considering relevant literature, as these parameters significantly influence the final mechanical properties of the printed parts. Tensile and flexural tests were performed to compare the mechanical properties of the additively manufactured parts, focusing on the diverse materials used. The findings revealed that the filament type played a pivotal role in determining the mechanical properties. PLA exhibited superior strength and stiffness, while Tritan demonstrated greater deformability. However, it is important to note that the chosen printing parameters also impacted the mechanical properties. The parameters employed in this study struck a suitable balance between printing time and mechanical characteristics. To summarize, this research provides valuable insights into the mechanical properties of commonly used thermoplastics in 3D printing. Furthermore, it underscores the significance of selecting appropriate printing parameters to achieve desired mechanical properties in additively manufactured parts. The evaluation of Tritan as a potential alternative for food packaging materials contributes to the advancement of sustainable and environmentally friendly materials.

The third chapter "**Strengthening of additive manufactured parts by using**

different type of fibre reinforcements." presents strategies for enhancing the mechanical properties of 3D printed components, which currently fall short of meeting the requirements for structural applications. The objective is to surpass the limitations of 3D printed parts and broaden their potential range of applications. To achieve this, the strategic implementation of reinforcements holds great promise in augmenting the mechanical, chemical, and thermal characteristics of 3D printed thermoplastics. Long and short fibres represent one such reinforcement method, offering a diverse array of benefits for both conventionally manufactured and additively manufactured parts. Furthermore, the utilization of natural fibres, such as jute and curauá, allows for the preservation of the biodegradability and recyclability of 3D printed thermoplastics, features that would be compromised or forfeited by the use of synthetic fibres. The present investigation focuses on the mechanical properties of fiber-reinforcements with different types of fibres. The findings demonstrate that the incorporation of fiber reinforcements leads to improvements in mechanical properties. Notably, synthetic fibres exhibit superior overall mechanical properties, while the curauá fiber-reinforced composite demonstrates a superior weight-to-strength ratio for tensile strength in comparison to glass fiber-reinforced specimens. This approach, along with the utilization of fibres, offers a straightforward and cost-effective solution for enhancing the mechanical properties of 3D printed parts, rendering it an attractive area for further investigation.

The fourth chapter refers to the "**Performance enhancement of adhesive joints of additive manufactured parts by using different types of fibre reinforcements**". The previous studies yielded valuable insights into the potential of reinforcement methods in composite materials. The incorporation of fibres has demonstrated significant improvements in mechanical properties, enabling potential applications in complex parts and 3D printed structures. However, the size limitations of print beds and machine dimensions impose constraints on these applications. Additionally, the joining of different reinforced parts presents an important area for investigation, as each composite can be tailored to specific applications. Of particular interest is the examination of reinforced composites' behaviour in adhesive joining. In this study, a manufacturing methodology consistent with previous work was employed, utilizing a structural adhesive commonly employed in the automotive industry for joining

purposes. The adhesive joint provided critical insights into the interaction between the reinforcement layer and the 3D printed core. Failure modes indicated that while joint strength was sufficient, delamination between the reinforcing layer and polymer core was the predominant failure mechanism. This highlighted the need for further investigation to compare methodologies and address this issue. To tackle the problem, two viable solutions were considered. The first solution involved integrating fiber reinforcements within the filament itself, thereby eliminating the interface between the reinforcement layer and the core. This approach will be expounded upon in subsequent sections of this thesis. The second solution entailed employing a non-planar (wavy) joint surface. Due to time limitations, however, the latter method was deferred for future studies. In conclusion, this chapter provides a comprehensive investigation into the behaviour of reinforced composites in adhesive joining. The findings from this research contribute to the advancement of advanced composites with enhanced mechanical properties and open avenues for their broader utilization across various applications.

The fifth chapter "**Development and mechanical characterization of short curauá fibre-reinforced PLA composites made via fused deposition modelling** outlines the development of a novel short fiber filament for 3D printing, aiming to provide an alternative to existing reinforcement methods. Although the utilization of resin and a reinforcement layer offered numerous advantages to the 3D printed core, the approach was contingent upon the interfacial strength between the reinforcement and the core. Delamination failures arising from this interface proved problematic, particularly when implementing such composites in adhesive joints. To tackle these challenges, a fresh methodology was explored. The incorporation of curauá fiber, indigenous to Brazil, emerged as a pertinent choice due to its impressive mechanical properties, positioning it as a potential substitute for glass fiber. The investigation centred on the mechanical characterization of PLA additive manufactured parts reinforced with short curauá fiber, as scarce data was available in the relevant literature at the time of publication. The inclusion of short curauá fibres notably enhanced the mechanical properties of reinforced PLA compared to its neat form. However, when compared to alternative methods, it still exhibited comparatively lower overall mechanical properties. Nonetheless, the methodology presented here holds potential for improvement through enhanced mixing and extrusion techniques. Additionally,

numerous studies indicate that thermal, chemical, and mechanical treatments can augment overall properties by improving interfacial interactions between the fiber and the polymer. In conclusion, the study presented in this chapter contributes to the advancement of novel materials with enhanced mechanical properties for additive manufacturing applications. The findings suggest that curauá fibres could serve as an appealing alternative to glass fibres, providing a sustainable and cost-effective solution for reinforcing filaments. The methodology outlined herein lays the foundation for further investigations that could lead to the development of even more sophisticated materials with superior mechanical properties.

The sixth and last chapter of this study encompasses the conclusion and outlines potential future directions for research. The findings and insights obtained from the investigation of the mechanical properties, characterization of additive manufactured polymeric parts reinforced with different types of fibres, and evaluation of adhesive joints have shed light on the significant improvements achieved through fiber reinforcement.

REFERENCES

1. Standard, A., F2792. 2012. standard terminology for additive manufacturing technologies. ASTM F2792-10e1, 2012: p. 24.

2. Bikas, H., P. Stavropoulos, and G. Chryssolouris, Additive manufacturing methods and modelling approaches: a critical review. The International Journal of Advanced Manufacturing Technology, 2016. 83(1): p. 389-405.

3. Ngo, T.D., et al., Additive manufacturing (3D printing): A review of materials, methods, applications and challenges. Composites Part B: Engineering, 2018. 143: p. 172-196.

4. Harris, M., et al., Effect of material and process specific factors on the strength of printed parts in fused filament fabrication: A review of recent developments. Materials, 2019. 12(10).

5. Kiendl, J. and C. Gao, Controlling toughness and strength of FDM 3D-printed PLA components through the raster layup. Composites Part B: Engineering, 2020. 180: p. 107562.

6. Ahmed, S.W., et al., On the Effects of Process Parameters and Optimization of Interlaminate Bond Strength in 3D Printed ABS/CF-PLA Composite. Polymers, 2020. 12(9): p. 2155.

7. Lay, M., et al., Comparison of physical and mechanical properties of PLA, ABS and nylon 6 fabricated using fused deposition modeling and injection molding. Composites Part B: Engineering, 2019. 176: p. 107341.

8. Schmitt, M., R.M. Mehta, and I.Y. Kim, Additive manufacturing infill optimization for automotive 3D-printed ABS components. Rapid Prototyping Journal, 2020. 26(1): p. 89-99.

9. Atahan, M.G. and M.K. Apalak, Loading-rate effect on tensile and bending strength of 3D-printed polylactic acid adhesively bonded joints. Journal of Adhesion Science and Technology, 2021.

10. Yao, T., et al., Tensile failure strength and separation angle of FDM 3D printing PLA material: Experimental and theoretical analyses. Composites Part B: Engineering, 2020. 188: p. 107894.

11. Wang, K., et al., Flexure behaviors of ABS-based composites containing carbon and Kevlar fibers by material extrusion 3D printing. Polymers, 2019. 11(11): p. 1878.

12. Ivanov, E., et al., PLA/Graphene/MWCNT Composites with Improved Electrical and Thermal Properties Suitable for FDM 3D Printing Applications. Applied Sciences, 2019. 9(6): p. 1209.

13. Caminero, M.Á., et al., Additive Manufacturing of PLA-Based Composites Using Fused Filament Fabrication: Effect of Graphene Nanoplatelet Reinforcement on Mechanical Properties, Dimensional Accuracy and Texture. Polymers, 2019. 11(5): p. 799.

14. Camargo, J.C., et al., Mechanical properties of PLA-graphene filament for FDM 3D printing. The International Journal of Advanced Manufacturing Technology, 2019. 103(5): p. 2423-2443.

15. Galatas, A., et al., Additive manufactured sandwich composite/ABS parts for unmanned aerial vehicle applications. Polymers, 2018. 10(11): p. 1262.

16. Yang, C., et al., 3D printing for continuous fiber reinforced thermoplastic composites: mechanism and performance. Rapid Prototyping Journal, 2017. 23(1): p. 209-215.

17. Singh, S., S. Ramakrishna, and R. Singh, Material issues in additive manufacturing: A review. Journal of Manufacturing Processes, 2017. 25: p. 185-200.

18. Weng, Z., et al., Mechanical and thermal properties of ABS/montmorillonite nanocomposites for fused deposition modeling 3D printing. Materials & Design, 2016. 102: p. 276-283.

19. Sood, A.K., R.K. Ohdar, and S.S. Mahapatra, Parametric appraisal of mechanical property of fused deposition modelling processed parts. Materials & Design, 2010. 31(1): p. 287-295.

20. Auras, R.A., et al., Poly (lactic acid): synthesis, structures, properties, processing, and applications. Vol. 10. 2011: John Wiley & Sons.

21. Afrose, M.F., et al., Effects of Build Orientations on Tensile Properties of PLA Material Processed by FDM. Advanced Materials Research, 2014. 1044-1045: p. 31-34.

22. Aliheidari, N., et al., The impact of nozzle and bed temperatures on the fracture resistance of FDM printed materials. SPIE Smart Structures and Materials + Nondestructive Evaluation and Health Monitoring. Vol. 10165. 2017: SPIE.

23. Kovan, V., G. Altan, and E.S. Topal, Effect of layer thickness and print orientation on strength of 3D printed and adhesively bonded single lap joints. Journal of

Mechanical Science and Technology, 2017. 31(5): p. 2197-2201.

24. Maroti, P., et al., Printing orientation defines anisotropic mechanical properties in additive manufacturing of upper limb prosthetics. Materials Research Express, 2018. 6(3): p. 035403.

25. Wang, L., et al., Effect of fused deposition modeling process parameters on the mechanical properties of a filled polypropylene. Progress in Additive Manufacturing, 2018. 3(4): p. 205-214.

26. Harris, M., et al., Effect of Material and Process Specific Factors on the Strength of Printed Parts in Fused Filament Fabrication: A Review of Recent Developments. Materials, 2019. 12(10): p. 1664.

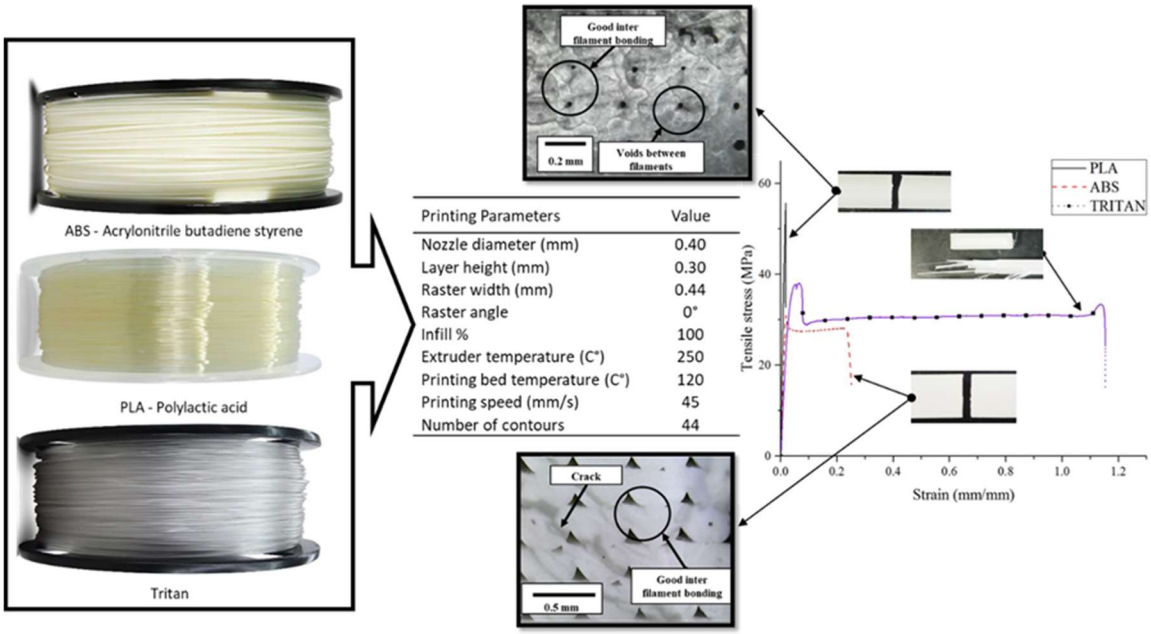
27. Nakagawa, Y., K.-i. Mori, and T. Maeno, 3D printing of carbon fibre-reinforced plastic parts. The International Journal of Advanced Manufacturing Technology, 2017. 91(5): p. 2811-2817.

28. Justo, J., et al., Characterization of 3D printed long fibre reinforced composites. Composite Structures, 2018. 185: p. 537-548.

CHAPTER 2

Chapter 2 is based on the following article: D.K.K. Cavalcanti, M.D Banea, H.F.M. de Queiroz, Effect of material on the mechanical properties of additive manufactured thermoplastic parts, Annals of Dunarea de Jos University of Galati Fascicle XII. https://doi.org/10.35219/awet.2020.01

Graphical abstract



Effect of material on the mechanical properties of additive manufactured thermoplastic parts

ABSTRACT

Additive manufacturing (AM) also called 3D printing, is an emerging process in the manufacturing sector with increasing new applications in aerospace, prototyping, medical devices and product development, among others. The resistance of the AM part is determined by the chosen material and the printing parameters. As novel materials and AM methods are continuously being developed, there is a need for the development and mechanical characterization of suitable materials for 3D printing. In this study, the influence of the material and the 3D-printing parameters on the mechanical properties of additive manufactured thermoplastic parts was investigated. Three different filaments that are commercially available: Polylactic acid (PLA), acrylonitrile butadiene styrene (ABS) and Tritan were used. Tensile and flexural tests were carried out, in accordance to ASTM standards, to investigate and compare the mechanical properties of the AM parts as a function of material used. The results showed that the type of filaments had the greatest influence on the mechanical properties of the AM parts. The maximum strength and stiffness were obtained for the PLA specimens. Tritan displayed the highest deformation, while the PLA manifested the lowest deformation capacity. The mechanical properties of the printed parts also depend on the printing parameters. The parameters used in this work are a good compromise between the printing time and the mechanical properties.

Keywords: Additive manufactured parts, PLA, ABS, Tritan, Mechanical properties.

2.1. INTRODUCTION

Additive manufacturing (3D printing technology) is a process in which 3D components, with high precision and complexity, are made by depositing materials in a layer-by-layer fashion, as opposed to conventional machining or forming methods [1]. One of the most common methods for 3D printing of polymeric materials is the Fused Filament Fabrication (FFF) or Fused Deposition Modelling (FDM) technique [2]. The resistance of the AM part is determined by the chosen material and printing parameters [3,4]. Therefore, using the correct process parameters for the FDM technique is essential to ensure that the material can be printed with a good surface

finish and high precision. These process parameters are: the layer thickness, raster orientation and infill density, build orientation, printing temperature and speed. Each parameter may have different settings for different materials, depending on their flow properties [5]. For example, the mechanical properties of 3D printed parts seem to be strongly dependent on the printing orientation (i.e. the tensile strength of FDM printed samples printed in the XYZ direction can be 5 times higher than those printed vertically). Sood et al. [6] showed that the mechanical properties of the AM parts are related to the number of printed layers. This is due to the thermal cycles (heating and cooling) that will cause cumulative residual stresses, distortion, interlayer cracking and delamination. The nature of the AM technique limits the choice of materials. The majority of the materials used for AM are thermoplastics (i.e. Polylactic Acid (PLA) and Acrylonitrile Butadiene Styrene (ABS)). PLA is a linear aliphatic thermoplastic polyester, produced from renewable biodegradable materials. PLA has excellent mechanical properties, thermal stability, good processing capability, and low environmental impact. However, one disadvantage is that PLA is relatively expensive when compared to other petroleum-based polymers [7]. The ABS thermoplastic material has good mechanical properties, but it emits an unpleasant odour during processing [5]. However, novel materials for 3D printing are continuously being developed. Thus, in order to further understand the mechanical properties of these AM materials and stimulate their use in new applications in the industry, more research work is needed. The main objective of this work was to characterise three different filament materials that are commercially available in order to understand the mechanical behaviour of 3D printed materials and to stimulate their use in new applications.

2.2. MATERIALS AND METHODS

2.2.1. Materials

All the materials used in this work were provided by GTMax3D (Americana, SP, Brazil) under the form of filaments. The basic mechanical properties as per supplier can be seen in table 1. The PLA and ABS thermoplastic materials are well known in the industry. Tritan is an amorphous copolyester, a modified polyester with diacids and diols), that offers some advantages, such as clarity, toughness, heat resistance, chemical resistance, resulting in more robust parts in the context of 3D printing.

Table 1. Mechanical properties of the materials used.

Material	Tensile strength (MPa)	Flexural modulus (GPa)	Tensile strain (%)
PLA	53	3.50	6
ABS	29	0.26	18
Tritan	43	1.55	210

2.2.2. Specimens' fabrication

The AM specimens were fabricated using a Core A1v2 3D printer form GTMax3D (Americana, SP, Brazil). The printing process parameters used in this work are presented in Table 2 and were chosen based on the literature and some in-house laboratory trials. The layer height was 0.3 mm, as it was shown in the literature it presented the best mechanical properties and lower production times for FDM 3D printing [8].

Table 2. Printing parameters used for all specimens.

Printing Parameters	Value
Nozzle diameter (mm)	0.40
Layer height (mm)	0.30
Raster width (mm)	0.44
Raster angle	0°
Infill %	100
Extruder temperature (C°)	250
Printing bed temperature (C°)	120
Printing speed (mm/s)	45
Number of contours	44

The raster width chosen was 0.44 mm since this will reduce internal voids (see Fig. 1) produced by overlapping the rasters [9]. The raster angle chosen was 0º, in the literature a raster angle of 0° is the optimum direction of depositions if high tensile strength is desired. The infill chosen

was 100%, since the properties of printed parts are associated to internal voids [8]. The printing speed used was 45 mm/s as it was shown in the literature that this printing speed presented the best results by providing increased diffusion, larger interfacial width and lower internal voids. The slower speed also permits a longer exposure to heat, increasing diffusion between rasters and layers [10]. Finally, the extruder and bed temperature values used were chosen based on the fact that the temperature has a significant impact in the part's properties. Within the relevant literature a continuous rise in material properties was observed as the nozzle temperature increased, while the bed temperature (i.e. 120 ºC) was chosen to reduce a possible temperature gradient between the top and bottom layers [11].

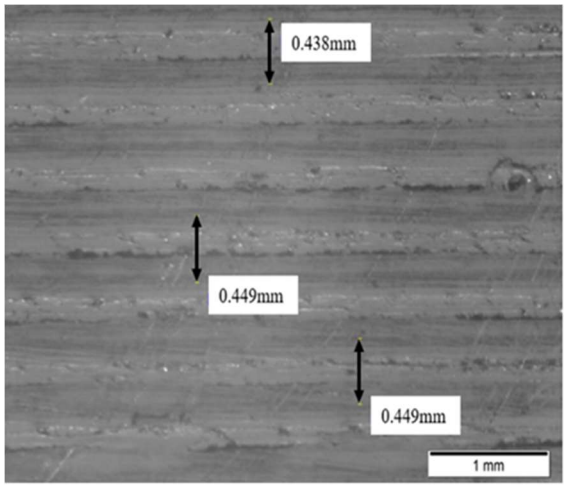


Fig. 1. Magnification of printed ABS core with indications of raster width (contrast was done using graphite powder).

Slicing was performed with Simplify3D® and all test specimens were fabricated in a flat-edge orientation as shown in Fig. 2. The number of contours was high enough in order to ensure that the raster angle was 0° (see Fig. 3). The configuration used is independent of the XY build orientation.

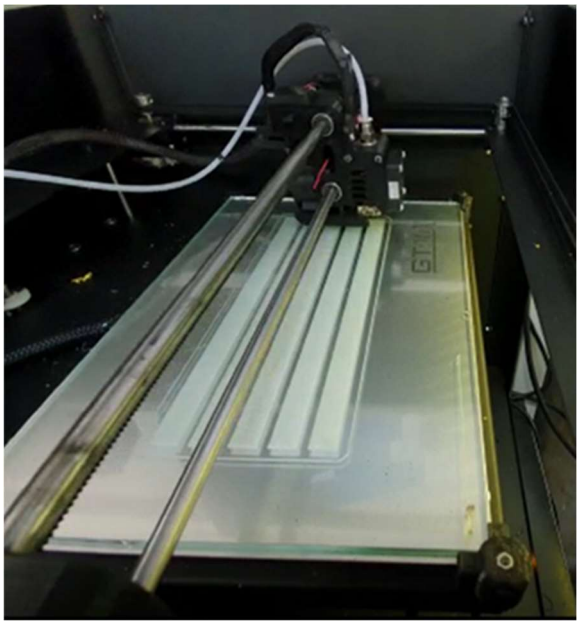


Fig. 2. 3D printing process fabrication of AM specimens.

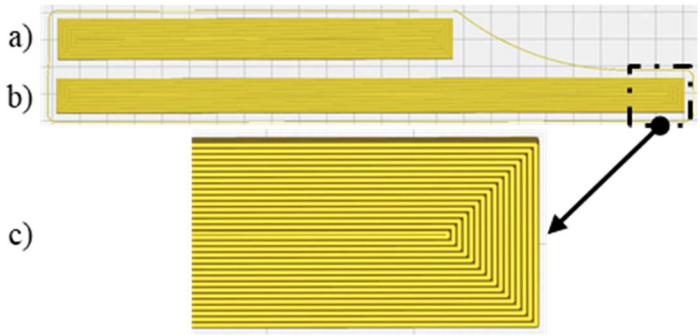


Fig. 3. Preview of the specimens and their layering after slicing (taken from the Simplify3D® program): a) flexural, b) tensile and c) magnification of specimen surface.

The specimen dimensions (in mm) can be seen in Fig. 4. As there are no recognized standards in the literature for the quantification of the mechanical properties of FDM parts, the specimen dimensions of the tensile specimens were chosen after in-house laboratory experimentation (the configuration chosen presented consistent failure within the specimen width of the tab or grip). The tabs were added to the specimen by using an acrylic adhesive (TEK Bond 793), this was chosen due to their low ductility and relatively high strength, therefore, not affecting the tests.

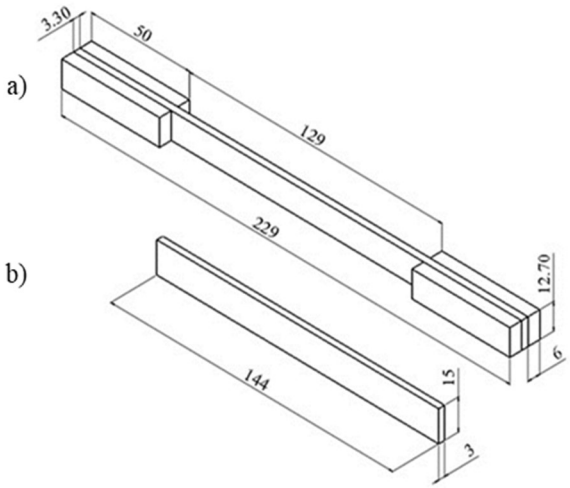


Fig. 4. Scheme of AM parts specimens: a) tensile; b) flexural, dimensions in mm.

2.2.3. Test method

The tensile and flexural tests were performed at room temperature using a testing machine INSTRON® model 5966 (Norwood, Massachusetts, USA). The tensile tests were done with a cross head speed of 2 mm/min and a load cell of 10kN. A strain gauge extensometer was used to record the strain, as seen in Fig. 5. A 50x15x6mm tab was used on either side or extremity of the specimen in order to ensure that all failures occurred in the proper area. For the flexural tests a three-point bending rig with a span of 120 mm, cross head speed of 1 mm/min and a 1 kN load cell were used, as per ASTM D790 standard. Four specimens were tested for each condition.

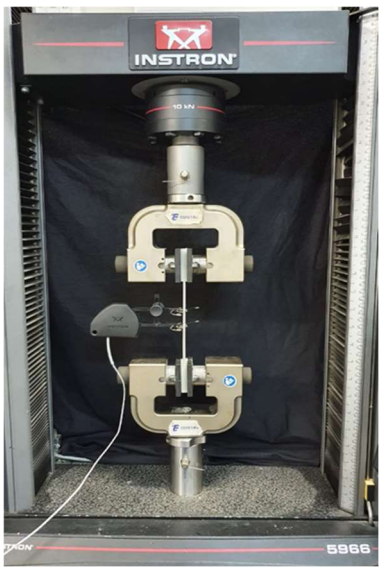


Fig. 5. Tensile test set-up.

2.2.4. Preliminary parametric study

Prior to the mechanical tests, a preliminary study was performed in order to verify if the printing temperature chosen (i.e. 250 °C) is adequate for printing the Tritan material as this temperature is lower than the minimum temperature recommended by the supplier (i.e. 260 °C). Therefore, the Tritan was also printed with an extruder temperature of 280 °C. All other parameters are maintained the same (see Table 2). Representative stress-strain curves for the two cases studied are presented in Fig. 6. From these curves the tensile properties were calculated and it was found that the difference between the tensile strength of the samples printed with 250°C (i.e. 37.79 ± 1.45 MPa) and the 280°C (i.e. 38.29 ± 0.43 MPa) is negligible. Furthermore, the failure surfaces of the specimens after the tensile tests were examined visually. Figure 7 presents the failure modes of both cases. It can be seen, that the specimens printed with an extruder temperature of 250 °C presented a SAT (Splitting, at grip/tab and top) type failure (see Fig. 7a), while the 280 °C case (Fig. 7b) presented an AAT (Angled, at grip/tab and Top) failure as per ASTM D3039 standard.

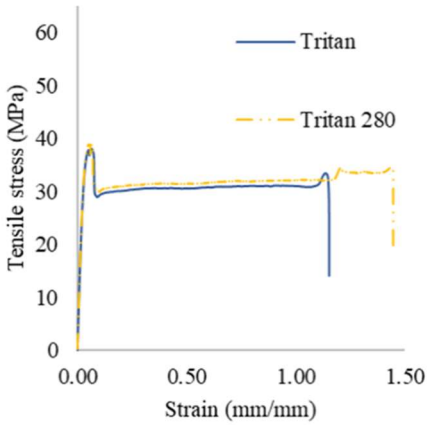


Fig. 6. Representative stress-strain curves for the 250°C and 280°C printed Tritan specimens.

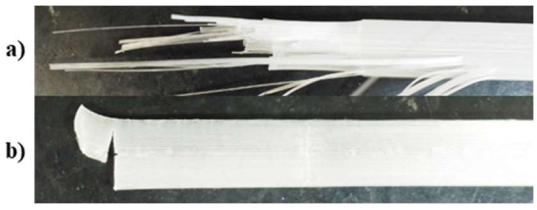


Fig. 7. Representative failures mode of Tritan tensile specimens printed at: a) 250°C and b) Tritan at 280°C.

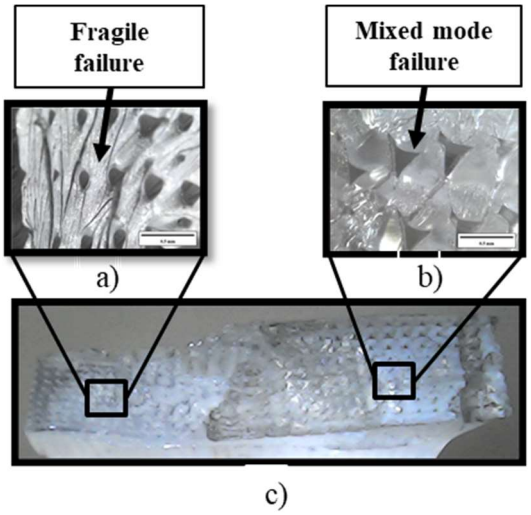


Fig. 8. Cross-section of the Tritan printed at 280 °C, where a) fragile failure area, b) mixed mode failure area and c) the cross-section.

For further clarification of the failure modes, an optical microscope was used to produce micrographs of the failure surfaces. Figure 8 presents the macro cross section view of the Tritan tensile specimen printed at 280ºC as well as micrographs of two distinct failure zones. From Fig. 8a, the micrograph from the leftmost side of the cross-section can be seen, where a smooth surface is visible, indicative of a fragile failure, as well as multiple crack fronts. From Fig. 8b, a micrograph of the zone opposite to the previously described can be observed and a more ductile surface is visible, indicating a mixed mode failure.

Figure 9 depicts a more detailed view of the cross-section micrographs. From Fig. 9a, inter filament voids are visible as well as significant crack nucleation following these voids. Furthermore, a very homogeneous and smooth surface is visible where even the deposition layering sequence is not discernible. On the other hand, from Fig. 9b, a detailed view of the opposite end of the cross-section can be seen. Here, significant fracture surface differences can be observed. First, the layering sequence is clearly visible, along with the inter filament voids. However, crack nucleation and propagation is visible through the filaments with a ductile (wavy)/ fragile (smooth) transition zone. Moreover, despite of these differences in failure mode, the ultimate failure load was not significantly affected by the extruder temperature. Thus, the 250ºC temperature was chosen for the Tritan specimens.

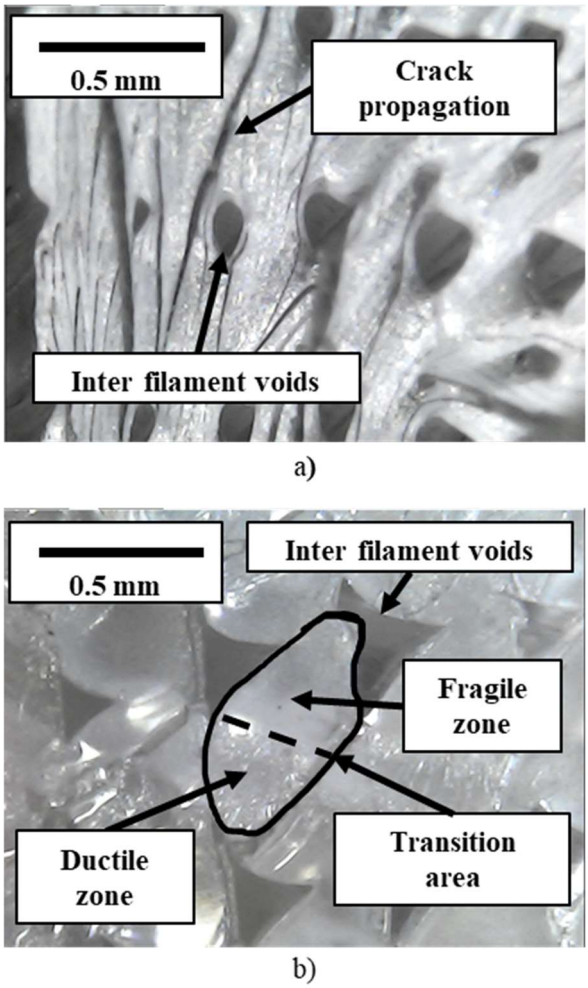


Fig. 9. Cross-section micrograph of the Tritan printed tensile specimens with a 280 °C extruder temperature.

2.3. RESULTS AND DISCUSSION

2.3.1. Tensile tests

Figure 10 shows representative tensile stress-strain curves obtained from the tensile tests of the FDM parts as a function of material. From the stress/strain curves, the tensile data were calculated (tensile strength, Young's modulus and elongation at break), and the results are presented in Table 3. The material properties varied significantly as a function of the filament material. PLA presented the highest tensile strength, with an increase of approx. 40% and 28% when compared to ABS and Tritan, respectively. The stiffness of AM parts also varied as a function of filament material with the highest value for the PLA and lowest for Triran. Finally, the highest deformation was found for Tritan, while the lower, as expected, was found for PLA.

Table 3. Tensile data for the materials studied.

Material	Tensile strength (MPa)	Young's modulus (GPa)	Strain (%)
PLA	51.88 ± 3.92	3.72 ± 0.17	2.18 ± 0.68
ABS	31.03 ± 0.11	2.18 ± 0.05	24.98 ± 0.1
Tritan	37.79 ± 1.45	1.38 ± 0.01	104.14 ± 30.98

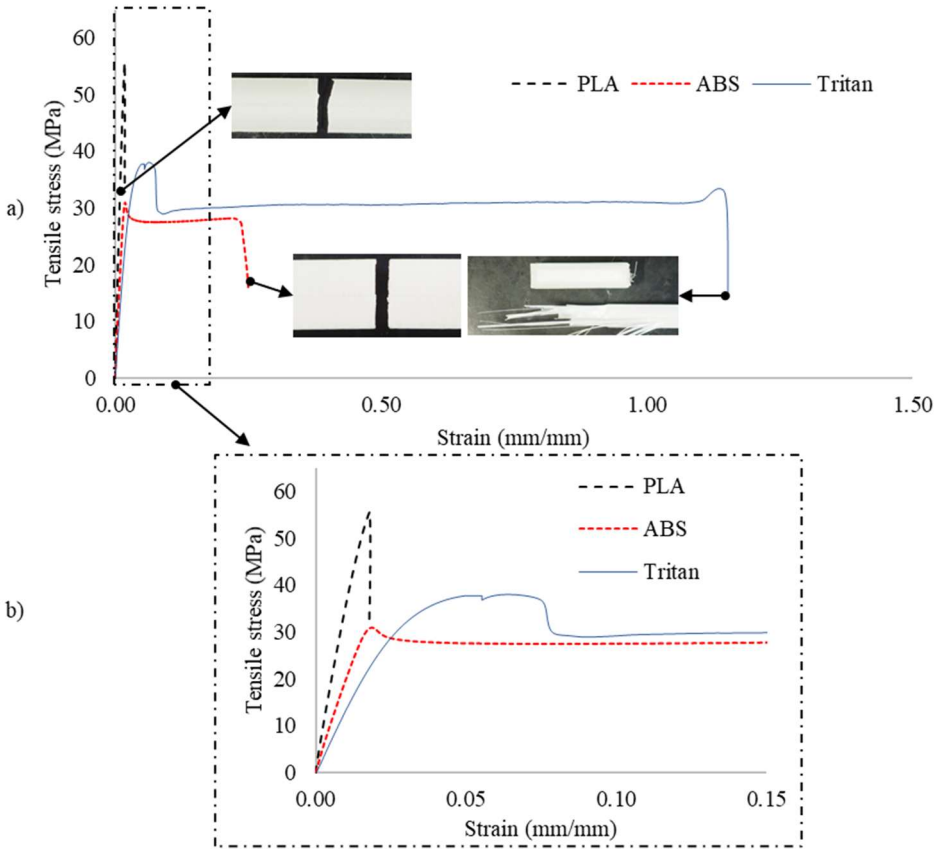


Fig. 10. Representative tensile stress-strain curves in function of material (a) and b) Magnification of the linear part of the stress-strain curves.

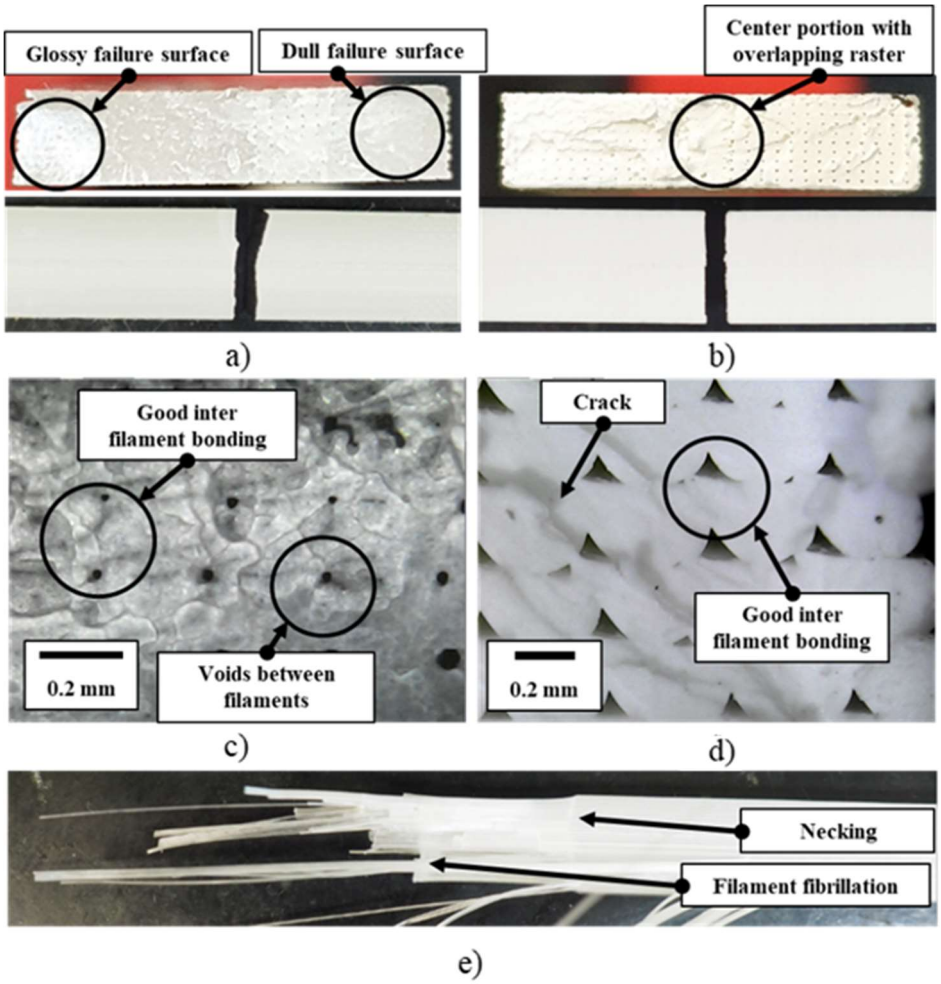


Fig. 11. Representative tensile failures of a) cross-section of PLA specimen, b) cross-section of ABS specimen, c) PLA micrograph, d) ABS micrograph and e) Tritan fibrillation failure.

From Fig. 10, it can be seen that the behaviour of the PLA material was predominantly brittle, while both ABS and Tritan presented a significantly more ductile behaviour. For a better conception of the initial slope, a magnified view of that area of the stress-strain curves can be seen in Fig. 10b. (the differences in stiffness in function of material presented in Table 3 can be seen more easily).

If the values from Table 3 are compared to the supplier material properties (see Table 1), little variation was found in terms of tensile strength (bellow 10%) for PLA. However, a lower deformation was observed (approx. 28%). Similar results were found for the ABS and Tritan, where the tensile strength presented little variation when compared to the supplier data. However, the elongation at break is higher for the ABS (by approx. 28%), while for Tritan is lower (by approx. 50%), compared to the supplier data. These variations are likely due to different printing parameters used in this work.

Representative macro failure surfaces of the tested materials can be seen in Fig 11. As stated by the ASTM D3039 standard, the PLA and ABS both presented AGM (Angled, gage and middle) failure, Figs. 11a and b, respectively. For all specimens, the centre portion of the printed part presented very few to no internal voids, as shown in Fig. 11b. This is due to the slicing program that created an overlap in this portion of the sample. Magnified views of the failure surfaces taken with the aid of an optical microscope can be seen for PLA and ABS in Figs. 11c and d, respectively. From Fig. 11c, a very uniform failure surface is visible, with relatively small internal printing voids and essentially no layering is observable. In other words, the material is very cohesive with little to no visible deposition interphase. This is due to the temperature used during the printing process, which changes the void geometry [12]. This improvement in inter filament bonding is promoted by a higher diffusion time. The crack propagation was ductile in its progression with smooth fragile patches in between crack fronts. Crack nucleation points were predictably close to the internal voids.

The ABS micrograph can be seen in Fig. 11d and significant failure surface differences can be observed. For example, the layering sequence is clearly visible and uniform as well as the printing voids. In addition, while the crack propagation here was also ductile in progression, it was more uneven in its topography. The macro failure mode of the Tritan can be seen in Fig. 11e, and a SAT (Splitting, at grip/tab and top), failure mode is observable. This has been described in this work as a fibre "fibrillation", as individual deposition fibres split and failed at the interphase during loading. Also, a "necking" front was observed during tensile testing where significant Poisson deformation was visible, ending with the previously described fibrillation failure close to the top tab.

2.3.2. Flexural tests

Figure 12 presents representative flexural stress-strain curves of the AM parts in function of material. From the stress/strain curves the flexural data were calculated and are presented in Table 4.

Similar to the tensile properties, the flexural data varied significantly with the printed material. The PLA presented a brittle behaviour, while a ductile behaviour was observed for the ABS and Tritan specimens, as expected. It is important to note that both the ABS and Tritan's flexural tests took a significant amount of time and were ultimately stopped due to specimen slippage.

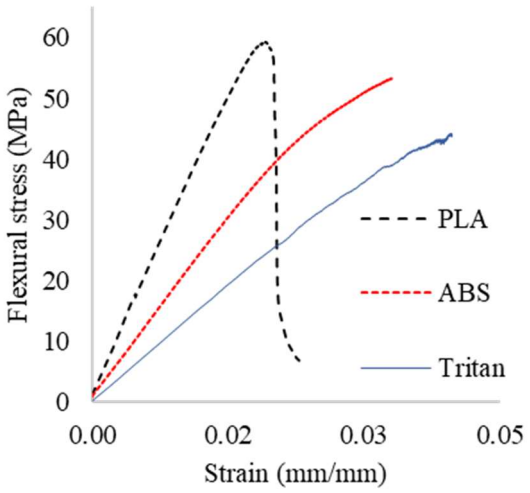


Fig. 12. Representative flexural stress-strain curves as a function of material.

Table 4. Flexural data.

Material	Flexural strength (MPa)	Flexural Modulus (GPa)
PLA	60.85 ± 1.57	3.11 ± 0.11
ABS	53.32 ± 1.54	1.6 ± 0.15
Tritan	43.53 ± 0.74	1.08 ± 0.08

A higher flexural strength of approx. 30% and 22% was found when PLA is compared to Tritan and ABS, respectively. Similarly, in terms of flexural modulus, significant increases are also observed (i.e. enhancements of approx. 50% and 66% when PLA is compared to ABS and Tritan). If the data obtained here is compared to the data provided by the supplier, a significant higher flexural modulus for the ABS can be seen (approx. 84% higher). However, for the PLA and Tritan, lower values were obtained in the present study (approx. 12% and 47% lower than those provided by the supplier). The difference in values can be explained by the different layer thickness and filament orientation used in this study. It was shown in the literature that the layer thickness will directly impact void size and inter filament bonding [12, 16]. Also, the filament orientation impacts the specimen rigidity [19]. This will be discussed further in the next section 3.3.

Table 5. Tensile data.

Material	Parameters	Tensile strength (MPa)	Young's modulus (GPa)	Ref.
ABS	0.2 mm Layer heigh / ±45° Orientation / 100% Infill	29.70	1.84	[13]
ABS	0/90 Orientation / 100% Infill	27.60	1.74	[13]
ABS	0.4 mm Layer height / 0/90 Orientation / 100% Infill	28.20	1.88	[13]
ABS	0.127 mm Layer height / ±45° Orientation / 12 Contour layers / 100% Infill	30.66	1.80	[14]
ABS	0.254 mm Layer height / 12.7 mm/s Printing speed	26.50	2.14	[15]
PLA	0.30 mm Layer height / 85% Infill	37.90	0.36	[8]
PLA	0/90 Orientation/ 100% Infill	60.40	3.48	[13]
PLA	0.3 mm Layer height / ±45° Orientation / 100% Infill	48.50	3.34	[13]
PLA	0.06 mm Layer height / Flat edge / 50 mm/s Printing speed	89.10	4.19	[16]
PLA	0.24 mm Layer height / Flat edge / 50 mm/s Printing speed	72.30	3.77	[16]
PLA	0.2 mm Layer height / 0° Orientation / 3 shell	55.60	3.74	[17]
PLA	0.15 mm Layer height / ±45° Orientation / 2 Contour layers	42.28	2.80	[17]
PLA	0.2 mm Layer height / ±45° Orientation / 60 mm/s Printing speed	61.42	3.96	[18]

Table 6. Flexural data.

Material	Parameters	Flexural strength (MPa)	Flexural modulus (GPa)	Ref.
ABS	100% Infill / +45/-45 Orientation	42.69	0.50	[19]
ABS	0.10 mm Layer height / ±45° Orientation / 60 mm/s Printing speed	48.38	1.50	[20]
PLA	0.06 mm Layer height / Flat edge / 80 mm/s Printing speed	56.00	1.60	[16]
PLA	0.06 mm Layer height / On-edge / 80 mm/s Printing speed	65.00	1.85	[16]
PLA	0.12 mm Layer height / On-edge / 20 mm/s Printing speed	64.80	1.77	[16]
PLA	0.27 mm Layer height / 78% Infill	60.90	2.47	[8]
PLA	0.13 mm Layer height / 78% Infill	45.70	2.18	[8]

2.3.3 Comparative analysis

Table 5 and 6 present a comparative analysis of the properties of the PLA and ABS which was done in order to evaluate the impact of the methodology and the results obtained in the present work using relevant published literature [13-20]. It can be seen that the values found in the literature varied for the same material. For instance, the tensile strength found in this study for the ABS (i.e. 31.03 ± 0.11) were close to the values found in some studies [13, 14] and superior to values found in [15]. The difference in values compared to the study of Rodríguez et al. [15] may be explained by the fact that the larger layer height value used in the present study promotes fewer internal voids and consequently improved tensile properties. The printing speed is also a factor that influences the tensile properties of the printed parts. It was shown in the literature that a slower printing speed promotes a better molecular alignment and allows each layer to

cool down before the next one is printed, and in this way, the inter filament bonding is improved.

The tensile strength of the PLA printed parts found in the literature varied from approx. 37 to 89 MPa [8, 13, 16-18]. The layer thickness of the printed parts varied between 0.06 and 0.3 mm, which can be the reason behind the superior variability in the values found for this material compared to ABS. For example, Chacón et al. [16], studied the effect of printing parameters (i.e. layer thickness, printing orientation and speed) on the material properties of PLA. It was found that a smaller layer height along with an average printing speed and flat orientation was the best parameter combination for optimum tensile properties. The smaller layers can result in fewer voids, with the consequence of also greatly increasing the printing time. For example, an increase in printing time of approx. 255% was reported when the 0.06 mm layer height case is compared to the 0.27 mm case [16]. However, the parameters used in this work for the PLA, presented a good compromise between printing time (~35 min per tensile sample) and mechanical properties, where gains or losses in tensile and flexural properties are compensated by the greatly reduced printing time. Finally, the values for the Young's modulus found in this work for ABS and PLA are in line with those found in the literature.

Similarly to the tensile properties, the flexural material characteristics were also found to be dependent on the printing parameters (see Table 6). For ABS, the flexural strength found in this study presented a higher value when compared to those found in the literature. This is mainly due to the raster orientation used, where the totally aligned filaments provide better resistance to tensile loads, consequently increasing the flexural strength and modulus [19]. Regarding the PLA, little variation was found when the flexural strength found in this work is compared to the available literature. However, the flexural modulus of PLA, found in this study is approx. 68% higher than the value found in [16]. On the other hand, the values obtained in this study are close to those obtained in the flat edge configuration by Chacón et al. [16]. Therefore, it can be concluded that the print orientation has a higher impact in flexural properties than the layer thickness or printing speed.

2.4. CONCLUSIONS

In this study, the influence of material and the 3D-printing parameters on the mechanical properties of additive manufactured thermoplastic parts was investigated. In the literature the use of these parameters was not combined into a single work. The results show that the type of

filaments had the biggest influence on the mechanical properties of the AM parts. Among the tested materials, the one with the highest tensile strength was the PLA (51.88 MPa), followed by the Tritan (37.79 MPa) and finally, the ABS (31.03 MPa). In terms of stiffness, PLA is the best material, followed by ABS and Tritan which presented the lowest value. Finally, Tritan presented the highest deformation, while PLA displayed the lowest deformation capacity. Regarding the flexural properties, PLA presented the best properties, followed by ABS and Tritan. The mechanical properties of the printed parts also depend on the printing parameters. The printing parameters used in this work presented a good compromise between printing time and the mechanical properties of the AM parts. The mechanical properties of the AM materials were optimised in order to stimulate their use in new applications in the industry.

REFERENCES

[1]. ASTM Standard F2792, Standard terminology for additive manufacturing technologies, vol. 2012, ASTM International, West Conshohocken, Pa, USA (2012)

[2]. Cavalcanti D. K. K., Banea M. D., de Queiroz H. F. M., Mechanical characterization of bonded joints of additive manufactured adherends, Annals of Dunarea de Jos University of Galati Fascicle XII, Welding Equipment and Technology, vol. 29, 2019, pp. 27-33.

[3]. Popescu, D., Zapciu, A., Amza, C., Baciu, F., Marinescu, R., FDM process parameters influence over the mechanical properties of polymer specimens: A review, Polymer Testing 69, 2018, pp. 157–166.

[4]. Solomon, A., Rosenthal, Y., Ashkenazi, D. and Stern, A., Structure and mechanical behavior of additive manufactured fused deposition modeling ABS, Annals of" Dunarea de Jos" University of Galati. Fascicle XII, Welding Equipment and Technology 29, 2018, pp. 47–56.

[5]. Ngo T. D., Kashani A., Imbalzano G., Nguyen K. T. Q., Hui D., Additive manufacturing (3D printing): A review of materials, methods, applications and challenges, Composites Part B: Engineering. vol. 143, 2018, pp. 172-196.

[6]. Sood A. K., Ohdar R. K., Mahapatra S. S., Parametric appraisal of mechanical property of fused deposition modelling processed parts, Materials & Design, vol. 31(1), 2010, pp. 287-295.

[7]. Carrasco F., Pagès P., Gámez-Pérez J., Santana O. O., Maspoch M. L., Processing of poly(lactic acid): characterization of chemical structure, thermal stability and mechanical properties, Polymer Degradation and Stability, vol. 95, 2010, pp. 116-125.

[8]. Camargo J. C., Machado A. R., Almeida E. C., Silva E. F. M. S., Mechanical properties of PLA-graphene filament for FDM 3D printing, The International Journal of Advanced Manufacturing Technology, vol. 103(5), 2019, pp. 2423-2443.

[9]. Harris M., Potgieter J., Archer R., Arif K. M. E., Effect of Material and Process Specific Factors on the Strength of Printed Parts in Fused Filament Fabrication: A Review of Recent Developments, Materials, vol. 12(10), 2019, pp. 1664.

[10]. Wang L., Sanders J. E., Gardner D. J., Han Y., Effect of fused deposition modeling process parameters on the mechanical properties of a filled polypropylene, Progress in Additive Manufacturing. vol. 3(4), 2018, pp. 205-214.

[11]. Aliheidari N., Tripuraneni R., Hohimer C., Christ J., Ameli A., Nadimpalli S., The impact of nozzle and bed temperatures on the fracture resistance of FDM printed materials, Smart Structures and Materials + Nondestructive Evaluation and Health Monitoring, vol. 10165. 2017, pp. 1016512.

[12]. Kuznetsov V. E., Solonin A. N., Tavitov A. G., Urzhumtsev, O. D., Vakulik A., Increasing of strength of FDM (FFF) 3D printed parts by influencing on temperature-related parameters of the process, Rapid Prototyping Journal, 2018, pp. 1-32.

[13] Tymrak B. M., Kreiger M., Pearce J. M., Mechanical properties of components fabricated with open-source 3-D printers under realistic environmental conditions, Materials & Design, vol. 58, (2014), pp 242-246.

[14] Schmitt M., Mehta R. M., Kim I. Y., Additive manufacturing infill optimization for automotive 3D-printed ABS components, Rapid Prototyping Journal, vol. 26, 2020, pp 89-99.

[15] Rodríguez J. F., Thomas J. P., Renaud J. E., Mechanical behavior of acrylonitrile butadiene styrene (ABS) fused deposition materials. Experimental investigation, Rapid Prototyping Journal, vol. 7, 2001, pp. 148-459.

[16] Chacón J. M., Caminero M. A., García-Plaza E., Núnez P. J., Additive manufacturing of PLA structures using fused deposition modelling: Effect of process parameters on mechanical properties and their optimal selection, Materials & Design, vol. 124, 2017, pp. 143-157.

[17] Pei E., Lanzotti A., Grasso M., Staiano G., Martorelli M., The impact of process parameters on mechanical properties of parts fabricated in PLA with an open-source 3-D printer Rapid Prototyping Journal, vol. 21, 2015, pp. 604-617.

[18] Wang K., Li S., Rao Y., Wu Y., Peng Y., Yao, S., Zhang, H., Ahzi, S., Measurements of the mechanical response of unidirectional 3D-printed PLA, Materials & Design, vol. 123, 2017, pp. 154-164.

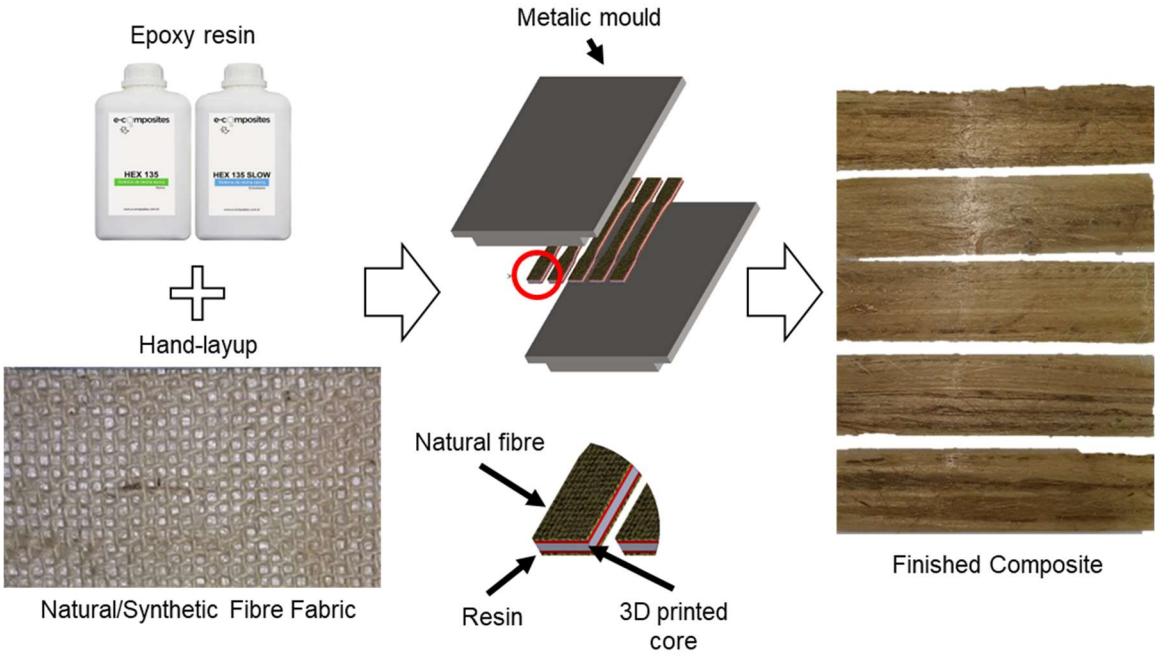
[19] Weng Z., Wang J., Senthil T., Wu L., Mechanical and thermal properties of ABS/montmorillonite nanocomposites for fused deposition modeling 3D printing, Materials & Design, vol. 102, 2016, pp. 276-283.

[20] Wang K., Li S., Rao Y., Wu Y., Peng Y., Yao S., Zhang H., Ahzi S., Flexure behaviors of ABS-based composites containing carbon and Kevlar fibers by material extrusion 3D printing, Polymers, vol. 11, 2019, pp. 1-12.

CHAPTER 3

Chapter 3 is based on the following article: D. K. K. Cavalcanti, H. F. M. de Queiroz, J. S. S. Neto, M.D Banea, strengthening of additive manufactured parts by using different type of fibre reinforcements, The International Journal of Advanced Manufacturing Technology, vol. 29, 2022, ISSN 1221-4639, pp. 27-33. https://doi.org/10.1007/s00170-022-10327-8

Graphical abstract



Strengthening of additive manufactured parts by using different type of fibre reinforcements

ABSTRACT

The main objective of this work was to investigate the mechanical properties of additive manufactured (AM) polymeric parts (Polylactic Acid (PLA) and Acrylonitrile Butadiene Styrene (ABS)) reinforced by different types of fibres. Natural (jute and curauá) and synthetic (glass) fibre fabrics were laminated on the outer sides of the AM parts by using an epoxy resin. The reinforcement was applied to the AM parts as 1 and 2-layers for each fibre type. The mechanical characterization of the AM reinforced composites was performed through tensile and flexural tests. It was found that the addition of the reinforcement fibres improved the mechanical properties of the AM parts for both materials tested. In general, the glass fibre reinforced specimens presented better mechanical properties when compared to the natural fibre reinforced AM parts. The curauá fibre reinforced specimens presented improved performance when compared to the jute composites and matched the mechanical properties of the 1-layer glass fibre reinforced AM specimens. The failure modes significantly varied as a function of the material. The PLA specimens showed a brittle failure, while the ABS specimens presented delamination in the resin/printed part interface. Adding different fibre fabrics to 3D printed materials may be a promising innovation in order to improve their mechanical properties and these improvements might enable these materials to serve for high load bearing purposes.

Keywords: Fused deposition modelling; additive manufacturing; fibre reinforcements; mechanical properties; ABS; PLA.

3.1. INTRODUCTION

Additive manufacturing (AM), also known as 3D printing, is a relatively new manufacturing sector in the industry that has rapidly gained space in both home and industrial applications. AM presents many advantages over traditional fabrication methods, such as: lower costs for complex parts less waste and simple implementation [1-4]. However, the AM parts have high anisotropy, with the layering sequence and process parameters influencing the final product's mechanical and aesthetics characteristics. Fused Filament Fabrication (FFF) or Fused

Deposition Modelling (FDM) is one of the most widely used AM technique due to its ability to manufacture complex and relatively high strength parts from low-cost materials. The most commonly materials used with FDM are acrylonitrile butadiene styrene (ABS) and polylactic acid (PLA) [5-10]. ABS has good mechanical properties but emits unpleasant odour during processing whereas PLA is environmentally friendly but has relatively poor mechanical and thermal properties [11]. However, these materials without any modification have relatively low mechanical properties (i.e. they have typical bulk strengths between 30–100 MPa and elastic moduli in the range of 1.3–3.6 GPa), which means that the printed parts cannot be used for high-performance applications [12,13].

There are various methods explored in the literature to enhance the original properties of the materials used for FDM processes (e. g. incorporation of nanoparticles within the material and the use of fibres or fabrics as reinforcements) [14-20,7,10,6,21-25]. For instance, Dul et al. [15] investigated the mechanical properties of 3D-printed ABS modified with 2, 4 and 8 wt.% graphene and found that, the presence of graphene substantially increased the elastic modulus and the dynamic storage modulus, but decreased the maximum tensile strength and elongation at break of the modified material. However, it was shown that reinforcement of the filaments by particles, affects the melt flowability and viscosity of the filament. In addition, during printing, particle reinforcement may lead to nozzle clogging due to particle aggregation, void formation, and variation in curing time [26]. Another emerging method for increasing the mechanical properties of 3D printed materials is the use of continuous fibre reinforced filaments [17,19,24,27,28,25,29]. Nevertheless, this method requires specialized equipment and is limited in printing parameters [19]. In addition, when compared to conventional manufactured composites, they exhibit low strength due to poor bonding between the layers, which significantly affects the mechanical performance of the resulting composites. Hence, a simpler solution would be to reinforce only the surface of the printed parts. For example, Galatas et al. [17] found that the addition of carbon fibre fabric to an ABS printed part using a bi-component epoxy resin resulted in an increase of both strength and rigidity. This increase was directly related to the number of carbon fibre layers. Gohar et al. [30], studied the mechanical performance of sandwich structures built by FDM printing technique. The reinforcing face sheets were 3D printed using a PLA + 15% carbon fibre filament. They found that the main form of the specimen's failure was delamination, therefore, the bond strength between face sheet and core is highly influential in the load capacity of the composites. Therefore, this solution can be a faster and more direct form of improving the mechanical properties of AM

parts when compared to continuous fibre reinforced AM parts and may be relevant mainly for prostheses and applications where the printing parameters may not be compatible with the continuous printing method [31,32] due to the above mentioned limitations.

The use of natural fibres has gained interest in many industries as a possible substitute to the already established synthetic fibres [33,34]. The transport sector has been the most interested in these fibres, mainly due to their eco-friendly properties [35]. Natural fibres present many advantages, such as: biodegradability, low density, and good acoustic isolation, low cost and renewable source. However, these approaches are not without inherent disadvantages. These include the variability in fiber properties and their hygroscopic characteristics, which contribute to the absorption of moisture by the fibres. This moisture absorption, in turn, leads to low interfacial adhesion between the hydrophobic matrix and the fibres, consequently resulting in a reduction in the overall mechanical properties of the composite material [36]. Nonetheless, these fibres still offer a good alternative to synthetic fibres, especially glass fibre. Although, several researchers studied the possibility of reducing and/or substituting glass fibre as a reinforcement in fibre reinforced composites, to reduce cost, weight and environmental benefits, using natural fibre as reinforcing agents to AM parts is not fully explored [34].

The main objective of this work was to investigate the mechanical properties of composite materials made by 3D printed (PLA and ABS) parts reinforced by different types of fibres. Natural (jute and curauá) and synthetic (glass) fibre fabrics were laminated on the outer sides of the AM parts by using an epoxy resin via compression moulding. The reinforcement was applied to the AM parts as 1 and 2-layers for each fibre type. The mechanical characterization of the resulting composites was performed through tensile and flexural tests in accordance with their respective ASTM standards. The current work provides an alternative to the more common reinforcement method, by using a hybrid manufacturing alternative: 3D printing+ compression moulding. The application of novel manufacturing methodologies allied with renewable biodegradable fibres can provide an interesting path forward for fabricating high-performance 3D printed thermoplastic composites.

3.2. MATERIALS AND METHODS

3.2.1 Materials

The 3D printed parts were produced using PLA plus and ABS (tradename SABIC Cycolac® MG94), provided in the form of a 1.75 mm natural filament by GTMax3D (Americana, SP, Brazil). Bidirectional jute and glass fibre fabrics and curauá fibres were used as reinforcements.

The HEX SLOW epoxy resin and the glass fibre fabric (tradename RE200P) were supplied by Barracuda Advanced Composites (Rio de Janeiro, Brazil). The jute fabric was supplied by Sisalsul (São Paulo, Brazil), while the curauá was kindly provided by the Federal University of Pará (Universidade Federal do Pará, Brazil). The fibre fabrics, both natural and synthetic, presented a simple weave configuration, with 0°, 90° weave orientation. Typical properties of the natural fibres used can be seen in Table 1 [37,38].

Table 1. Properties of the natural fibres used [37,38].

Properties	**Jute fibre**	**Curauá fibre**
Density (g/cm3)	1.3	1.4
Bundle diameter (mm)	0.55–0.65	0.6–0.7
Tensile strength (MPa)	393–773	500–1150
Young's modulus (GPa)	26.5	11.8
Elongation at break (%)	1.5–1.8	3.7–4.3
Cellulose (%)	58–63	58.8
Hemicellulose (%)	12	23.8
Lignin content (%)	12–14	14.7
Lumen area (μm2)	1014	162
Cellular wall thickness (μm)	2.5	3.5
Lumen diameter (μm)	6.7	4
Microfibril angle	8º	15-18.8

3.2.2. Specimen fabrication

3.2.2.1. 3D printed part fabrication

The 3D printed parts were fabricated using a Core A1v2 3D printer GTMax3D (Americana, SP, Brazil). As there is no universal or widely accepted specimen form and dimensions for the tensile testing of FDM parts [14], the specimen dimensions for the tensile tests were chosen after an in-house laboratory experimentation (the configuration chosen presented consistent failure within the specimen width of the tab or grip). The schematic representation of the specimens (dimensions in millimetres) can be seen in Fig.1.

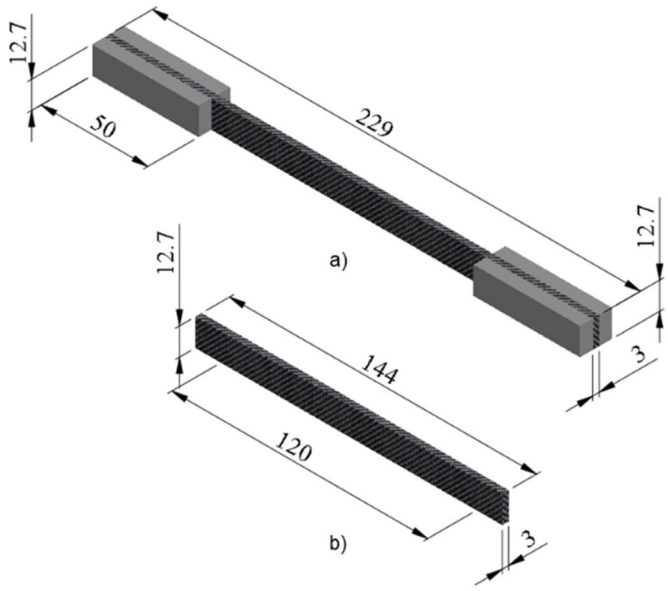


Fig. 1. Schematic representation of the specimen: a) tensile specimen with tabs and b) flexural specimen. (Dimensions in millimetres).

The printing process parameters used in this work are presented in Table 2 and were chosen based on the literature and some in-house laboratory trials and present a good relation between mechanical properties and production times [12,13,39]. The 3D printed parts were sliced with Simplify3D® and all specimens were fabricated in a flat-edge orientation. The number of contours ensures that the raster angle was always 0°. The configuration used is independent of the XY build orientation.

Table 2. The printing parameters used for the 3D printed parts.

Printing Parameters	**Value**
Nozzle diameter (mm)	0.40
Layer height (mm)	0.30
Raster width (mm)	0.44
Raster angle	0°
Infill %	100
Extruder temperature (C°)	250
Printing bed temperature (C°)	120
Printing speed (mm/s)	45
Number of contours	44

3.2.2.2. Composite specimens' fabrication

Different configurations were produced by using 1 or 2 layers of reinforcements on either side of the ABS and PLA printed part. A schematic representation of the specimen fabrication can be seen in Fig 2. The reinforcements (jute, curauá and glass fibre) were laminated to ABS and PLA core using the Hex Slow bicomponent epoxy resin. Prior to the fabrication process, the curauá fibres were immersed in distilled water for one hour and then rinsed with tap water and subsequently they were dried in an oven at 100 ºC for one hour. The other reinforcements used did not undertake any treatment. The curing process was done using metal plates and a small pressure was applied using a hotplate hydraulic press (SL 12, Solab, São Paulo) for 3h at 60 ºC. This process (compression moulding) ensures a flat surface and proper resin curing.

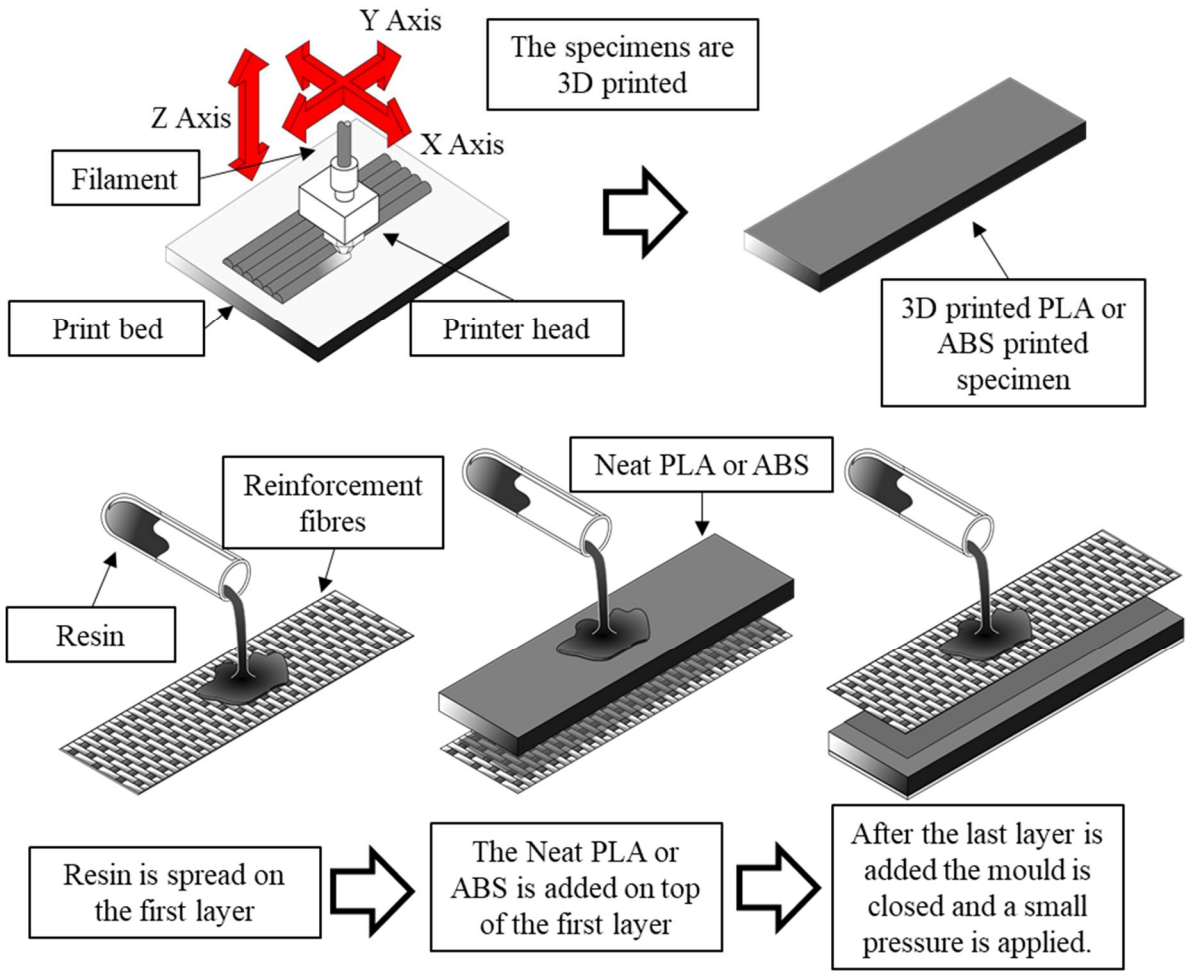


Fig. 2. Schematic representation of the specimen fabrication.

3.2.3. Test method

The tensile and flexural tests were carried out in an Instron®5966 (Norwood, Massachusetts, USA) universal testing machine. The tensile tests were performed with a crosshead speed of 2 mm/min using a 10 kN load cell (see Fig. 3). A 50 x 12.7 x 6 mm tab was used on both sides and extremity of the tensile specimens in order to ensure that the failure occurs in the proper area. For the flexural tests, a three-point bending rig with a span of 120 mm was used. A cross head speed of 1mm/min and a 1 kN load cell was used, as recommended by the ASTM D790 standard. Load-displacement curves were recorded for each case. A minimum of 5 specimens were tested for each case for both tensile and flexural tests. The nomenclature used in this study can be seen in Table 3.

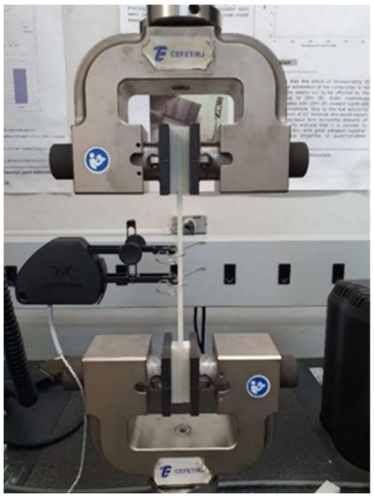


Fig. 3. Tensile test setup.

Table 3. Nomenclature of the specimens as a function of material and reinforcement.

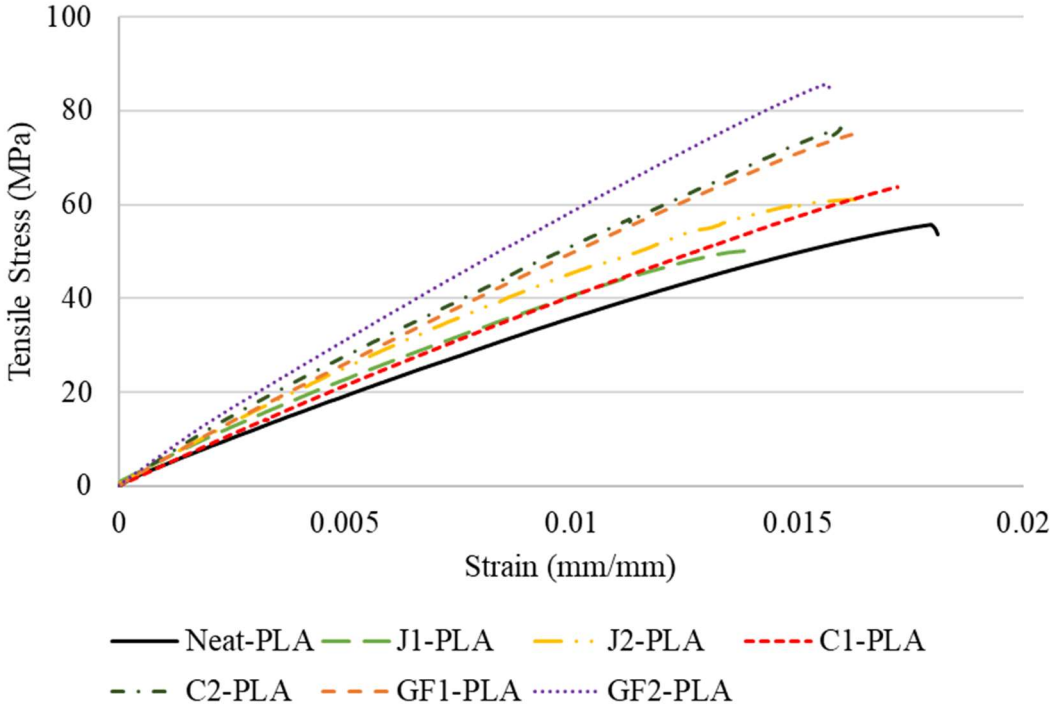
Reinforcement	PLA	ABS
Neat	Neat-PLA	Neat-ABS
Jute 1 layer	J1-PLA	J1-ABS
Jute 2 layer	J2-PLA	J2-ABS
Curauá 1 layer	C1-PLA	C1-ABS
Curauá 2 layer	C2-PLA	C2-ABS
Glass fibre 1 layer	GF1-PLA	GF1-ABS
Glass fibre 2 layer	GF2-PLA	GF2-ABS

3.3. RESULTS AND DISCUSSION

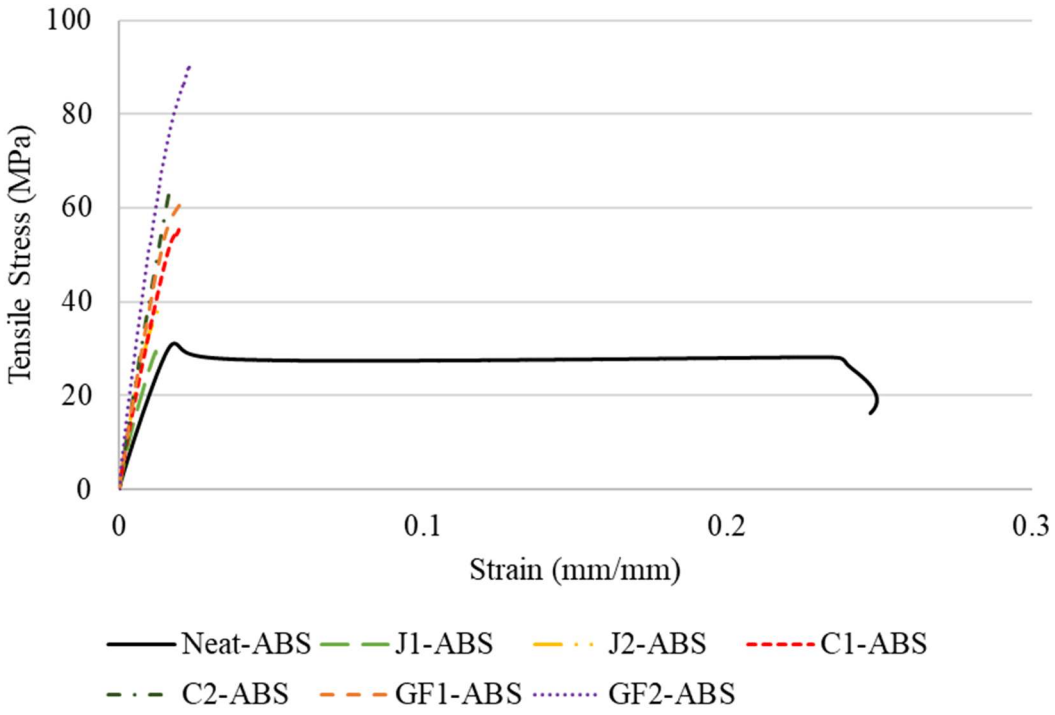
3.3.1. Tensile tests

The representative stress-strain curves obtained from the tensile tests as a function of material of additive manufactured parts and reinforcement can be seen in Fig. 4. It can be seen that the fibre reinforcement generally positively affected the tensile stress and stiffness of the reinforced PLA and ABS specimens. The only exception was the 1 layer jute-reinforced specimens which presented an negligible variation in tensile strength.

The tensile data (tensile strength, Young's modulus and elongation at break) was calculated from the stress-strain curves and the results are summarised in Table 4 and Fig. 5.



a)

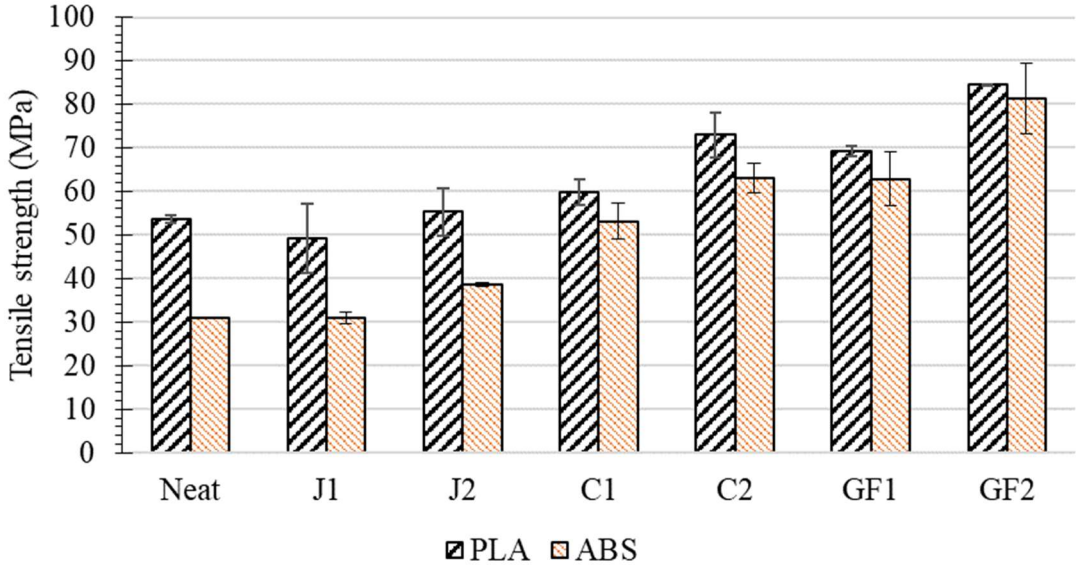


b)

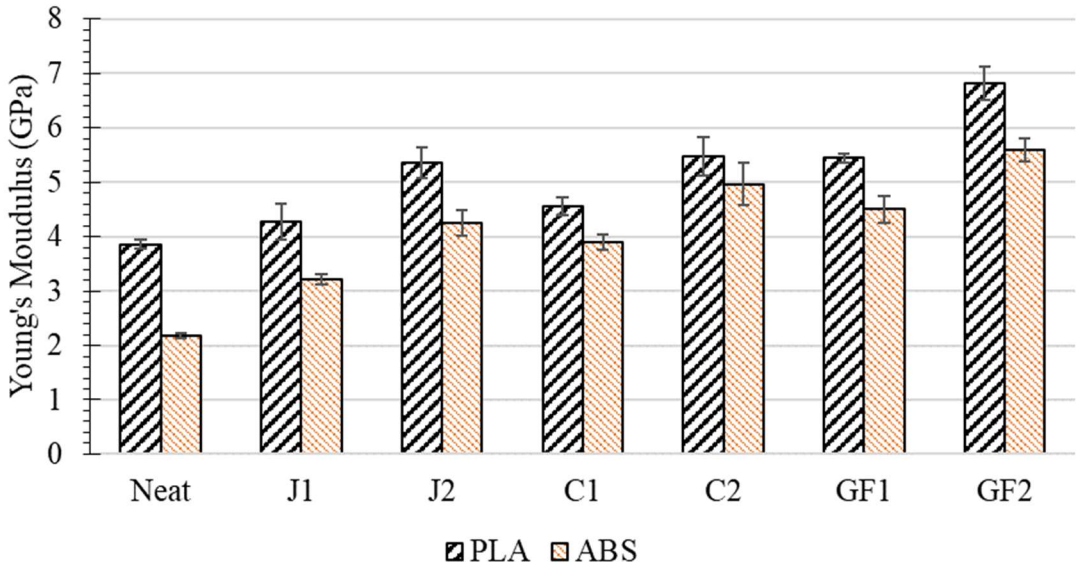
Fig. 4. Representative tensile stress-strain curves as a function of reinforcement: a) PLA and b) ABS.

Table 4. Tensile data of all composites as a function of material and reinforcement type.

Composite type	Tensile Strength (MPa)	Young's Modulus (GPa)	Strain (%)	Fibre weight (g)
Neat-PLA	51.88 ± 3.9	3.85 ± 0.08	2.18 ± 0.68	-
J1-PLA	49.22 ± 0.90	4.28 ± 0.33	1.41 ± 0.04	2.73 ± 0.09
J2-PLA	54.50 ± 7.58	5.27 ± 0.14	1.51 ± 0.12	5.25 ± 0.12
C1-PLA	59.95 ± 5.48	4.55 ± 0.16	1.57 ± 0.15	0.60 ± 0.05
C2-PLA	72.98 ± 2.94	5.48 ± 0.35	1.49 ± 0.08	1.2 0± 0.01
GF1-PLA	69.25 ± 5.23	5.44 ± 0.08	1.45 ± 0.16	1.61 ± 0.16
GF2-PLA	84.56 ± 1.11	6.82 ± 0.30	1.47 ± 0.09	3.13 ± 0.22
Neat-ABS	31.03 ± 0.11	2.18 ± 0.05	24.98 ± 0.10	-
J1-ABS	30.85 ± 1.30	3.21 ± 0.09	1.25 ± 0.04	2.82 ± 0.13
J2-ABS	38.65 ± 0.44	4.25 ± 0.24	1.25 ± 0.08	5.10 ± 0.10
C1-ABS	53.09 ± 4.11	3.90 ± 0.15	1.72 ± 0.31	0.59 ± 0.03
C2-ABS	63.05 ± 3.45	4.97 ± 0.40	1.53 ± 0.14	1.18 ± 0.05
GF1-ABS	62.86 ± 6.14	4.50 ± 0.25	2.12 ± 0.24	1.42 ± 0.08
GF2-ABS	81.33 ± 7.98	5.58 ± 0.21	1.94 ± 0.35	2.90 ± 0.18



a)



b)

Figure 5. Average values as a function of reinforcement type, a) Tensile strength and b) Young´s modulus.

For the PLA reinforced specimens, significant tensile strength enhancements were observed for all cases, when compared to the Neat-PLA, except for the J1-PLA which presented a slightly decrease in tensile strength. For the curauá fibre reinforced specimens the increase was by

approx. 15% for C1-PLA and approx. 36% for C2-PLA. Thus, a linear enhancement of tensile strength is obtained by increasing the layers. Similarly, when the synthetic-fibre reinforced PLA specimens are compared to the Neat-PLA, an almost linear tensile strength enhancements (approx. 29% and 58%) were reported as a function of increasing fibre weight (layers).

The stiffness of the PLA reinforced specimens also varied as a function of reinforcement fibres and number of layers, with increases in Young's modulus of approx. 11% (J1-PLA) to 77% (GF2-PLA) when compared to the Neat-PLA. The jute and glass fibre reinforced specimens presented a similar improvements in rigidity (~25%), while the curauá had a slightly lower variation (~20%), in terms of Young's modulus, when comparing the 1-layer and 2-layers reinforced PLA specimens are compared.

Finally, the PLA reinforced specimens presented a reduction in strain at failure with the addition of the reinforcement fibres. These reductions range from approx. 15% (J1-PLA) to 12% (GF2-PLA) when compared to the Neat-PLA. The addition of subsequent layers had negligible effect in the PLA reinforced specimen's strain at failure.

The tensile characteristics observed are due to the reinforcement fibre and the printed core material properties as well as the core/reinforced epoxy multi-material interface. The core material properties will ultimately dictate failure. A strong and stiff material such as the PLA, will fail at a high load and low strain at failure. On the other hand, the reinforcement fibre and matrix properties will rule the stress state at the multi-material interface. A significant mismatch between the printed core and reinforcement fibre/matrix properties will lead to a considerable stress state asymmetry and concentration at the interface [40]. For instance, the jute fibre presents a lower ductility when compared to the PLA core [12,41]. This leads to little tensile property variation as a function of fibre layers, especially strength, since the natural fibres will begin to fail prior to the core material. Moreover, this was not observed for the curauá and the glass fibre-reinforced PLA specimens, where both fibres present higher ductility when compared to the core material.

For the ABS reinforced specimens, significant improvements in tensile strength were reported for all specimens when compared to the Neat-ABS, except for the J1-ABS which presented no significant variation. Also, a tendency of considerable tensile strength enhancement as a function of fibre layers was reported for all specimens. The J2-ABS presented an increase in tensile strength of approx. 25% when compared to J1-ABS, the C2-ABS presented an increase of approx. 19% when compared to C1-ABS, while the glass reinforced ABS specimens showed an increase of approx. 29%.

Young's modulus also benefited from the addition of reinforcement layers, with increases of approx. 48% (J1-ABS) to 157% (GF2-ABS), when compared to the Neat-ABS. All ABS fibre-reinforced specimens presented enhanced stiffness with the addition of subsequent reinforcement layers. For example, the J2-ABS specimens exhibited an improvement of approx. 32% when compared to the J1-ABS. On the other hand, the GF2-ABS specimens presented an enhancement of approx. 24% when compared to the GF1-ABS.

The strain at failure was considerably influenced by the fibre reinforcements, presenting reductions ranging from approx. 95% (J1-ABS) to 91% (GF1-ABS) when compared to the Neat-ABS. The addition of subsequent layers of reinforcement fibres had no significant impact in the strain at failure (see Table 4).

The behaviour seen in the ABS fibre reinforced specimens can also be explained by the reinforcement fibres properties. The Neat-ABS presented lower tensile strength (~42%) and rigidity (~43%) than the Neat-PLA, and the reinforcement fibres tend to dominate the tensile properties of the reinforced specimens when their tensile properties are higher than the core. Thus, the jute fibres had a larger positive impact in the ABS reinforced specimens than in the PLA. Furthermore, the curauá fibres present higher tensile strength and rigidity than the jute fibre [41], diminishing the effects the core has on the specimen. This is further confirmed by the small difference in tensile strength between the C1-PLA and C1-ABS (~13%) and the insignificant differences between GF2-PLA and GF2-ABS.

In general, the tensile strength found in this study for the best case (84.56 ± 1.11 for the GF2-PLA specimens) was higher compared to the values found in the literature. For instance, Heidari-Rarani et al. [42] found values of 61.4 ± 2.1 MPa and 8.28 ± 0.56 GPa for tensile strength and modulus, respectively, for continuous carbon fibre reinforced PLA composite. The use of Poly vinyl alcohol (PVA) as a surface treatment for the carbon fibres presented a positive impact in both tensile and flexural properties of the 3D printed specimens. However, in line with what was found in the present work, even with prior surface treatment, it was found that the dominant failure mode was delamination and delamination-induced-matrix cracking [42].

The ABS core composites also consistently presented higher or similar values to values found in the literature. Galatas et al. [17], used a similar methodology (the lamination of fibre reinforced layers on to a 3D printed ABS core) and found that the carbon fibre reinforced ABS (CFRP/ABS/CFRP) presented improved specific strength and elastic modulus with increasing the number of CFRP (i.e. for 3 layers of CFRP, 93.2 ± 2.6 MPa for the tensile strength while for Young's modulus values of 10.2 ± 0.52 GPa, were found). The authors also, reported delamination as the common failure mode for the reinforced ABS specimens [17]. The trends

in tensile properties found in the literature can be explained by the different fabrication methodologies and printing parameters used. For example, variations in infill density, raster angle and direction were shown to be very significant regarding the final material properties [39].

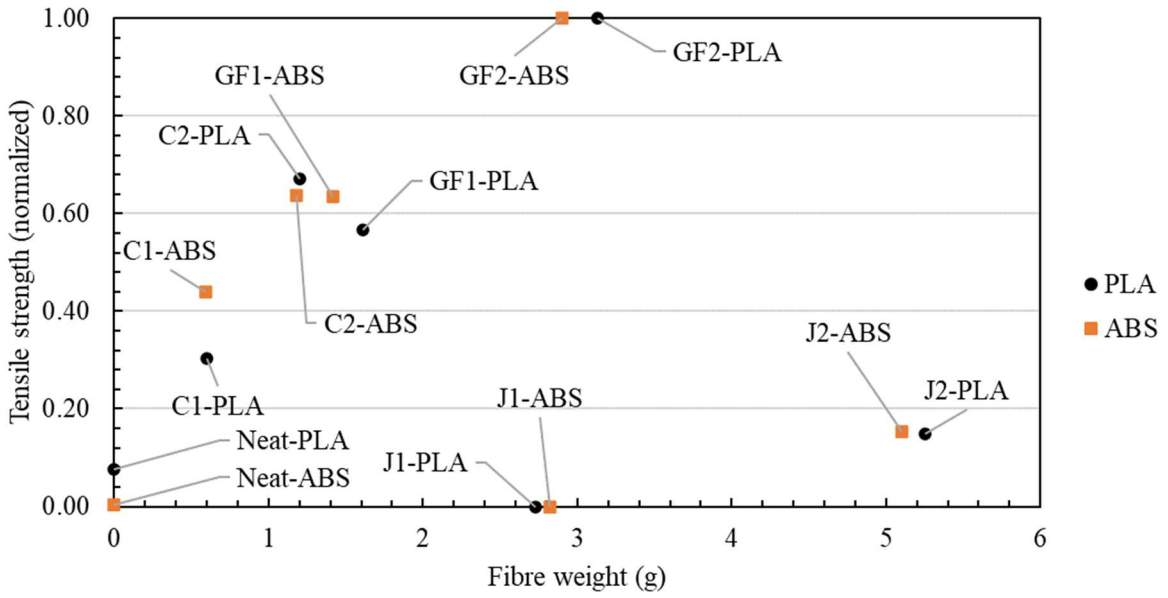
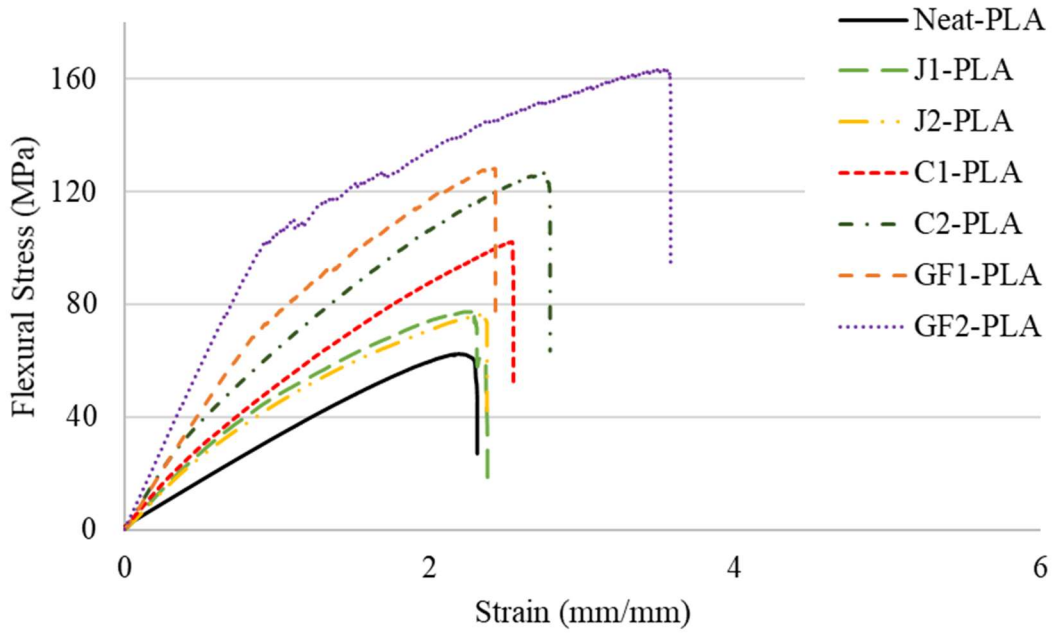


Fig. 6. Normalized (min-max scaling) tensile strength as a function of fibre weight.

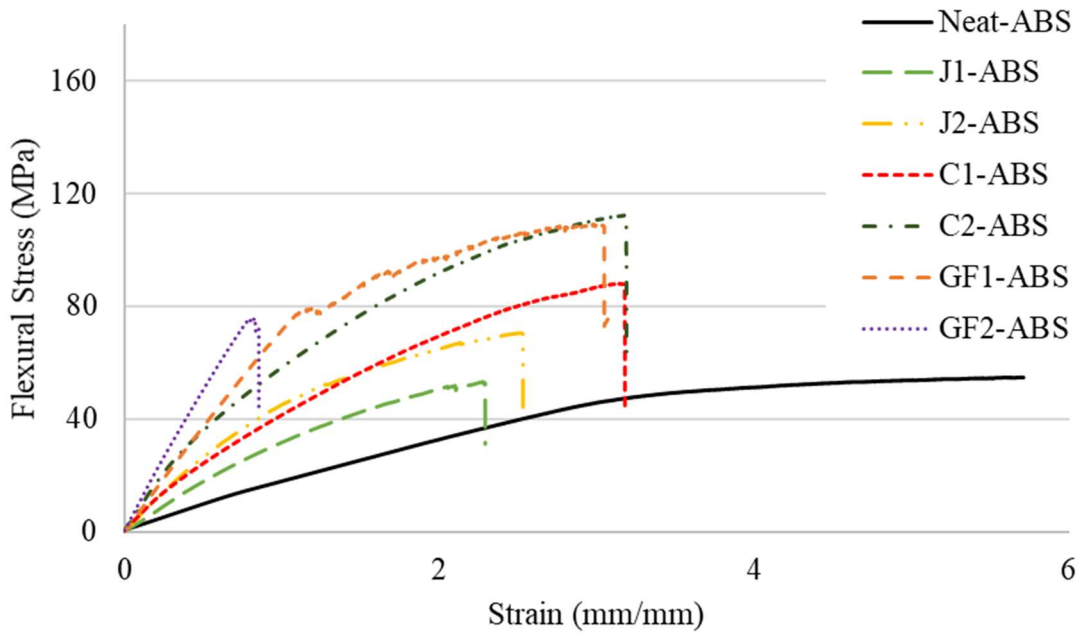
Figure 6 presents the normalized (min-max scaling) tensile strength as a function of fibre weight, where the 0 and 1 on the y axis represent the lowest and highest values for the PLA and ABS groups, respectively. Therefore, the ideal strength to weight ratio is in the upper left area of the graph, having the highest tensile strength with the lowest possible fibre weight. It can be seen that the PLA reinforced specimens did not present a proportional increase in tensile strength in relation to the number of layers. For instance, the jute reinforced specimens presented little tensile strength gain for each layer. The curauá reinforced specimens displayed an increase in tensile strength per fibre weight, where the C2-PLA presented similar tensile strength to the GF1-PLA, but with approx. 25% lower fibre weight. This is mainly due to similar curauá and glass fibre tensile properties, as found in a previous study [41]. The ABS reinforced specimens had analogous behaviour to the PLA reinforced specimens, as related to the strength gain per fibre weight. The C2-ABS, again, presented tensile strength values similar to the GF1-ABS, but with a reduction of approx. 17% in weight.

3.3.2. Flexural tests

The stress-strain representative curves obtained from the flexural tests as a function of material and reinforcement can be seen in Fig. 7. The flexural data (flexural strength and flexural modulus) was calculated from the stress-strain curves and the results are summarised in Table 5 and Fig. 8.



a)

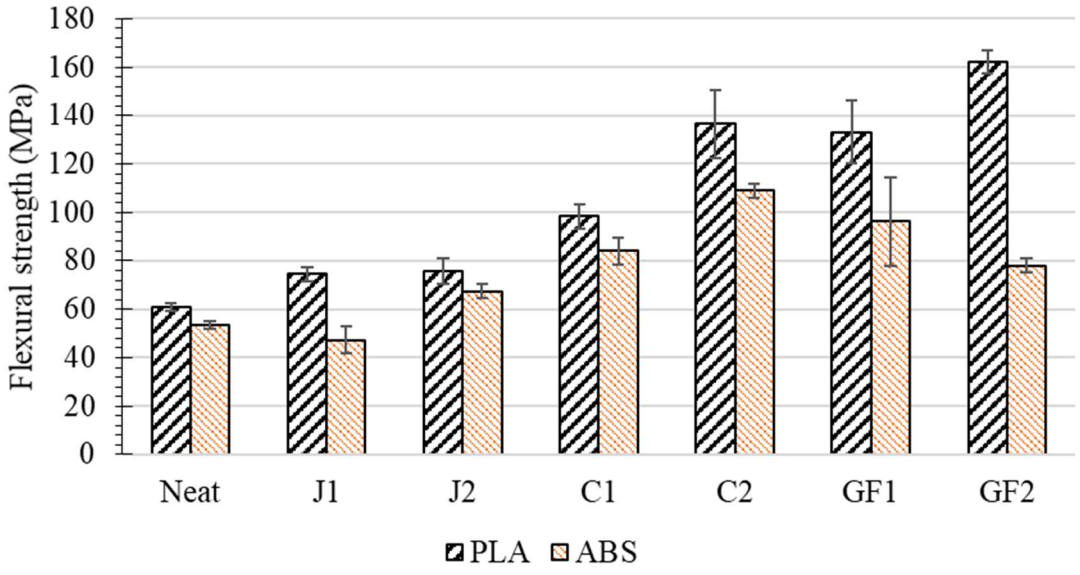


b)

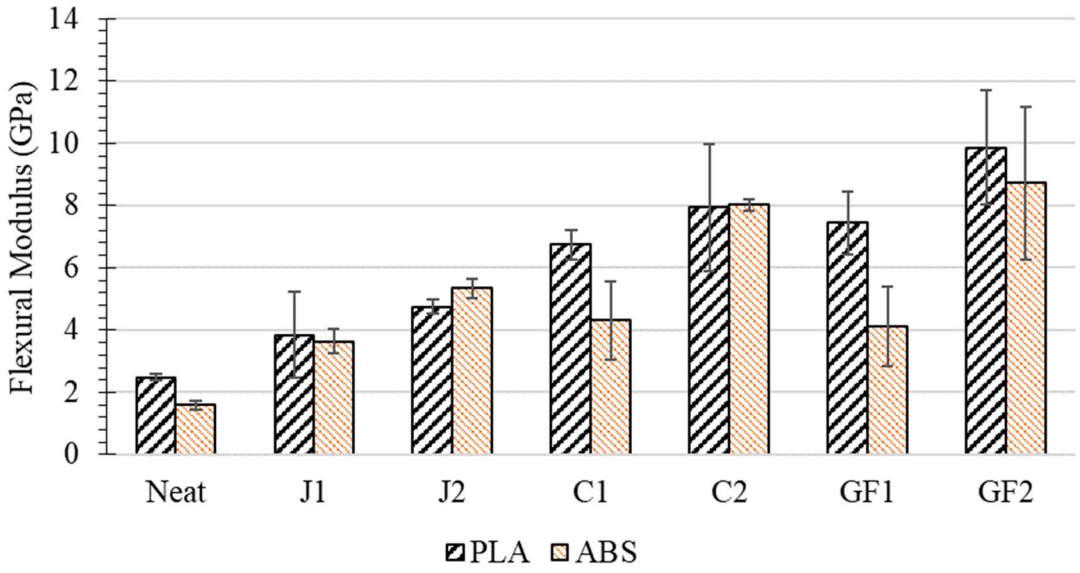
Fig. 7. Representative flexural stress-strain curve as a function of reinforcement: a) PLA and b) ABS.

Table 5. Flexural data of all composites as a function of core material and reinforcement type.

Composite type	**Flexural Strength (MPa)**	**Flexural Modulus (GPa)**
Neat-PLA	60.85 ± 1.57	2.49 ± 0.09
J1-PLA	74.47 ± 3.11	3.85 ± 1.37
J2-PLA	75.88 ± 5.42	4.76 ± 0.21
C1-PLA	98.35 ± 5.06	6.74 ± 0.48
C2-PLA	136.56 ± 14.10	7.95 ± 2.05
GF1-PLA	133.18 ± 13.02	7.44 ± 0.99
GF2-PLA	162 ± 4.89	9.86 ± 1.83
Neat-ABS	53.32 ± 1.54	1.60 ± 0.15
J1-ABS	47.30 ± 5.59	3.64 ± 0.38
J2-ABS	67.33 ± 2.91	3.82 ± 2.65
C1-ABS	84.09 ± 5.56	4.31 ± 1.27
C2-ABS	108.93 ± 3.05	8.02 ± 0.18
GF1-ABS	96.32 ± 18.24	4.12 ± 1.27
GF2-ABS	78.06 ± 3.02	8.72 ± 2.44



a)



b)

Fig. 8. Average flexural properties as a function of reinforcement type: a) flexural strength; b) flexural modulus.

From Table 5 and Fig. 8, it can be seen that the fibre reinforcement generally positively affected the flexural properties of the reinforced PLA specimens. When compared to the Neat-PLA, all the fibre reinforced PLA specimens presented considerably enhanced flexural strength. The improvements increased as a function of reinforcement fibre (going from jute to curauá to glass, from lowest to highest, respectively). Furthermore, the effect of increasing the fibre layers

presented a similar trend to that observed for the tensile strength. The jute reinforced specimens presented no significant variation, while both the curauá and glass reinforced specimens presented a trend of considerable flexural strength enhancement as a function of fibre layers. For example, C1-PLA displayed an enhancement in flexural strength of approx. 62%, while for the C2-PLA an increase of approx. 124% in flexural strength when compared to Neat-PLA (roughly a linear property variation as a function of fibre layers) was found. The G1-PLA displayed an enhancement of approx. 119% in flexural strength when compared to Neat-PLA, while the GF2-PLA approx. 166%.

The flexural modulus presented a trend of enhancement when the fibre reinforced PLA specimens are compared to the Neat-PLA in an almost linear fashion, up to the C2-PLA/GF1-PLA specimens. These specimens presented no significant variation in flexural stiffness. The highest improvement in flexural modulus was reported for the GF2-PLA, when compared to Neat-PLA (~296%). A progressive enhancement in flexural modulus was seen for all fibre reinforced PLA specimens with increasing fibre layers. The jute and curauá reinforced specimens presented a similar improvement in flexural rigidity (i.e., ~24% for the jute and ~18% for the curauá), while the glass fibre had a higher variation (~33%), when 2-layer specimens are compared to the single layer ones. The increase in layers also resulted in a growth of flexural strength in all specimens, except for the jute, where no significant increase in properties was seen (i.e., when the 2-layer specimens are compared to the single layers ones). For the curauá fibre reinforced specimens, this increase was more expressive (~39%) than the one seen for the glass fibre (~22%).

The literature is scarce, and few results have been reported for flexural properties of materials with similar fabrication techniques. For example, Heidari-Rarani et al. [42] used continuous carbon fibre reinforcements with PLA (CCFR-PLA) in a custom 3D printer and found values of 152.1 ± 2.2 MPa and 13.42 ± 0.31 GPa for flexural strength and modulus, respectively. It is interesting to note that the C2-PLA (136.56 ± 14.10 for flexural strength and 7.95 ± 2.05 for flexural modulus) specimens produced in this study, present great potential in this context, especially given the inherent carbon footprint reduction afforded by the natural fibres.

For ABS reinforced specimens, the flexural strength is also improved by adding the fibre reinforcements. However, the enhancement linked to fibre weight was not observed for the synthetic fibre reinforced specimens. Specifically, the curauá reinforced specimens displayed flexural strength improvement when compared to the Neat-ABS, in an almost linear fashion. However, for the glass reinforced ABS, a decrease in flexural strength is observed when the reinforcement layers are increased. This is likely linked to the resin/ABS interface and how the

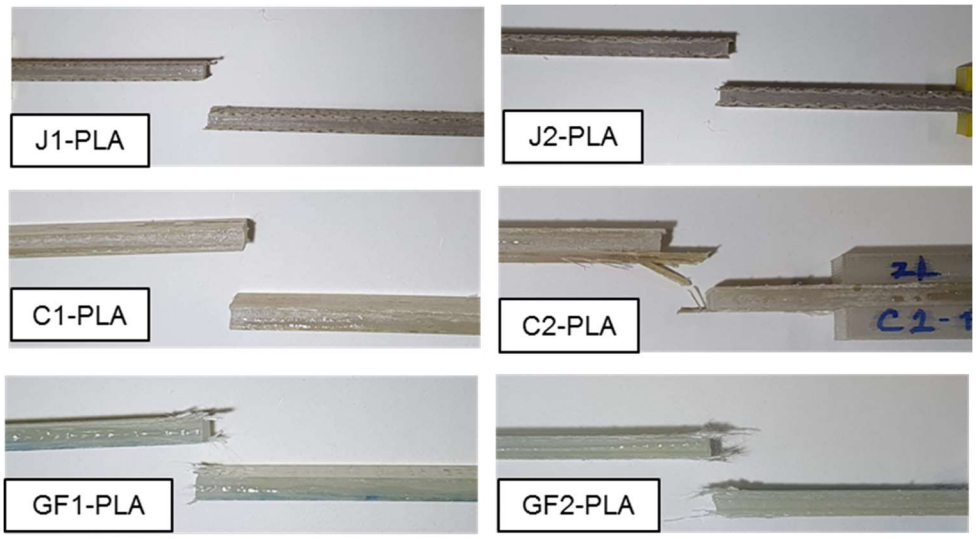
critical debonding and buckling stresses [43] may be considerably affected by an increase in stiffness (see section 4).

The flexural modulus of the ABS specimens was improved by the addition of all fibre reinforcements. For instance, increases of approx. 128% (J1-ABS) to approx. 446% (GF2-ABS) in flexural stiffness were observed when compared to Neat-ABS. The increase in number of fibre layers also enhanced the flexural modulus of the specimens (the jute composite presented an increase of approx. 47%, while the curauá fibre specimens presented an increase of approx. 86%, when the 2-layer specimens are compared to the single layer ones). Furthermore, the highest increase displayed was for the glass fibre reinforced specimens at approx. 111%. This is linked to the effect of the fibre properties in the reinforced specimen, where an increase in layers generates an increase in stiffness.

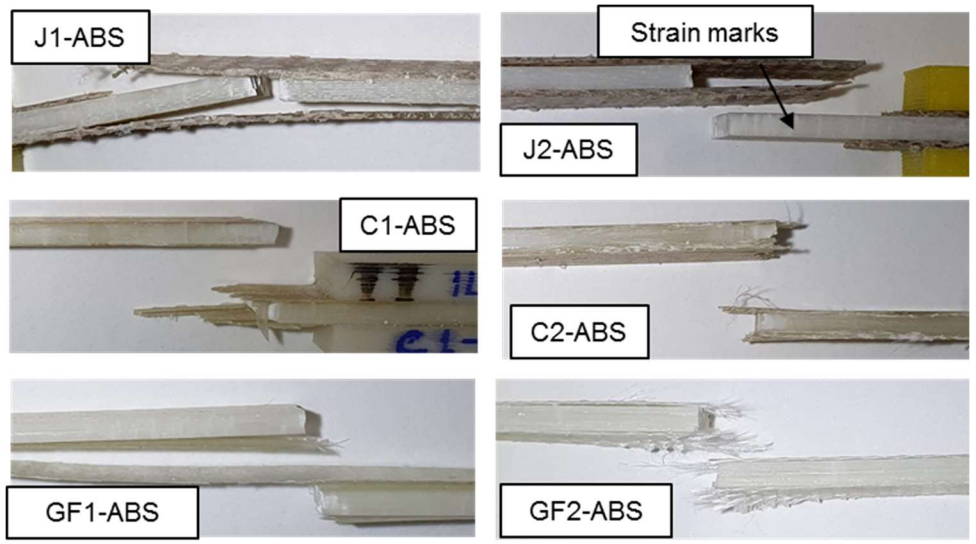
To summarise, the flexural properties of the fibre reinforced PLA and ABS specimens were affected by fibre type and number of layers. Generally, the flexural strength and stiffness increased in an almost linear fashion as a function of increasing the fibre properties (i.e., from jute to curauá and finally glass) as well as higher reinforcement fibre weight (layers).

3.3.3. Fracture analysis

The fractured specimens were visually examined after each test. Representative failure modes can be seen in Fig. 9. The fracture analysis of the composites shows two distinct behaviours in accordance with the core material. The PLA reinforced specimens presented a clearly brittle behaviour with little to no delamination between the fibre reinforcement and the PLA core, while the ABS reinforced specimens presented mostly delamination of the fibre layer, with a brittle core failure on some occasions. For both materials core breakage occurred after fibre failure.



a)



b)

Fig. 9. Images of the fractured tensile specimens: a) PLA; b) ABS.

The PLA reinforced specimens presented better interfacial adhesion with all reinforcements used, therefore most failures occurred first in the reinforcing fibre, followed by the PLA core with little to no delamination (see Fig. 9a).

From Fig. 9b it can be seen that the ABS reinforced specimens showed signs of elongation in the core (stain marks and coloration change on its surface) followed by the delamination of the reinforcing layer. Catastrophic core failure was observed after reinforcement breakage. It should be noted that, in all ABS cases, some form of delamination occurred. However, for the curauá fibre reinforced specimens (C1-ABS), delamination was less prominent, and the failure was similar to the one seen in the glass fibre reinforced specimens (GF1-ABS). A similar behaviour was seen in the literature. For example, Galatas et al. [17] studied ABS printed parts

reinforced with carbon fibre and found that failure occurred within the reinforcing layer before it propagated to the core.

Photos of representative PLA and ABS fractured flexural specimens are presented in Fig. 10. It can be seen that the PLA reinforced specimens presented better interaction (adhesion) with the fibre reinforced layer compared to the ABS reinforced specimens. All PLA specimens presented fibre and core breakage in the bottom side, while little to no fibre buckling was seen in the top side of the specimen. However, some delamination was seen in the natural fibre reinforced specimens (Fig 10a and Fig. 10c). Finally, for glass fibre reinforced specimens compressive damage was also seen (Fig. 10e).

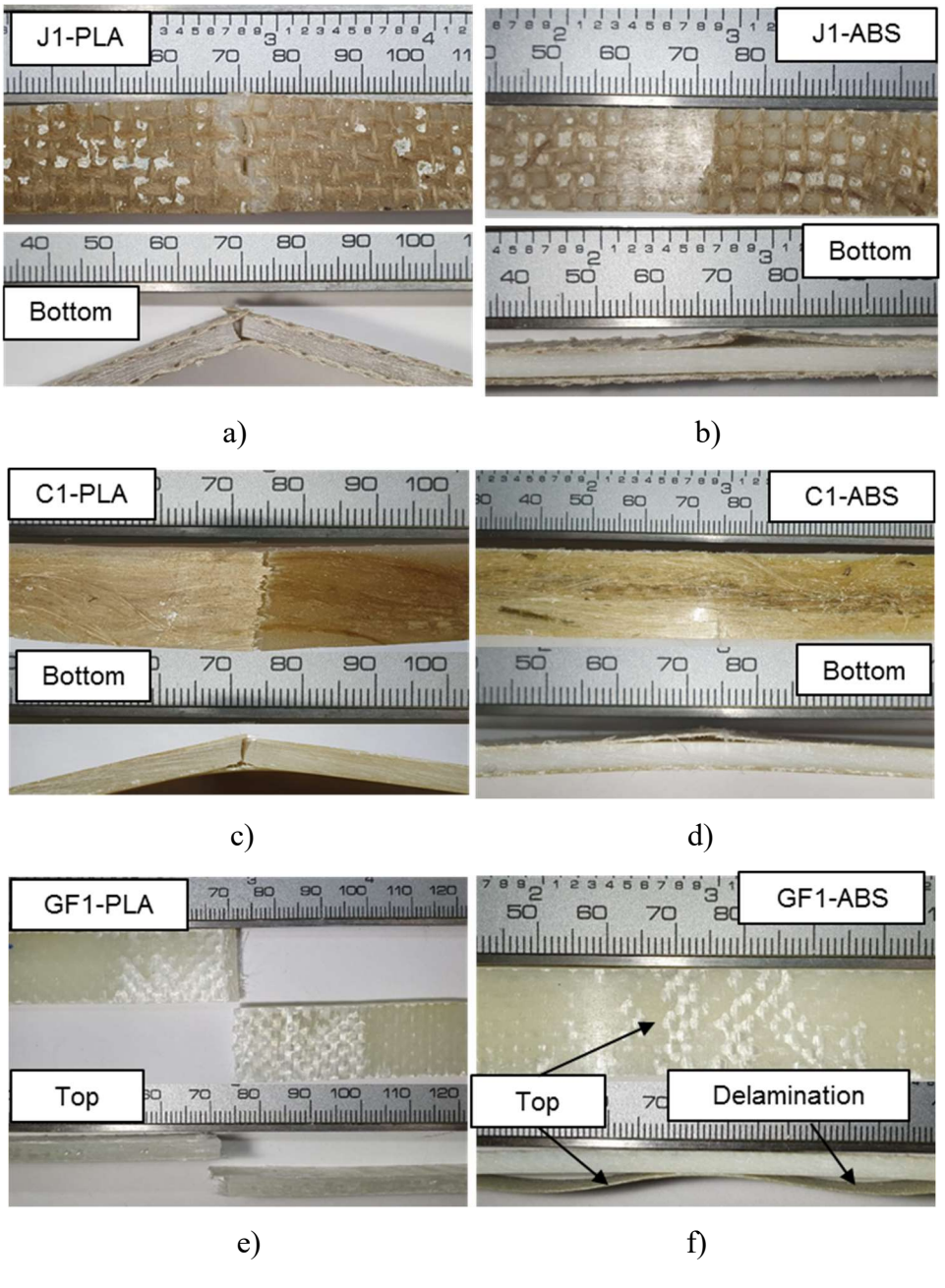


Fig. 10. Images of representative PLA and ABS fractured flexural specimens: a) J1-PLA, b) J1-ABS, c) C1-PLA, d) C1-ABS, e) GF1-PLA, f) GF1-ABS.

The ABS specimens presented clear delamination in all cases with the exception to the jute fibre reinforced specimens (Fig. 10b). This can be explained by the fact that the jute reinforcement has a lower tensile strength and suffers mainly brittle failure. A similar failure mode was seen for both ABS glass fibre reinforced specimens (GF1-ABS and GF2-ABS), where significant fibre buckling was observed. Furthermore, substantial delamination due to compressive loads can be noted (Fig. 10f). The natural fibre reinforced specimens did not present major fibre bucking before failure. From Fig. 10c and d, it can be seen that both the jute and curauá specimens presented fibre and delamination failures on the bottom side of the specimens. The number of layers did not significantly impact specimens' failure modes and for this reason only I layer reinforced specimens are showed in Fig. 10. Gohar et al. [30] also observed a similar behaviour with sandwich ABS core reinforced with composite material face sheets, where the delamination was the main failure mode seen in flexural tests. They state that the failure was mainly due to the low interfacial strength between the carbon fibre layer and core. The contact angle analysis of the ABS material was show to be approx. 118 degrees [43], which indicates poor wettability. Therefore, the fracture observed in this study for the ABS reinforced specimens seen are in line with the current literature.

3.4. CONCLUSIONS

In this work, the effect of fibre reinforcement on the mechanical properties of AM polymeric parts (PLA and ABS) was investigated. Natural (jute and curauá) and synthetic (glass) fibre (1 and 2-layers) were laminated on the outer sides of the AM parts by using an epoxy resin via compression moulding. The following conclusions can be drawn:

- In general, adding of fibre reinforcements to the 3D printed parts promoted an increase in mechanical properties and a reduction in elongation.
- The mechanical properties of the PLA and ABS reinforced specimens varied as a function of reinforced material (fibre type and number of layers). Generally, the properties of reinforced AM specimens increased as a function of increasing the fibre properties (i.e., from jute to curauá and finally glass) as well as higher reinforcement fibre weight (layers). The glass fibre reinforced specimens presented better mechanical properties when compared to the natural fibre reinforced AM parts. However, the curauá fibre reinforced specimens presented improved performance when compared to the jute

composites and matched the mechanical properties of the 1-layer glass fibre reinforced specimens.

- The type of the material of 3D printed cores affected the mechanical properties of the reinforced 3D printed specimens. The PLA reinforced specimens presented higher tensile and flexural properties compared to ABS reinforced specimens. This is mainly due to two factors: the PLA's higher mechanical properties when compared to the ABS, and the better interfacial interaction/adhesion between the resin and 3D printed core. The ABS core composites presented an increase in mechanical properties in spite of apparent low interfacial strength. The use of chemical and thermal surface treatments can further increase the mechanical properties of ABS fibre reinforced specimens.
- The curauá fibres can be a promising substitute to the glass fibres, especially when considering the strength to weight ratio of both fibres. The C2 composites had similar properties to the GF1, but with a significant mass reduction (the C2-PLA and C2-ABS had a reduction of approx. 25% and 17% in specimen weight for a variation of less than 6% in tensile strength when compared to the GF1-PLA and GF1-ABS).
- Strengthening of additive manufactured parts by using different type of fibre reinforcements is a promising innovation in order to improve their mechanical properties and these improvements might enable these materials to serve for high load bearing purposes.

REFERENCES

1. Baca Lopez DM, Ahmad R (2020) Tensile Mechanical Behaviour of Multi-Polymer Sandwich Structures via Fused Deposition Modelling. Polymers 12 (3):651

2. Harris M, Potgieter J, Archer R, Arif KM (2019) Effect of Material and Process Specific Factors on the Strength of Printed Parts in Fused Filament Fabrication: A Review of Recent Developments. Materials 12 (10):1664

3. Abdulhameed O, Al-Ahmari A, Ameen W, Mian SH (2019) Additive manufacturing: Challenges, trends, and applications. Advances in Mechanical Engineering 11 (2):1687814018822880. doi:10.1177/1687814018822880

4. Bandyopadhyay A, Heer B (2018) Additive manufacturing of multi-material structures. Materials Science and Engineering: R: Reports 129:1-16. doi:https://doi.org/10.1016/j.mser.2018.04.001

5. Lalehpour A, Janeteas C, Barari A (2018) Surface roughness of FDM parts after post-processing with acetone vapor bath smoothing process. The International Journal of Advanced Manufacturing Technology 95 (1):1505-1520. doi:10.1007/s00170-017-1165-5

6. Wu H, Fahy WP, Kim S, Kim H, Zhao N, Pilato L, Kafi A, Bateman S, Koo JH (2020) Recent developments in polymers/polymer nanocomposites for additive manufacturing. Progress in Materials Science 111:100638. doi:https://doi.org/10.1016/j.pmatsci.2020.100638

7. Parandoush P, Lin D (2017) A review on additive manufacturing of polymer-fiber composites. Composite Structures 182:36-53. doi:https://doi.org/10.1016/j.compstruct.2017.08.088

8. Ning F, Cong W, Hu Y, Wang H (2017) Additive manufacturing of carbon fiber-reinforced plastic composites using fused deposition modeling: Effects of process parameters on tensile properties. Journal of Composite Materials 51 (4):451-462. doi:10.1177/0021998316646169

9. McIlroy C, Olmsted PD (2017) Disentanglement effects on welding behaviour of polymer melts during the fused-filament-fabrication method for additive manufacturing. Polymer 123:376-391. doi:https://doi.org/10.1016/j.polymer.2017.06.051

10. Weng Z, Wang J, Senthil T, Wu L (2016) Mechanical and thermal properties of ABS/montmorillonite nanocomposites for fused deposition modeling 3D printing. Materials & Design 102:276-283. doi:https://doi.org/10.1016/j.matdes.2016.04.045

11. Wang X, Jiang M, Zhou Z, Gou J, Hui D (2017) 3D printing of polymer matrix composites: A review and prospective. Composites Part B: Engineering 110:442-458. doi:https://doi.org/10.1016/j.compositesb.2016.11.034

12. Cavalcanti DKK, Banea MD, de Queiroz HFM (2019) Mechanical characterization of bonded joints made of additive manufactured adherends. Annals of "Dunarea de Jos" University of Galati, Fascicle XII, Welding Equipment and Technology 30:27-33. doi:10.35219/awet.2019.04

13. Cavalcanti DKK, Banea MD, de Queiroz HFM (2020) Effect of material on the mechanical properties of additive manufactured thermoplastic parts. Annals of "Dunarea de Jos" University of Galati, Fascicle XII, Welding Equipment and Technology 31:5-12. doi:10.35219/awet.2020.01

14. Caminero MÁ, Chacón JM, García-Plaza E, Núñez PJ, Reverte JM, Becar JP (2019) Additive Manufacturing of PLA-Based Composites Using Fused Filament Fabrication: Effect of Graphene Nanoplatelet Reinforcement on Mechanical Properties, Dimensional Accuracy and Texture. Polymers 11 (5):799

15. Dul S, Fambri L, Pegoretti A (2016) Fused deposition modelling with ABS–graphene nanocomposites. Composites Part A: Applied Science and Manufacturing 85:181-191. doi:https://doi.org/10.1016/j.compositesa.2016.03.013

16. Falck R, Goushegir SM, dos Santos JF, Amancio-Filho ST (2018) AddJoining: A novel additive manufacturing approach for layered metal-polymer hybrid structures. Materials Letters 217:211-214. doi:10.1016/j.matlet.2018.01.021

17. Galatas A, Hassanin H, Zweiri Y, Seneviratne L (2018) Additive manufactured sandwich composite/ABS parts for unmanned aerial vehicle applications. Polymers 10 (11):1262

18. Ivanov E, Kotsilkova R, Xia H, Chen Y, Donato RK, Donato K, Godoy AP, Di Maio R, Silvestre C, Cimmino S, Angelov V (2019) PLA/Graphene/MWCNT Composites with Improved Electrical and Thermal Properties Suitable for FDM 3D Printing Applications. Applied Sciences 9 (6):1209

19. Justo J, Távara L, García-Guzmán L, París F (2018) Characterization of 3D printed long fibre reinforced composites. Composite Structures 185:537-548. doi:https://doi.org/10.1016/j.compstruct.2017.11.052

20. Melnikova R, Ehrmann A, Finsterbusch K (2014) 3D printing of textile-based structures by Fused Deposition Modelling (FDM) with different polymer materials. IOP Conference Series: Materials Science and Engineering 62:012018. doi:10.1088/1757-899x/62/1/012018

21. Yamamoto BE, Trimble AZ, Minei B, Ghasemi Nejhad MN (2018) Development of multifunctional nanocomposites with 3-D printing additive manufacturing and low graphene loading. Journal of Thermoplastic Composite Materials 32 (3):383-408. doi:10.1177/0892705718759390

22. Sugiyama K, Matsuzaki R, Ueda M, Todoroki A, Hirano Y (2018) 3D printing of composite sandwich structures using continuous carbon fiber and fiber tension. Composites Part A: Applied Science and Manufacturing 113:114-121. doi:https://doi.org/10.1016/j.compositesa.2018.07.029

23. Mohamed OA, Masood SH, Bhowmik JL (2015) Optimization of fused deposition modeling process parameters: a review of current research and future prospects. ADVANCES IN MANUFACTURING 3 (1):42-53. doi:10.1007/s40436-014-0097-7

24. Calles AF, Carou D, Ferreira RTL (2022) Experimental Investigation on the Effect of Carbon Fiber Reinforcements in the Mechanical Resistance of 3D Printed Specimens. Applied Composite Materials 29 (3):937-952. doi:10.1007/s10443-021-09996-7

25. Kong X, Luo J, Luo Q, Li Q, Sun G (2022) Experimental study on interface failure behavior of 3D printed continuous fiber reinforced composites. Additive Manufacturing 59:103077. doi:https://doi.org/10.1016/j.addma.2022.103077

26. Shanmugam V, Pavan MV, Babu K, Karnan B Fused deposition modeling based polymeric materials and their performance: A review. Polymer Composites n/a (n/a). doi:https://doi.org/10.1002/pc.26275

27. Yang C, Tian X, Liu T, Cao Y, Li D (2017) 3D printing for continuous fiber reinforced thermoplastic composites: mechanism and performance. Rapid Prototyping Journal 23 (1):209-215. doi:10.1108/RPJ-08-2015-0098

28. Dickson AN, Abourayana HM, Dowling DP (2020) 3D Printing of Fibre-Reinforced Thermoplastic Composites Using Fused Filament Fabrication—A Review. Polymers 12 (10):2188

29. Zhang Z, Long Y, Yang Z, Fu K, Li Y (2022) An investigation into printing pressure of 3D printed continuous carbon fiber reinforced composites. Composites Part A: Applied Science and Manufacturing 162:107162. doi:https://doi.org/10.1016/j.compositesa.2022.107162

30. Gohar S, Hussain G, Ali A, Ahmad H Mechanical performance of honeycomb sandwich structures built by FDM printing technique. Journal of Thermoplastic Composite Materials 0 (0):0892705721997892. doi:10.1177/0892705721997892

31. Jin Y-a, Plott J, Chen R, Wensman J, Shih A (2015) Additive Manufacturing of Custom Orthoses and Prostheses – A Review. Procedia CIRP 36:199-204. doi:https://doi.org/10.1016/j.procir.2015.02.125

32. Maroti P, Varga P, Abraham H, Falk G, Zsebe T, Meiszterics Z, Mano S, Csernatony Z, Rendeki S, Nyitrai M (2018) Printing orientation defines anisotropic mechanical properties in additive manufacturing of upper limb prosthetics. Materials Research Express 6 (3):035403. doi:10.1088/2053-1591/aaf5a9

33. Neto J, Queiroz H, Aguiar R, Lima R, Cavalcanti D, Banea M-D (2022) A Review of Recent Advances in Hybrid Natural Fiber Reinforced Polymer Composites. Journal of Renewable Materials 10 (3):561--589

34. Le Duigou A, Correa D, Ueda M, Matsuzaki R, Castro M (2020) A review of 3D and 4D printing of natural fibre biocomposites. Materials & Design 194:108911. doi:https://doi.org/10.1016/j.matdes.2020.108911

35. de Queiroz HFM, Banea MD, Cavalcanti DKK (2021) Adhesively bonded joints of jute, glass and hybrid jute/glass fibre-reinforced polymer composites for automotive industry. Applied Adhesion Science 9 (1). doi:10.1186/s40563-020-00131-6

36. Cavalcanti DKK, Banea MD, Neto JSS, Lima RAA, da Silva LFM, Carbas RJC (2019) Mechanical characterization of intralaminar natural fibre-reinforced hybrid composites. Composites Part B: Engineering 175:107149. doi:https://doi.org/10.1016/j.compositesb.2019.107149

37. de Queiroz HFM, Banea MD Methods to increase the mechanical performance of composite adhesive joints: An overview with focus on joints with natural fibre composite adherends. Journal of Composite Materials 0 (0):00219983221125906. doi:10.1177/00219983221125906

38. Fabio T, Thais H, Kestur G (2007) Studies on lignocellulosics fibre of Brazil. Part II: Morphology and properties of Brazilian coconut fibre. Composites: Part A 38:1710-1721

39. Wang L, Sanders JE, Gardner DJ, Han Y (2018) Effect of fused deposition modeling process parameters on the mechanical properties of a filled polypropylene. Progress in Additive Manufacturing 3 (4):205-214. doi:10.1007/s40964-018-0053-3

40. Fernandes Medeiros de Queiroz H, Banea MD, Kioshi Kawasaki Cavalcanti D, de Souza e Silva Neto J (2021) The effect of multiscale hybridization on the mechanical properties of natural fiber-reinforced composites. Journal of Applied Polymer Science 138 (41):51213. doi:https://doi.org/10.1002/app.51213

41. de Araujo Alves Lima R, Kawasaki Cavalcanti D, de Souza e Silva Neto J, Meneses da Costa H, Banea MD (2020) Effect of surface treatments on interfacial properties of natural intralaminar hybrid composites. Polymer Composites 41 (1):314-325

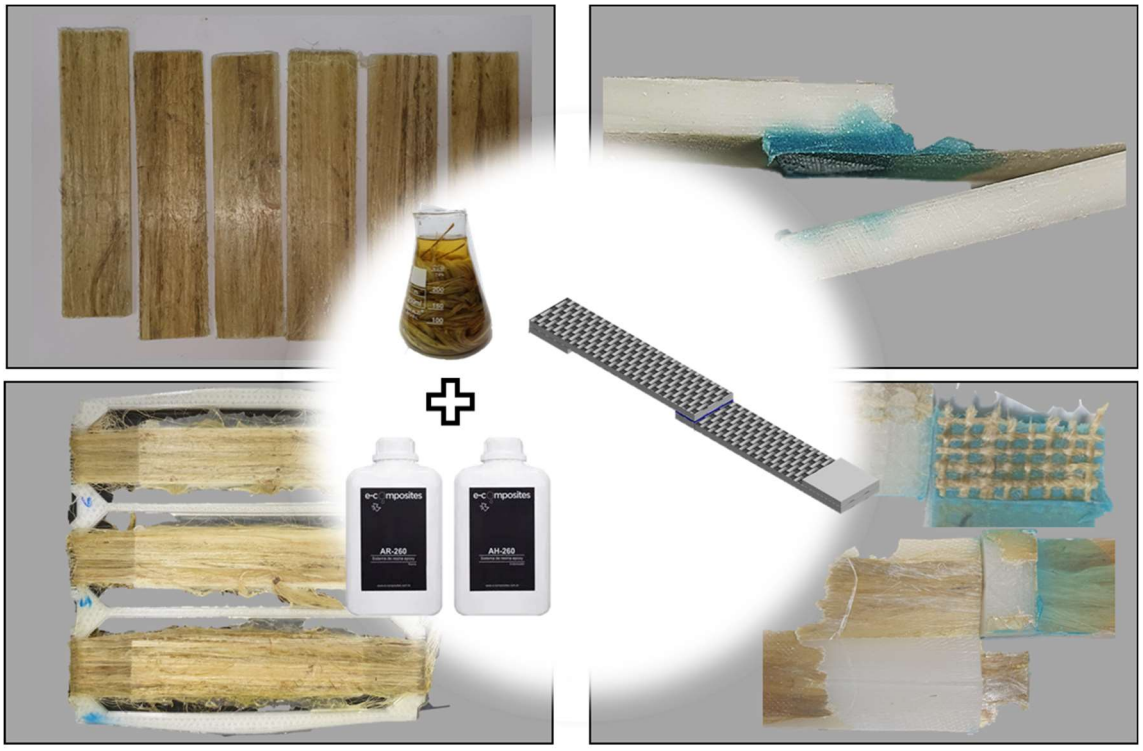
42. Heidari-Rarani M, Rafiee-Afarani M, Zahedi AM (2019) Mechanical characterization of FDM 3D printing of continuous carbon fiber reinforced PLA composites. Composites Part B: Engineering 175:107147. doi:https://doi.org/10.1016/j.compositesb.2019.107147

43. Zaldivar RJ, McLouth TD, Patel DN, Severino JV, Kim HI (2017) Strengthening of plasma treated 3D printed ABS through epoxy infiltration. Progress in Additive Manufacturing 2 (4):193-200. doi:10.1007/s40964-017-0032-0

CHAPTER 4

Chapter 4 is based on the following article: D.K.K. Cavalcanti, H.F.M. de Queiroz, M.D Banea, Performance enhancement of adhesive joints of additive manufactured parts by using different types of fibre reinforcements, International Journal of Adhesion and Adhesives, 2023, Vol. 124, 103371. https://doi.org/10.1016/j.ijadhadh.2023.103371

Graphical abstract



Performance enhancement of adhesive joints of additive manufactured parts by using different types of fibre reinforcements

ABSTRACT

The main objective of this study was to investigate experimentally the mechanical performance of adhesive joints made of additive manufactured (AM) polymeric parts reinforced with different types of fibres. PLA (PolyLactic Acid) and ABS (acrylonitrile butadiene styrene) AM adherends were fabricated by fused deposition modelling (FDM). Further, natural (jute and curauá) and synthetic (glass) fibre reinforcement fabrics were laminated on the outer sides of the AM parts using an epoxy resin via compression moulding. The type of reinforcement (natural or synthetic) and the effect of the number of the layers (1 and 2 layers) on the performance of the bonded joints was studied by testing single lap joints (SLJs) bonded with an epoxy structural adhesive. It was found that the mechanical performance of adhesively bonded SLJs is improved by using different types of fibre reinforcements to the 3D printed core adherends. The failure load varied as a function of fibre type and number of layers used as reinforcement, as well as the material used for the core of the adherends. The ABS SLJs presented lower strength compared to PLA SLJs, mainly due to the ABS adherend inferior mechanical properties. In addition, the PLA core specimens presented a better interface adhesion with the epoxy resin used in this study to laminate the reinforcements, when compared to the ABS core reinforced specimens. The best results in terms of improvement in failure load were obtained for the curauá fibre reinforced PLA 3D printed SLJ specimens (the average joint strength was more than 1.5 times higher than the neat-PLA SLJ specimens).

Keywords: additive manufactured parts, natural fibres, synthetic fibres, adhesively bonded joints, mechanical testing.

4.1. INTRODUCTION

Additive manufacturing (AM) or 3D printing technology is a process in which 3D components, with high precision and complexity, are made by depositing materials in a layer-by-layer fashion as opposed to conventional machining or forming methods. AM has been called the next industrial revolution and has experienced a huge development in the last decade [44]. Fused Deposition Modelling (FDM) is one of the most widely used AM technique due to its ability to manufacture complex and relatively high strength parts from low-cost materials. The

most commonly materials used with FDM are acrylonitrile butadiene styrene (ABS) and polylactic acid (PLA) [45]. However, these materials without any modification have relatively low mechanical properties (i.e. they have typical bulk strengths between 30–100 MPa and elastic modulus in the range of 1.3–3.6 GPa), which means that the printed parts cannot be used for high-performance applications [12]. There are various methods explored in the literature to enhance the original properties of the materials used for FDM processes (e. g. incorporation of nanoparticles within the material and the use of fibres or fabrics as reinforcements) [17,46,47,18,19,48,49].

The use of natural fibres has gained interest in many industries as a possible substitute to the already established synthetic fibres [33]. Natural reinforcements are beneficial due to the eco-friendliness, lower weight and cost, while synthetic reinforcements such as glass, have higher strength, lower water absorption and increased fibre/matrix interfacial strength [50,35]. The use of jute fibres is related to the attractive strength and toughness properties of this material and its wide use in several industries. The density of jute is nearly half that of glass fibres (i.e. 1.3 g/cm³ compared to approx. 2.5 g/cm³), which makes it a viable replacement, allowing to match the stiffness of glass fibre components at a smaller weight. On the other hand, the stiffness of jute fibres is nearly 80% that of glass fibres and cost (the jute fibre presented itself as a cost-effective alternative to the glass fibre, presenting a ninth of the price at the time of publication). On the other hand, due to the limitations of 3D printers to produce large parts, the parts often have to be printed in several separate components and further joined together to obtain the final printed part. In addition, 3D printing can be used to produce only the most complex parts, which can be further combined with simple, non-printed parts from other materials to make the final product [51]. One way to join additive manufactured parts is by adhesive bonded method. Adhesively bonded joints are used in structural application, especially in automotive and aerospace sectors, because of high strength to weight ratio, design flexibility, damage tolerance, fatigue resistance, etc. [52].

The behaviour of adhesively bonded joints with 3D printed adherends was investigated by several researchers [53,54,12,55-60]. Most of the works concentred on the performance enhancement of adhesive joints of additive manufactured parts by optimizing the joint design and the surface properties of the adherends. For example, Yap et al. [57] used SLJs with 3D printed Acrylonitrile Styrene Acrylate (ASA) and Nylon 12 carbon fibre adherends to investigate the effect of adhesive type (epoxy and cyanoacrylate) on the joints performance. They found that the joint strength for cyanoacrylate joints is much higher than that of epoxy joints. Khosravani et al. [54] studied the fracture behaviour and mechanical performance of

adhesively bonded 3D printed SLJs made of Polyethylene terephthalate glycol (PETG) using different printing parameters (raster angle and raster width). They found that cohesive failure was the dominant failure mode (66% of samples), showing proper joint fabrication. In a different study, Khosravani et al. [53] studied the influence of printing parameters and adhesive layer thickness in the efficiency of SLJs with PLA adherends. The observed failure modes were adhesive, cohesive within the adhesive layer and stock breaks near the overlap edge. The stock break failure modes were correlated with the highest observed joint failure loads.

Several research works focused on the effects of tailored additively manufactured adherends on the joint performance. For instance, Cavalcanti et al. [12] investigated the effect of sinusoidal tailoring of the overlap coupled with different building directions (flat wise and edge wise) and found a good degree of compatibility between the PLA adherends and the epoxy adhesive used, as all joints presented failure in the adherends. Other researches concentrated on optimizing the surface properties and adhesion in order to improve the mechanical performance of joints with additive manufactured parts [61,62]. Frascio et al. [62] studied the effect of surface treatment (mechanical abrasion and plasma surface treatments) on the performance of adhesively bonded ABS adherends produced by FDM. Three different adhesives (a bi-component epoxy, a polyurethane and a silane modified polymer) were used. The highest reported failure load was for the epoxy adhesive in conjunction with the Low Pressure Plasma (LPP) surface treatment, where the failure modes progressed from adhesive (solvent cleaned, mechanically abraded specimens) to cohesive within the adhesive/adherend.

Although, several solutions are currently explored to enhance the mechanical performance of adhesively bonded joints made of 3D printed substrates, to the best of the authors' knowledge, there are still limited numbers of studies available in the literature focusing on the mechanical performance of adhesive joints with 3D-printed polymeric adherends and none about bonded joints with natural fibre reinforced 3D-printed polymeric adherends. The main objective of this study was to investigate experimentally SLJs made of 3D manufactured parts reinforced with different type of fibres (natural and synthetic). PLA (PolyLactic Acid) and ABS (acrylonitrile butadiene styrene) AM adherends were manufactured with a FDM (Fused Deposition Modelling) printer. Further, natural (jute and curauá) and synthetic (glass) fibre fabrics were laminated on the outer sides of the AM parts using an epoxy resin through compression moulding. The type of reinforcement (natural or synthetic) and the effect of the number of the layers (1 and 2 layers) on the performance of the bonded joints was studied by testing SLJs bonded with an epoxy structural adhesive.

4.2. MATERIALS AND METHODS

4.2.1. Materials

The 3D printed parts were produced using PLA plus and ABS (tradename SABIC Cycolac® MG94), provided in the form of a 1.75 mm natural filament by GTMax3D (Americana, SP, Brazil). Bidirectional jute and glass fibre fabrics and curauá fibres were used as reinforcements. The glass fibre fabric (Trade name RE200P) was supplied by Barracuda Advanced Composites (Rio de Janeiro, Brazil). The jute fabric was supplied by Sisalsul (São Paulo, Brazil), while the curauá was kindly provided in-natura by the Federal University of Pará (Universidade Federal do Pará, UFPA). A two-component epoxy resin, HEX 135 SLOW, supplied by Barracuda Advanced Composites (Rio de Janeiro, Brazil) was used to laminate the reinforcements on the 3D printed parts. A structural, two-component epoxy adhesive, Betamate™2096, supplied by DuPont (São Paulo, Brazil) was used in the fabrication of the SLJs. The tensile data for the adhesive and resin used were determined in previous studies and are summarized in Table 1.

Table 1: Tensile data of the adhesive and resin used [63-65].

Polymer	Tensile strength (MPa)	Young's Modulus (GPa)	Tensile strain (%)
Betamate 2096	34.27 ± 1.52	1.60 ± 0.10	8.04 ± 0.39
HEX 135 SLOW	60.92 ± 1.42	3.25 ± 0.008	3.20 ± 0.20

2.2 Substrate specimen fabrication

The printing process parameters used in this work are presented in Table 2 and were chosen based on the literature and some in-house laboratory trials and present a good relation between mechanical properties and production times [39,65]. The 3D printed parts were sliced with Simplify3D® and all specimens were fabricated in a flat-edge orientation. The number of contours ensures that the raster angle was always 0°. The configuration used is independent of the XY build orientation.

Table 2. The printing parameters used for the 3D printed parts.

Printing Parameters	Value
Nozzle diameter (mm)	0.40
Layer height (mm)	0.30
Raster width (mm)	0.44
Raster angle	0°
Infill %	100
Extruder temperature (C°)	250
Printing bed temperature (C°)	120
Printing speed (mm/s)	45
Number of contours	44

The fibre reinforced 3D printed parts were fabricated using the hand lay-up technique followed by hot press compression moulding via a steel mould and a heated plate hydraulic press, Solab SL-20 (São Paulo, Brazil). A schematic representation of the specimen fabrication can be seen in Fig. 1. Different configurations were produced by using 1 or 2 layers of fibre reinforcements on either side of the ABS and PLA 3D printed parts (the substrates were fabricated in such a way as to create a symmetrical fibre envelope around the 3D printed part). The reinforcements (jute, curauá and glass fibre) were laminated to ABS and PLA core using the HEX 135 SLOW epoxy resin (the resin cure was done at 60 C° for 3h). The unidirectional curauá fibre was laminated with the use of a 3D printed jig to ensure that the fibres are aligned in the direction of the load.

Prior to the fabrication process, the curauá fibres were treated by the following procedure: first they were immersed in distilled water for one hour and then rinsed with tap water and subsequently dried in an oven at 100 ºC for one hour. The other reinforcements used (jute and glass fabrics) did not receive any treatment. The neat-PLA and neat-ABS adherends did not receive any mechanical/physical/chemical treatment of the surface in order to preserve the as-manufactured morphology.

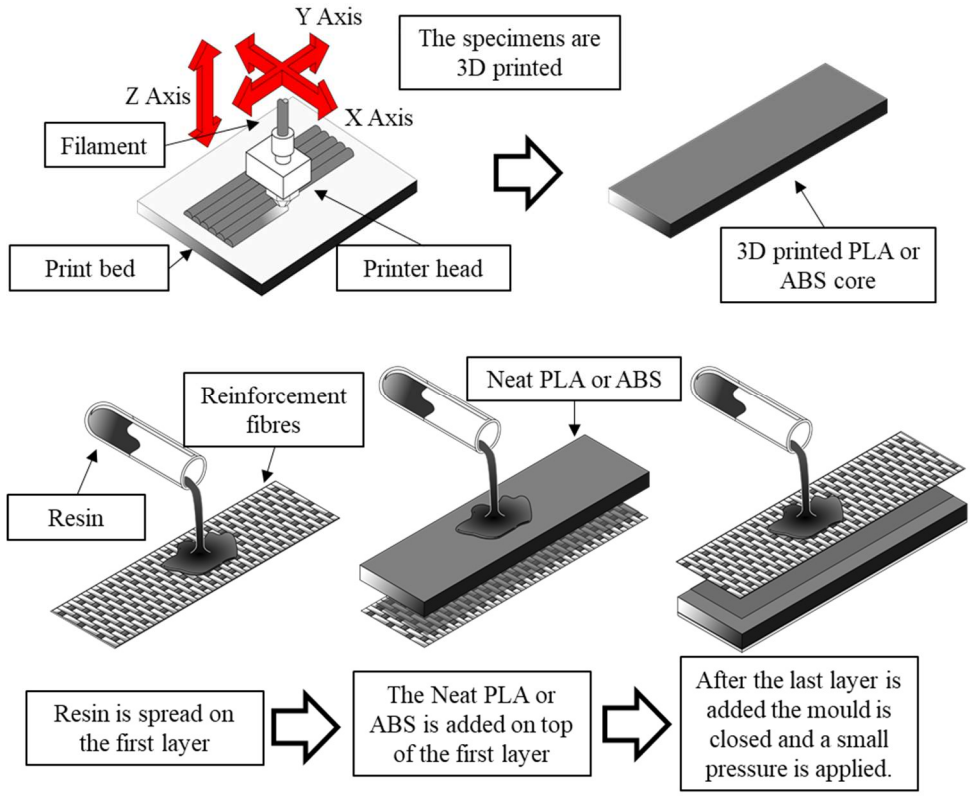


Fig. 1. Schematic representation of the specimen fabrication.

The fibre reinforced 3D printed parts used as specimens received specific nomenclature as a function of the fibre reinforcement (J-jute, C- curauá and GF-glass), layer number (1 or 2) and the material used for the core (PLA and ABS), as can be seen in Table 3.

Table 3. Nomenclature of the specimens as a function of material and reinforcement.

Neat-PLA	3D printed PLA without reinforcement
J1-PLA	1-layer Jute fibre reinforced PLA
J2-PLA	2-layer Jute fibre reinforced PLA
C1-PLA	1-layer Curauá fibre reinforced PLA
C2-PLA	2-layers Curauá fibre reinforced PLA
GF1-PLA	1-layer Glass fibre reinforced PLA
GF2-PLA	2-layers Glass fibre reinforced PLA
Neat-ABS	3D printed ABS without reinforcement
J1-ABS	1-layer Jute fibre reinforced ABS
J2-ABS	2-layer Jute fibre reinforced ABS
C1-ABS	1-layer Curauá fibre reinforced ABS
C2-ABS	2-layers Curauá fibre reinforced ABS
GF1-ABS	1-layer Glass fibre reinforced ABS
GF2-ABS	2-layers Glass fibre reinforced ABS

All the materials used as adherends were mechanically characterised through tensile (ASTM D3039, dimensions: 229x12.7x3mm) and flexural tests (ASTM D790, dimensions: 144x12.7x3mm) tests in a previous study by the authors. The tensile properties of the adherend materials are summarised in Table 4 [48]. In general, application of fibre reinforcements to the 3D printed parts promoted an increase in mechanical properties (strength and stiffness) and a reduction in elongation. The methodology used to manufacture the composite adherends provides an alternative to the more common reinforcement methods, by using a hybrid manufacturing method: 3D printing + compression moulding. The application of novel manufacturing methodologies allied with renewable biodegradable fibres can provide an interesting path forward for fabricating high-performance 3D-printed thermoplastic composites.

Table 4. Tensile data of the materials used as adherends.

Adherend material	Tensile Strength (MPa)	Young's Modulus (GPa)	Strain (%)
Neat-PLA	53.60 ± 2.31	3.85 ± 0.08	1.67 ± 0.12
J1-PLA	49.22 ± 0.9	4.28 ± 0.33	1.41 ± 0.04
J2-PLA	55.32 ± 7.99	5.27 ± 0.14	1.51 ± 0.12
C1-PLA	59.95 ± 5.48	4.55 ± 0.16	1.57 ± 0.15
C2-PLA	72.98 ± 2.94	5.48 ± 0.35	1.49 ± 0.08
GF1-PLA	69.25 ± 5.23	5.44 ± 0.08	1.45 ± 0.16
GF2-PLA	84.56 ± 1.11	6.82 ± 0.30	1.47 ± 0.09
Neat-ABS	31.03 ± 0.11	2.18 ± 0.05	24.98 ± 0.04
J1-ABS	30.85 ± 1.30	3.21 ± 0.09	1.25 ± 0.04
J2-ABS	38.65 ± 0.44	4.25 ± 0.24	1.25 ± 0.08
C1-ABS	53.09 ± 4.11	3.90 ± 0.15	1.72 ± 0.31
C2-ABS	63.05 ± 3.45	4.97 ± 0.40	1.53 ± 0.14
GF1-ABS	62.86 ± 6.14	4.50 ± 0.25	2.12 ± 0.24
GF2-ABS	81.33 ± 7.98	5.58 ± 0.21	1.94 ± 0.35

4.2.3 SLJ specimen fabrication

The geometry of the SLJ specimens can be seen in Fig. 2. A mould with steel spacers was used to maintain the correct alignment of the adherends and avoid spew fillets [66]. The spacers also ensured the adhesive layer thickness of 0.2 mm and the overlap length of 12.5 mm. The joints were cured using a hotplate hydraulic press (model SL-12/20, Solab) for 2 hours at 60ºC, as per adhesive manufacturer guidelines. The surface of the fibre reinforced substrates was manually abraded using a 100-grit sandpaper in crisscrossing 45º angles in order to increase the mechanical interlocking of the adhesive/adherend interface as well as to remove impurities and traces of releasing agents (all the samples were cleaned with alcohol 99% before the mechanical treatment). The area to be bonded was then cleaned with acetone to assure a clean surface in order to avoid adhesive failures due to chemical impurities.

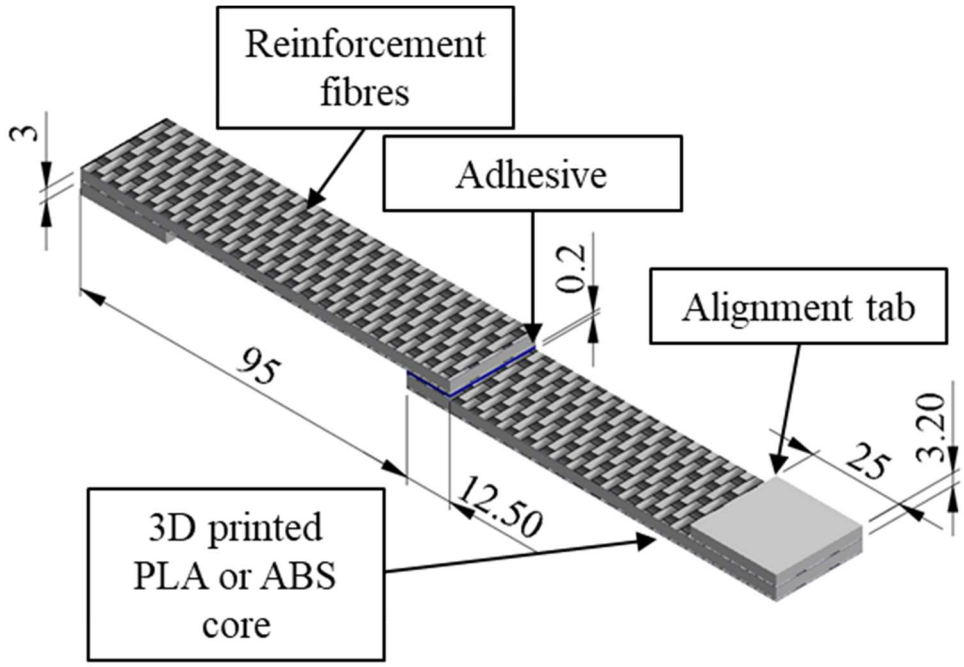


Fig. 2. SLJs specimen geometry (dimensions in mm).

2.4 Test method

All specimens were tested in tension via a universal testing machine INSTRON®5966 equipped with a 10 kN load cell, at a crosshead speed of 1 mm/min (see Fig. 3). At the grip areas, shims having dimensions 25 mm × 25 mm and 3.2 mm thickness were placed to ensure alignment of the bonded area in the grips. At least four specimens were tested for each case at room temperature. Load-displacement curves were recorded during the test.

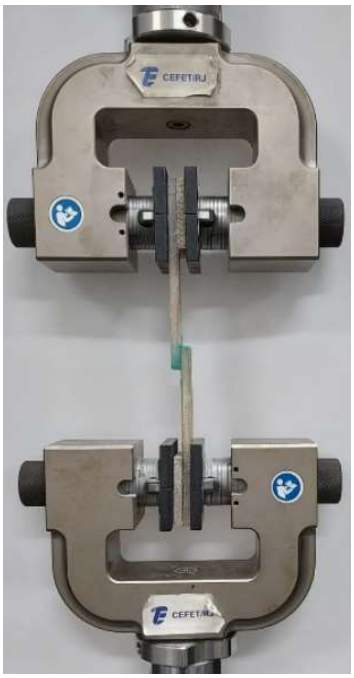


Fig. 3. Tensile test set-up.

4.3. RESULTS AND DISCUSSION

4.3.1. Effect of reinforcement type on the bonded joint performance

4.3.1.1. PLA core specimens

Figure 4 presents representative load-displacement curves of PLA core specimens SLJs as a function of reinforcement, while Table 5 and Fig. 5 summarizes the data obtained from the SLJs tests. It can be seen that the performance of the joints significantly varied as a function of reinforcement. For instance, a somewhat expected trend of joint rigidity (based on the substrate properties) was observed, increasing from lowest (Neat-PLA) to highest (GF2-PLA and C2-PLA). The stiffness of the PLA core reinforced specimens varied as a function of reinforcement fibres and number of layers, with increases in Young's modulus of approx. 11% (J1-PLA) to 77% (GF2-PLA) when compared to the Neat-PLA (see Table 4). However, despite the highest strength and rigidity of the glass fibre reinforced adherends, the highest failure load was found for the C2-PLA SLJ specimens. This may be linked to the failure modes, where the adhesive failure was observed for the GF2-PLA SLJs (see Fig. 6g), while for the C2-PLA SLJ specimens, the complete tearing of the fibre reinforcement envelope was observed after a multi-material interface failure zone (see Fig. 6e). However, even though the failure of the GF2-PLA was a typical LFT GFRP failure (Fig. 6g), the failure is significantly affected by the peel stress state of the overlap edge [35]. This, in turn, is also affected by the adherend's rigidity (the synthetic fibre reinforced specimens were not considerably more rigid than the curauá ones as can be

seen in Table 4). In a previous study by the authors, it was shown that a hybrid natural (jute)/synthetic (glass) composite SLJ reached the same joint efficiency of a fully synthetic glass fibre reinforced polymer (GFRP) joints (the adherend rigidity of GFRP adherend was approx. 10 GPa) [35].

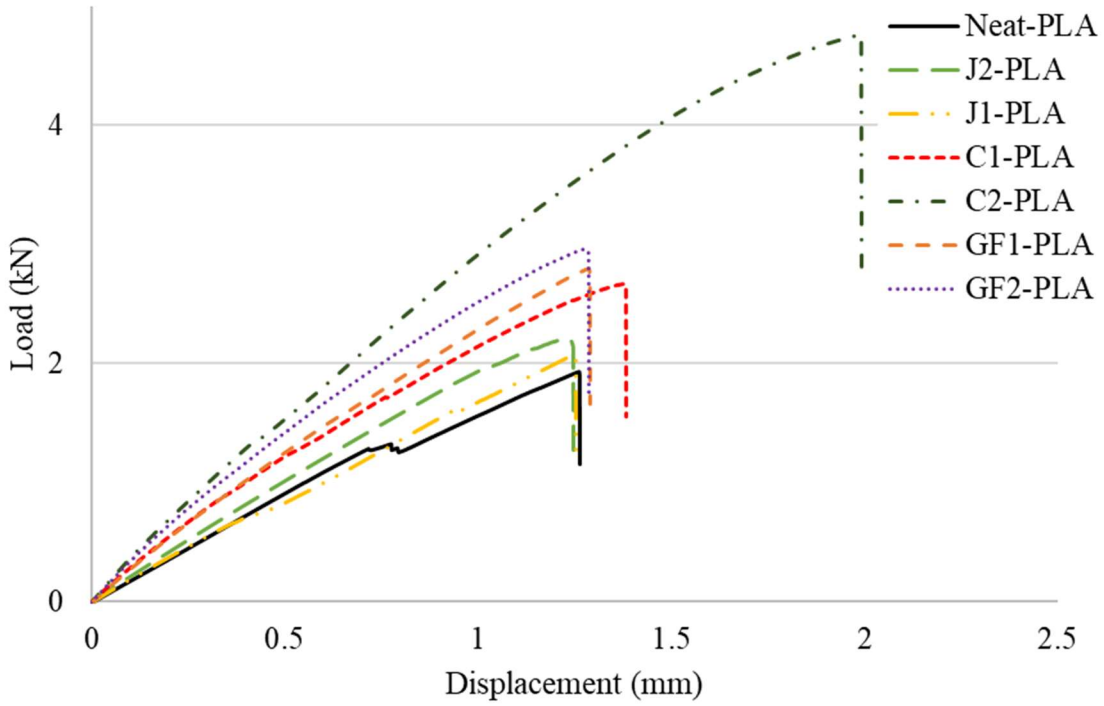


Fig. 4. Representative load-displacement curves of PLA core specimens SLJs as a function of reinforcement.

Table 5. SLJ PLA core test data.

Joint	Failure load (kN)	Displacement (mm)
Neat-PLA	1.83 ± 0.11	1.12 ± 0.12
J1-PLA	1.92 ± 0.14	1.24 ± 0.03
J2-PLA	1.82 ± 0.39	0.97 ± 0.27
C1-PLA	2.76 ± 0.12	1.19 ± 0.26
C2-PLA	4.60 ± 0.23	1.64 ± 0.33
GF1-PLA	2.61 ± 0.27	1.21 ± 0.14
GF2-PLA	3.05 ± 0.41	1.33 ± 0.26

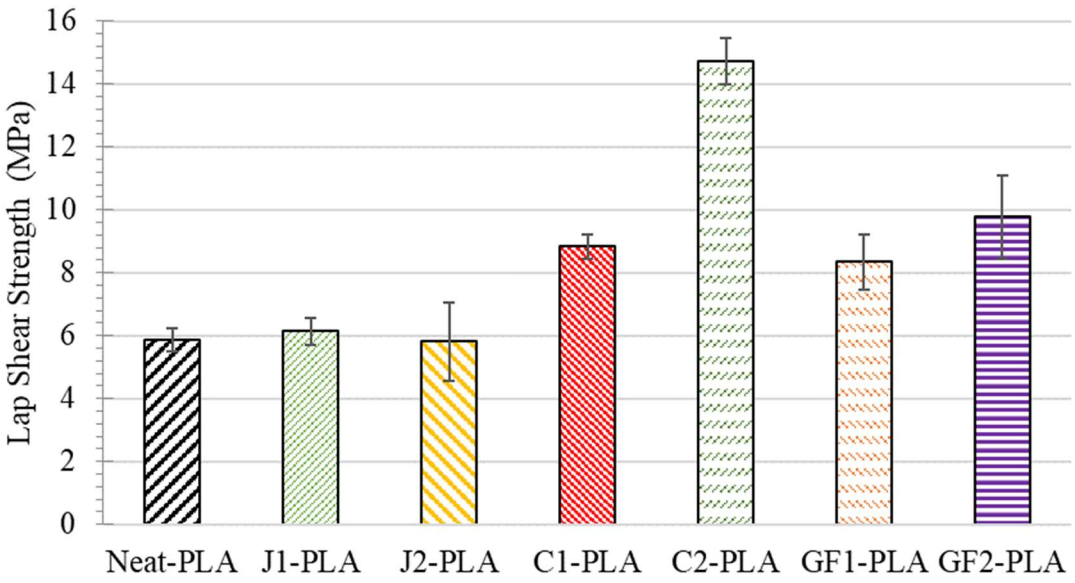


Fig. 5. Lap shear strength of the PLA core SLJs as a function of reinforcement.

From Fig. 5 it can be seen that the jute-fibre reinforced PLA SLJs presented an insignificant variation in joint lap shear strength when compared to the Neat-PLA. This is likely due to the jute fibre's low ductility and propensity to fail prematurely during the bending stresses at the overlap edge [50]. On the other hand, the curauá-fibre reinforced specimens presented improvements of approx. 50% and 150% when the C1-PLA and C2-PLA specimens are compared to the Neat-PLA, respectively. The glass-reinforced specimens presented an increase of failure load of approx. 42% and 66% when the GF1-PLA and GF2-PLA specimens are compared to the Neat-PLA, respectively.

The failure modes of the SLJ specimens were visually analysed after testing. The failure modes were analysed qualitatively based on the international standard ASTM 5573. Figure 6 shows representative failure modes for the PLA core group specimens.



a) b)

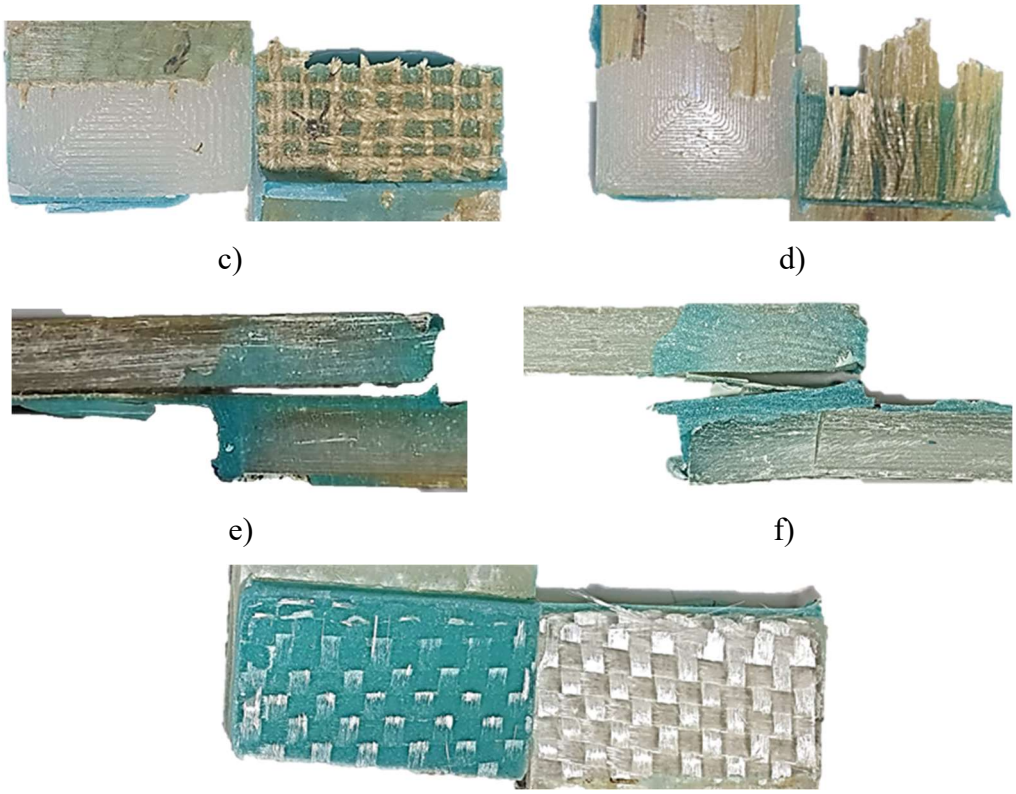


Fig. 6. Representative failure modes of the PLA joints: a) Neat-PLA, b) J1-PLA, c) J2-PLA, d) C1-PLA, e) C2-PLA, f) GF1-PLA and g) GF2-PLA.

From Fig. 6a, it can be seen that, for the neat-PLA SLJs, a mixed mode of adhesive failure/ thin layer cohesive failures (TLC) and stock break was observed. This mixed failure mode for the Neat-PLA specimens is in line with what has been previously observed in the literature [53]. For the fibre reinforced PLA specimens, the failure modes varied as a function of fibre type. For instance, for both the 1-layer natural fibre reinforced (J1-PLA and C1-PLA) SLJ specimens, a failure in the multi-material interface leading up to tearing of the reinforcement fibre at or near the overlap edge was observed. The resin/fibre envelope beneath the overlap area was debonded from the core (see Figs. 6b and d). This suggests an enhanced chemical interaction between the fibre-reinforced epoxy envelope and the epoxy adhesive when compared to the fibre-reinforced epoxy/printed core interface. Therefore, the crack propagation will occur within the less resistant multi-material interface.

For the J2-PLA SLJs, a delamination of the first printed PLA layer was observed (failure within the PLA printed core), up to the tearing of the entire jute fibre envelope at the overlap edge (see Fig. 6c), while for the C2-PLA SLJs, a generalized multi-material interfacial failure of the fibre envelope was observed as well as fibre tear/failure (see Fig. 6e). Finally, for the synthetic fibre

reinforced SLJ specimens, the failure mode also varied as a function of fibre layers. For the GF1-PLA specimens, a mixed mode of stock break, light fibre tear (LFT) failure at the adhesive/glass interface and failure at the epoxy resin/PLA interface was observed (see Fig. 6f). The fibre envelope/adhesive interface presented an LFT failure and can be observed by the few delaminated surface bundle fibres. This can be explained by the effect of the peak peel stresses at the overlap edges leading to different failure modes as a function of multi-material interfacial strength. For the GF2-PLA SLJ specimens, a generalized LFT failure was observed.

To conclude, the variation in failure mode for the PLA reinforced specimens is linked to the lowest energy path for the crack (the least resistance material interface will present the dominant crack path).

4.3.1.2. ABS core specimens

Figure 7 presents representative load-displacement curves of ABS core specimens SLJs as a function of reinforcement, while Table 6 and Figure 8 summarizes the data obtained from the SLJs tests.

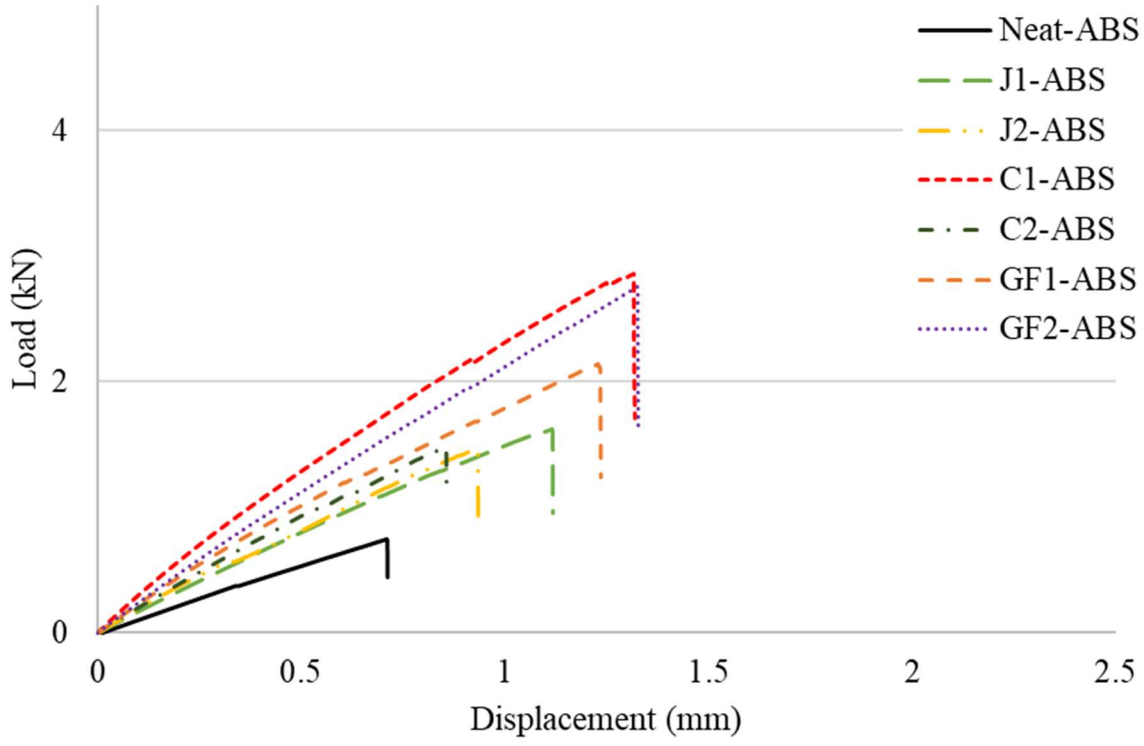


Fig. 7. Representative load-displacement curves of ABS core specimens SLJs as a function of reinforcement.

For the ABS reinforced SLJ specimens, the joint apparent rigidity also varied as a function of fibre type and number of layers as can be seen in Fig. 7. In terms of failure load, the ABS SLJs presented lower values compared to PLA SLJs. This is mainly explained by the fact that the Neat-ABS presented lower tensile strength (~42%) and rigidity (~43%) than the Neat-PLA (see Table 4).

For the ABS fibre-reinforced joints the lap shear strength also varied as a function of fibre type (see Fig. 8). The jute-fibre reinforced ABS SLJs presented no significant variation in joint failure load when compared to the Neat-ABS, similar to the PLA SLJs. The curauá-fibre reinforced specimens presented improvements of approx. 110% and 52% when the C1-ABS and C2-ABS specimens are compared to the Neat-ABS, respectively. However, for these cases significant standard deviations were observed (see Table 6) due to variations in the debonding failure zones and critical load to initiate damage. Finally, the glass-reinforced specimens presented an increase of failure load of approx. 57% and 98% when the GF1-ABS and GF2-ABS specimens are compared to the Neat-ABS, respectively. Given the failure mode similarity, the increase in joint failure load is due to the increase in adherend rigidity (see Table 4), where a more rigid adhered will rotate less under the peel stresses.

Table 6. SLJ ABS core specimen test data.

Joint	Failure load (kN)	Displacement (mm)
Neat-ABS	0.89 ± 0.20	0.89 ± 0.25
J1-ABS	1.06 ± 0.50	0.98 ± 0.35
J2-ABS	0.93 ± 0.47	1.25 ± 0.28
C1-ABS	1.87 ± 0.86	1.24 ± 0.58
C2-ABS	1.36 ± 0.28	0.72 ± 0.15
GF1-ABS	1.40 ± 0.67	0.61 ± 0.55
GF2-ABS	1.77 ± 0.57	0.98 ± 0.31

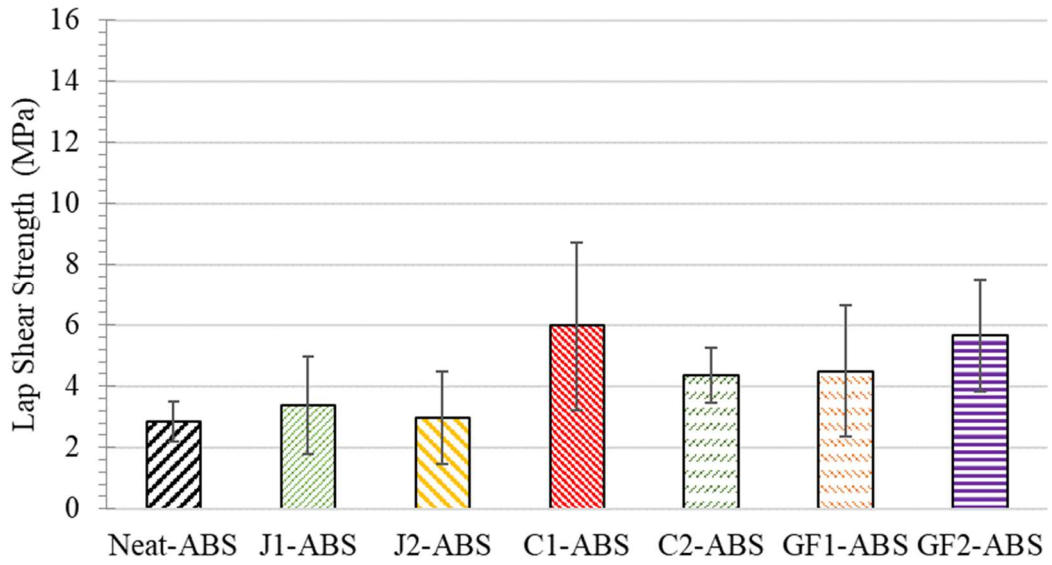
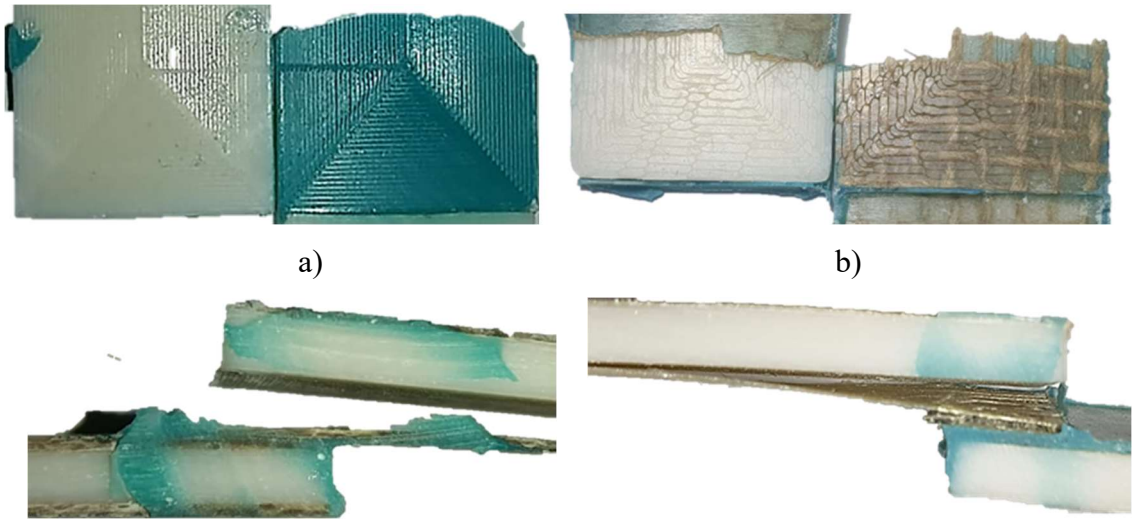


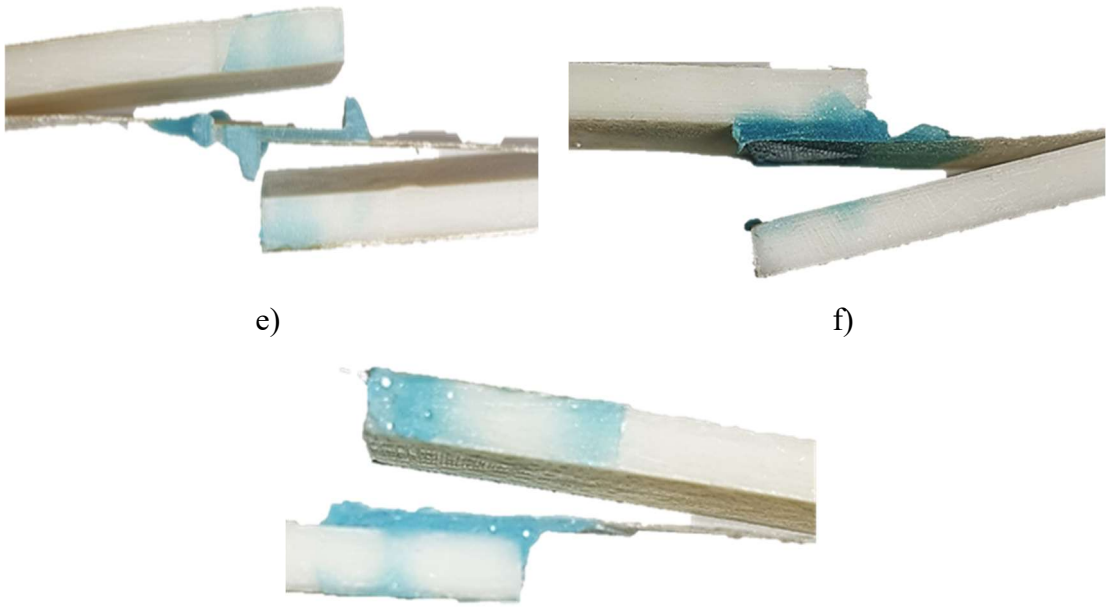
Fig. 8. Lap shear strength of the ABS core SLJs specimen as a function of reinforcement.

Figure 9 presents representative failure modes for the ABS core SLJ specimens. From Fig. 9a it can be seen that the Neat-ABS SLJ specimens presented a mixed adhesive/TLC failure. The detail of the failure surface presented in Fig. 10 clearly shows the adhesive dusting (blue specs) on the adherend, characteristic of the TLC failure. Adhesive failure was also reported in the literature for SLJs with ABS adherends bonded with structural epoxy adhesives. The joint strength can be maximized by applying pre-treatments by atmospheric pressure plasma, for example [62].



a) b)

c) d)



e) f)

g)

Fig. 9. Representative failure modes of the fibre reinforced ABS joints: a) Neat-ABS, b) J1-ABS, c) J2-ABS, d) C1-ABS, e) C2-ABS, f) GF1-ABS and g) GF2-ABS.

For the SLJs of fibre reinforced ABS specimens, in general, multi-material interfacial failure (failure at the fibre envelope/ABS core interface) was observed. For instance, the J1-ABS SLJ specimens presented delamination of the first layer of printed ABS material (see Fig. 9b). However, for the J2-ABS SLJ specimens, interfacial failure of the envelope (reinforcement) from one of the adherends was observed (see Fig. 9c). For the curauá fibre reinforced ABS joints, a similar interfacial failure was observed as a function of fibre layers for the C1-ABS and C2-ABS SLJs (Figs. 9d and e). Finally, regarding the synthetic fibre reinforced ABS SLJ specimens, a generalized single-sided interfacial failure was observed for both GF1-ABS and GF2-ABS SLJs (see Fig. 9f and g). The predominance of the multi-material interface failure is due to the lower energy required to initiate the crack propagation within the epoxy/ABS interface, similar to the PLA specimens. However, the debonded zones were much larger compared to the reinforced PLA SLJs and the failures initiated at lower loads.

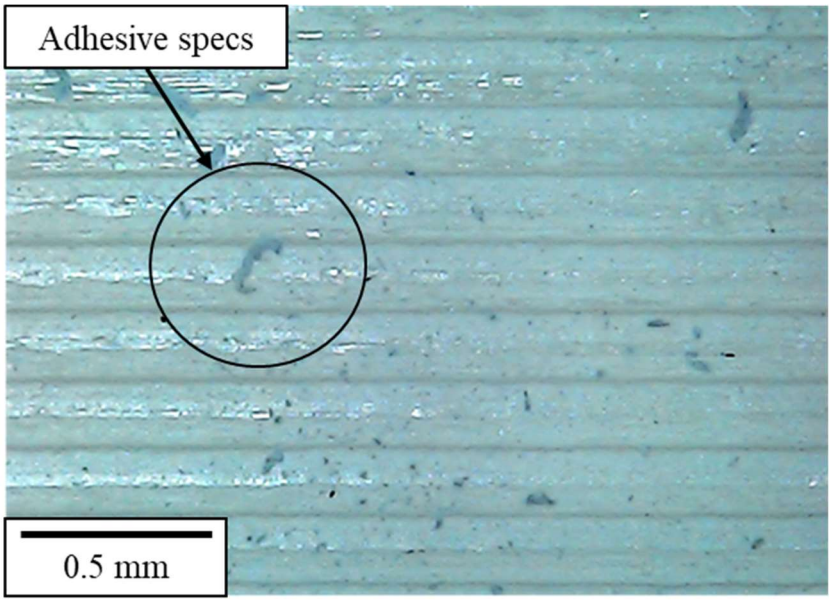


Fig. 10. Detail of the failure surface of the Neat-ABS joint.

The effect of the fibre reinforcement type on the adherend properties and thus, in the joint efficiency is directly linked to the fibre properties. The fibres chosen in this study represent a commonplace natural fibre (jute), a still relatively underused but promising natural fibre (curauá) and a staple of the synthetic fibre industry (glass). While, the high properties and good interfacial bonding of the glass/epoxy has been extensively described in the literature, the jute and curauá fibres, on the other hand, still have much investigation needed for wider industrial application, especially the curauá (this fibre presents an optimum compromise between low density, high ductility as well as very high tensile strength and rigidity [33]). These properties reflect in the failure load values for reinforced 3D printed core bonded joints as the best case reported.

In summary, significant improvement in bonded joint failure load was found as a function of fibre reinforcement for both PLA and ABS, except for the jute-reinforced SLJs. The best results were found for the curauá fibre reinforced SLJs, given the optimum compromise between fibre properties and mode of failure. This will be further discussed in the next section.

4.3.2 Effect of number of the fibre layers on the bonded joint performance

From Tables 5 and 6 and Figs. 5 and 9, it can be seen that the failure load and lap shear strength, respectively, of the reinforced PLA and ABS joints varied as a function of the number of fibre layers. For the PLA joints, a significant improvement was observed as a function of fibre layers for all specimens, except for the jute reinforced specimens. For instance, the C2-PLA presented

an enhancement in failure load of approx. 67% when compared to C1-PLA, while the GF2-PLA showed an enhancement in failure load of approx. 17%, when compared to the GF1-PLA. As was previously described, the curauá fibres fail completely following multi-material interfacial failure, while the glass fibre does not (see Fig. 6d and f). This represents the pattern to be expected if the number of layers continues to be increased as a function of fibre type for the PLA specimens. For instance, as can be seen in Table 5, a plateau-like trend is already visible for the glass-reinforced specimens (the LFT failure type will be a limiting factor). On the other hand, for the curauá-reinforced specimens, a trend of significant joint failure load improvement is reported as a function of fibre layers. This is due to the failure mode and high fibre properties where the natural fibre envelope presents a full "stock break" failure for the PLA specimens (see Fig. 6d).

Regarding the reinforced ABS joints, the failure load also varied as a function of fibre layers. Similar to the PLA specimens, the jute reinforced ABS SLJs did not present significant variation as a function of layers. This is related to the initiation and propagation of the failure, where the crack initiates in the multi-material interface and for the case of the 1-layer, the natural envelope fails (see Fig 10b). For the J2-ABS, given the more resistant envelope compared to J1-ABS, the crack initiates and propagates entirely within the interface (see Fig 10c), leading to similar failure loads. The C2-ABS SLJs presented a decrease of approx. 27% when compared to the C1-ABS SLJ specimens, but significant data scatter was observed due to the variation in the failure modes. It was shown in a previous study that for the curauá fibre–reinforced specimens (C1-ABS), delamination was less prominent compared to C2-ABS, and the failure is similar to the one seen in the glass fibre–reinforced specimens (GF1-ABS) [48]. In addition, the high rigidity and strength of the fibre envelope coupled with the observed low strength of the epoxy/ABS interface, may have generated a stress state that reached the critical epoxy/ABS debonding stresses, contributing to the observed behaviour.

Finally, the GF2-ABS SLJs presented an increase in failure load of approx. 26% when compared to the GF1-ABS SLJs. It should be noted that both PLA and ABS glass-reinforced specimens will likely present diminishing returns as a function of increasing the fibre layers due to their respective failure modes. The GF2-PLA specimens have reached a stable LFT failure surface while both GF1 and GF2-ABS specimens presented initiation and propagation of cracks in the epoxy/ABS interface. It was shown in a previous study [35], that by increasing the glass fibre layers (i.e., from 2 on either side to 3) in a synthetic envelope surrounding a jute/epoxy core, an approx. 29% enhancement in failure load was achieved. The failure load and mode were identical to the pure synthetic adherend bonded joint. The difference between

these studies lies in the existence of a single primary phase in the adherend material (i.e., a continuous epoxy resin phase) and two secondary phases (i.e., two reinforcement fibres). On the other hand, the current adherends studied present two primary phases, and as such, a significant multi-material (multi-primary phase) interface. The primary phases being the epoxy resin and the printed core's material. This will ultimately dictate the failure mode limitations and yield a state of diminishing returns on further fibre layer additions (plateau-like trend). Therefore, despite the significant improvement reported as a function of fibre layers for the GF-ABS specimens, further fibre addition will likely yield a similar failure mode and therefore represent a failure load limitation.

In summary, considerable enhancement of adhesive bonded joint efficiency of 3D printed polymer adherends by using different type of fibre reinforcements was found. The PLA core specimens revealed a superior interface adhesion with the epoxy resin used in this study to laminate the reinforcements, leading to higher SLJ failure loads, when compared to the ABS core reinforced specimens. Furthermore, the best results in terms of improvement in failure load were obtained for the curauá fibre reinforced 3D printed SLJ specimens (the average joint strength was more than 1.5 times higher than the neat SLJ specimens).

In general, for both PLA and ABS core materials, the epoxy/fibre laminated envelope reinforcement technique proved to be efficient in improving the bonded joint performance. However, given the observed failure modes and its correlation to the failure loads, a limiting factor was found (i.e., the epoxy resin/epoxy bi-component adhesive interface is significantly more resistant than the epoxy resin/printed core interface). This inevitably leads to the interfacial bonding failures and presents a limitation on the expected reinforcement improvements as a function of increasing the reinforcement fibre layers, especially for the ABS material.

4.4. CONCLUSIONS

In this study single-lap adhesively bonded joints made of additive manufactured polymeric parts reinforced with different types of fibres were experimentally investigated. The type of reinforcement (natural or synthetic) and the effect of the number of layers (1 and 2 layers) on the performance of the joints was studied by testing SLJs bonded with an epoxy structural adhesive. The following conclusions can be drawn:

- The mechanical performance of adhesively bonded SLJs is improved by using different types of fibre reinforcements to the 3D printed adherends. The curauá fibre reinforced

specimens presented the most significant improvements due to different factors: high fibre mechanical properties, good fibre/epoxy resin interfacial properties and high energy required for total fibre tearing. The highest improvement was found for the C2-PLA specimens that presented an increase in joint failure load of approx. 150% when compared to the Neat-PLA (unreinforced specimens), while for the ABS specimens, the highest improvement was found for the C1-ABS with an improvement of approx. 110% when compared to the Neat-ABS.

- The PLA core specimens presented a superior interface adhesion with the epoxy resin used in this study, leading to higher failure loads when compared to the ABS core fibre reinforced specimens.
- The failure modes of the bonded joints made of fibre-reinforced 3D printed parts presented significant differences as a function of adherend material. The Neat-PLA and Neat-ABS SLJs failed by a mixed mode of adhesive failure/thin layer cohesive failures (TLC) and stock break and a mixed adhesive/TLC failure, respectively. The reinforced PLA SLJs presented a mixed mode of multi-material interface failure (resin matrix/printed core) as well as fibre-reinforced envelope tearing. The reinforced ABS specimens presented multi-material interface failures predominantly, suggesting a weaker ABS core/epoxy resin interface compared to the PLA specimens. The epoxy resin/epoxy adhesive interface is significantly more resistant than the epoxy resin/printed core interface. This inevitably leads to the interfacial bonding failures and presents a limitation on the expected reinforcement improvements as a function of higher fibre layers, especially for ABS.

Strengthening of additive manufactured parts by using different type of fibre reinforcements is a promising innovation in order to improve their mechanical properties and these improvements might enable these materials to serve for high load bearing purposes. The methodology used in this study to manufacture the composite adherends provides an alternative to the more common reinforcement methods, by using a hybrid manufacturing method: 3D printing + compression moulding. The application of novel manufacturing methodologies allied with renewable biodegradable fibres can provide an interesting path forward for fabricating high-performance 3D-printed thermoplastic composites. In addition, the use of AM composite materials may further increase in many structural and non-structural applications if their joining behaviour is well-known and established.

REFERENCES

[1] Harris M., Potgieter J., Archer R., Arif K.M., Effect of material and process specific factors on the strength of printed parts in fused filament fabrication: A review of recent developments, Materials, 12 (2019).

[2] Ngo T.D., Kashani A., Imbalzano G., Nguyen K.T.Q., Hui D., Additive manufacturing (3D printing): A review of materials, methods, applications and challenges, Composites Part B: Engineering, 143 (2018) 172-96.

[3] Cavalcanti D.K.K., Banea M.D., de Queiroz H.F.M., Mechanical characterization of bonded joints made of additive manufactured adherends, Annals of "Dunarea de Jos" University of Galati, Fascicle XII, Welding Equipment and Technology, 30 (2019) 27-33.

[4] Galatas A., Hassanin H., Zweiri Y., Seneviratne L., Additive manufactured sandwich composite/ABS parts for unmanned aerial vehicle applications, Polymers, 10 (2018) 1262.

[5] Gama N., Magina S., Ferreira A., Barros-Timmons A., Chemically modified bamboo fiber/ABS composites for high-quality additive manufacturing, Polymer Journal, (2021).

[6] Long Y., Zhang Z., Fu K., Li Y., Efficient plant fibre yarn pre-treatment for 3D printed continuous flax fibre/poly(lactic) acid composites, Composites Part B: Engineering, 227 (2021).

[7] Ivanov E., Kotsilkova R., Xia H., Chen Y., Donato R.K., Donato K., et al., PLA/Graphene/MWCNT Composites with Improved Electrical and Thermal Properties Suitable for FDM 3D Printing Applications, Applied Sciences, 9 (2019) 1209.

[8] Justo J., Távara L., García-Guzmán L., París F., Characterization of 3D printed long fibre reinforced composites, Composite Structures, 185 (2018) 537-48.

[9] Cavalcanti D.K.K., de Queiroz H.F.M., Neto J.S.S., Banea M.D., Strengthening of additive manufactured parts by using different type of fibre reinforcements, International Journal of Advanced Manufacturing Technology, 123 (2022) 1889-903.

[10] Cavalcanti D.K.K., Neto J.S.S., Queiroz H.F.M.D., Wu Y., Neto V.F.S., Banea M.D., Development and Mechanical Characterization of Short Curauá Fiber-Reinforced PLA Composites Made via Fused Deposition Modeling, Polymers, 14 (2022).

[11] Neto J., Queiroz H., Aguiar R., Lima R., Cavalcanti D., Banea M.-D., A Review of Recent Advances in Hybrid Natural Fiber Reinforced Polymer Composites, Journal of Renewable Materials, 10 (2022) 561--89.

[12] de Queiroz H., Banea M., Cavalcanti D., Experimental analysis of adhesively bonded joints in synthetic-and natural fibre-reinforced polymer composites, Journal of Composite Materials, 54 (2020) 1245-55.
[13] de Queiroz H.F.M., Banea M.D., Cavalcanti D.K.K., Adhesively bonded joints of jute, glass and hybrid jute/glass fibre-reinforced polymer composites for automotive industry, Applied Adhesion Science, 9 (2021).
[14] Singh S., Ramakrishna S., Singh R., Material issues in additive manufacturing: A review, Journal of Manufacturing Processes, 25 (2017) 185-200.
[15] Budhe S., Banea M., De Barros S., Da Silva L., An updated review of adhesively bonded joints in composite materials, International Journal of Adhesion and Adhesives, 72 (2017) 30-42.
[16] Khosravani M.R., Soltani P., Weinberg K., Reinicke T., Structural integrity of adhesively bonded 3D-printed joints, Polymer Testing, 100 (2021) 107262.
[17] Khosravani M.R., Soltani P., Reinicke T., Fracture and structural performance of adhesively bonded 3D-printed PETG single lap joints under different printing parameters, Theoretical and Applied Fracture Mechanics, 116 (2021) 103087.
[18] Kovan V., Altan G., Topal E.S., Effect of layer thickness and print orientation on strength of 3D printed and adhesively bonded single lap joints, Journal of Mechanical Science and Technology, 31 (2017) 2197-201.
[19] Atahan M.G., Apalak M.K., Loading-rate effect on tensile and bending strength of 3D-printed polylactic acid adhesively bonded joints, Journal of Adhesion Science and Technology, (2021).
[20] Yap Y.L., Toh W., Koneru R., Lin R., Chan K.I., Guang H., et al., Evaluation of structural epoxy and cyanoacrylate adhesives on jointed 3D printed polymeric materials, International Journal of Adhesion and Adhesives, 100 (2020).
[21] Pizzorni M., Parmiggiani A., Prato M., Adhesive bonding of a mixed short and continuous carbon-fiber-reinforced Nylon-6 composite made via fused filament fabrication, International Journal of Adhesion and Adhesives, 107 (2021) 102856.
[22] Pizzorni M., Lertora E., Parmiggiani A., Adhesive bonding of 3D-printed short- and continuous-carbon-fiber composites: An experimental analysis of design methods to improve joint strength, Composites Part B: Engineering, 230 (2022) 109539.
[23] Pizzorni M., Prato M., Effects of hygrothermal aging on the tensile and bonding performance of consolidated 3D printed polyamide-6 composites reinforced with short and

multidirectional continuous carbon fibers, Composites Part A: Applied Science and Manufacturing, 165 (2023) 107334.

[24] Leicht H., Orf L., Hesselbach J., Vudugula H., Kraus E., Baudrit B., et al., Adhesive bonding of 3D-printed plastic components, The Journal of Adhesion, 96 (2020) 48-63.

[25] Frascio M., Mandolfino C., Moroni F., Jilich M., Lagazzo A., Pizzorni M., et al., Appraisal of surface preparation in adhesive bonding of additive manufactured substrates, International Journal of Adhesion and Adhesives, 106 (2021) 102802.

[26] dos Reis M., Banea M., da Silva L., Carbas R., Mechanical characterization of a modern epoxy adhesive for automotive industry, Journal of the Brazilian Society of Mechanical Sciences and Engineering, 41 (2019) 340.

[27] Bonaldo J., Banea M., Carbas R., Da Silva L., De Barros S., Functionally graded adhesive joints by using thermally expandable particles, The Journal of Adhesion, 95 (2019) 995-1014.

[28] Neto J.S.S., Banea M.D., Cavalcanti D.K.K., Queiroz H.F.M., Aguiar R.A.A., Analysis of mechanical and thermal properties of epoxy multiwalled carbon nanocomposites, Journal of Composite Materials, 54 (2020) 4831-40.

[29] Wang L., Sanders J.E., Gardner D.J., Han Y., Effect of fused deposition modeling process parameters on the mechanical properties of a filled polypropylene, Progress in Additive Manufacturing, 3 (2018) 205-14.

[30] Banea M.D., da Silva L.F., Campilho R.D., Moulds design for adhesive bulk and joint specimens manufacturing, Assembly Automation, 32 (2012) 284-92.

CHAPTER 5

Chapter 5 is based on the following article: D.K.K. Cavalcanti, J.S.S. Neto, H.F.M. de Queiroz, Y. Wu, V.F.S. Neto, M.D Banea, Development and mechanical characterization of short curauá fiber-reinforced PLA composites made via fused deposition modelling, Polymers 2022, 14(22), 5047; https://doi.org/10.3390/polym14225047 2022

Graphical abstract



Development and mechanical characterization of short curauá fibre-reinforced PLA composites made via fused deposition modelling

ABSTRACT

The increase in the use of additive manufacturing (AM) has led to the need for filaments with specific and functional properties in face of requirements of structural parts production. The use of eco-friendly reinforcements (i.e., natural fibres) as an alternative to those more traditional synthetic counterparts is still scarce and requires further investigation. The main objective of this work was to develop short curauá fibre reinforced Polylactic Acid (PLA) composites made via fused deposition modelling. Three different fibre lengths (3, 6 and 8 mm), and three concentrations in weight percentage (2%, 3.5% and 5% wt.%) were used to fabricate reinforced PLA filaments. Tensile and flexural tests in accordance with their respective American Society for Testing and Materials (ASTM) standards were performed. A thermal analysis was also carried out to investigate the thermal stability of the new materials. It was found that the main driving factor for the variation on mechanical properties was the fibre weight fraction. The increase in fibre length did not provide any significant benefit on the mechanical properties of the curauá fibre-reinforced PLA composite printed parts. The composites produced with PLA filaments reinforced by 3mm-2% curauá fibre presented the overall best mechanical and thermal properties of all studied groups. The curauá fibre-reinforced PLA composites made via fused deposition modelling may be a promising innovation to improve the performance of these materials which might enable them to serve for new applications.

Keywords: 3D printing; additive manufacturing; short fibre reinforcements; mechanical properties; PLA.

5.1. INTRODUCTION

Additive manufacturing (AM) also known as 3D printing technology is an innovative process in which parts can be manufactured with high precision and complexity. The feedstock used in the process is deposited layer by layer and these materials have been widely used in both household and industrial applications [1-4]. There is a wide variety of technologies used in 3D printing, where the Fused Filament Fabrication (FFF) or Fused Deposition Modelling (FDM) is one of the most widely used AM technique due to its ability to manufacture complex and

relatively high strength parts from low-cost materials [5-7]. The parts manufactured by FDM printers were found to be highly dependent on the feedstock material, processing parameters [8] and susceptible to printing defects (i.e. satellite droplets and nozzle clogging) [9,10]. The most common materials used in FDM are thermoplastics, of which polylactic acid (PLA) and acrylonitrile butadiene styrene (ABS) are the most common [11-19]. PLA is a linear aliphatic thermoplastic polyester, produced from renewable biodegradable materials, with good mechanical properties, thermal stability, processability, and low environmental impact [18]. The PLA presents many advantages over other thermoplastics used in FDM, including its lower melting temperature and reduced emissions of smells and plastic particles during printing. However, PLA still presents relatively lower mechanical properties compared to other plastics used in the industry. Therefore, to broaden the possible application of PLA printed parts numerous studies have focused on a wide range of reinforcing techniques [20]. The use of fibre reinforcements is common in composite materials and a similar trend can be seen for the filaments used in FDM.

The use of continuous fibre reinforced filaments has proven to be an effective method in increasing the mechanical properties of 3D printed composites. However, the necessity of specialized equipment to print and manufacture the filaments limits their applications, especially when printing parameters are concerned [21]. As an alternative, the use of short fibres as reinforcements for filaments can provide an increase in mechanical properties without the need of more complex fabrication and printing [22]. The reinforcements used to strengthen the filament can be either synthetic or natural [23-25]. However, the former presents problems for productions due to higher abrasion and production cost when compared to natural fibre alternatives. Furthermore, natural fibres present advantages such as lower overall production costs, renewable source, and low abrasiveness [26,22,27]. However, the study of short natural fibres as reinforcements to thermoplastic filaments is scarce and can provide a possible alternative to their synthetic counterparts.

The main objective of this work was to develop and investigate the mechanical and thermal properties of 3D PLA printed parts reinforced by short natural (curauá) fibre. Three different fibre lengths (3, 6 and 8 mm), and three concentrations in weight percentage (2%, 3.5% and 5% wt.%) were used to fabricate reinforced PLA filaments. Tensile and flexural tests in accordance with their respective ASTM standards were performed. A thermal analysis was also carried out in order to investigate the thermal stability of the new materials.

5.2. MATERIALS AND METHODS

5.2.1. Materials

The thermoplastic material used in this work was the PLA 4032D obtained as 6 mm pellets from Tucab (Leiria, Portugal). The reinforcement fibres were short curauá fibres, in-natura, by the Federal University of Pará (Universidade Federal do Pará, UFPA, Brazil). The mechanical properties of the materials used in this work are summarized in Table 1. The curauá is a type of natural fibre endemic to Brazil, they present excellent mechanical properties, with high cellulose count and low lignin content (70.4% cellulose, 10.8% hemicellulose and 11.1% lignin) [28]. The curauá fibres were manually cut, and their average size was measured through the Fiji image software [29]. The nomenclature used in this study can be seen in Table 2 (where C is curauá followed by average fibre length and fibre weight concentration).

Table 1. Material properties.

Material	Tensile strength (MPa)	Young's modulus (GPa)	Elongation at break (%)	Density (g/cm^3)
PLA 4032D [30]	51.00 ± 5.00	3.08 ± 0.30	5.76 ± 0.50	1.24
Curauá [31]	1929.80 ± 249.50	87.23 ± 15.40	3.94 ± 0.60	1.33

Table 2. Nomenclature of the specimens as a function of reinforcement (average fibre length and wt.%).

Specimen type	Fibre length (mm)	Weight concentration wt.% (%)
Neat-PLA	-	-
C -3mm-2%	3.02 ± 0.97	2
C-3mm-3.5%		3.5
C-3mm-5%		5
C-6mm-2%	6.53 ± 0.99	2
C-6mm-3.5%		3.5
C-6mm-5%		5
C-8mm-2%	7.97 ± 0.92	2
C-8mm-3.5%		3.5
C-8mm-5%		5

5.2.2. Filament and 3D part specimens' fabrication

The PLA-Curauá short fibre mixture was fabricated by means of a laboratory-scale mechanical melt-mixing Brabender® Plastograph torque rheometer (BRABENDER GMBH & CO.KG, Duisburg, Germany). The PLA pellets and curauá fibres were mixed at a temperature of 180 °C and a speed of 100 rpm. The batches were separated in 25g of PLA and the proportional wt.% in curauá fibres (i.e., 2%, 3.5% and 5%). The natural fibres were added after the PLA presented stable mixing (i.e., when the force measured by the Brabander mixer begins to stabilize). In Fig. 1, the representative curve of mixing force (Nm)/time (HH:MM:SS) is shown. After the fibres were added, they were let to mix for approx. 6 min. The speed and mixing time were chosen as to limit PLA degradation [32]. The temperatures used for mixing and extrusion were under the degradation onset for the curauá fibres [26].

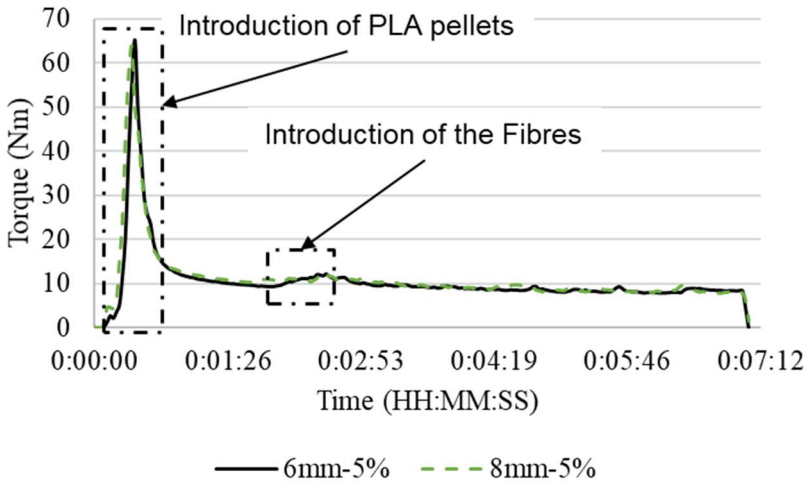


Fig. 1. Representative Torque/time of the PLA-curauá mixing process.

The resulting mixed composite was further grinded in a Wanner Technik GmbH B08.10 (Wertheim-Reicholzheim, Germany) to a size of approx. 6 mm. These pellets were then fed in the single screw Noztek pro filament extruder (Shoreham, England). The filaments with a variation in diameter of 1.5 ± 0.2 mm were manufactured with the aid of a Filafab (England) puller and spooler machine. The processing schematics can be seen in Fig. 2 and the extruded filament in Fig. 3.

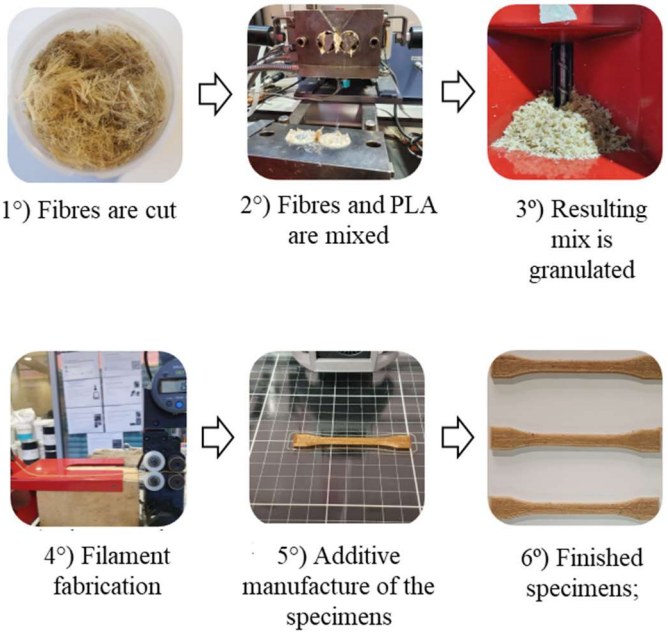


Fig. 2. Schematic representation of the specimen fabrication.

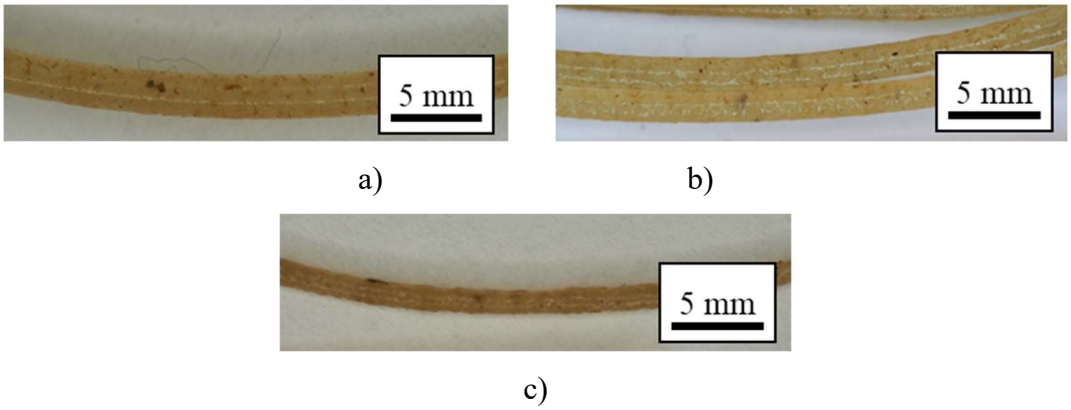
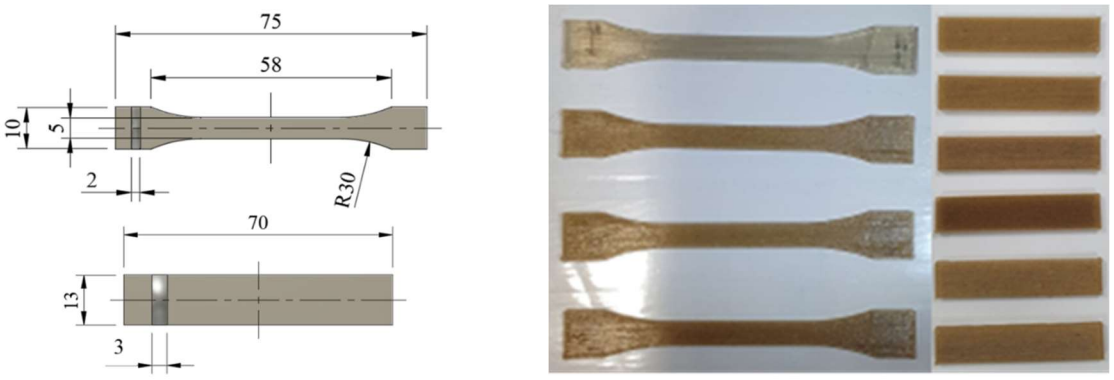


Fig. 3. Representative images of the extruded filaments of the 3 mm group: a) 2 wt.%, b) 3.5 wt.% and c) 5 wt.%.

The 3D part specimens were fabricated using a B2X300 3D printer from BEEVERYCREATIVE (Ílhavo – Portugal) using the in-house manufactured PLA-Curauá filament. The standards upon which the specimens were produced are ISO 527 for the tensile tests and ASTM D790 for the flexural tests. The schematic representation of the specimens can be seen in Fig.4. At least five specimens were tested for each condition.



(a) (b)

Fig. 4. Tensile and flexural specimens: a) Schematic of the specimens with dimensions in millimetres (in grey is the specimen thickness) and b) photos of the 3D printed specimens.

Table 3. The printing parameters used for the 3D printed specimens.

Printing Parameters	Value
Nozzle diameter (mm)	0.40
Layer height (mm)	0.20
Raster width (mm)	0.8
Raster angle	0°
Infill %	100
Extruder temperature (C°)	220
Printing bed temperature (C°)	50
Printing speed (mm/s)	30
Number of contours	1
Flow (%)	108

The printing process parameters used in this work are presented in Table 3 and were chosen based on the literature and in-house laboratory trials. The raster width chosen was 0.8 mm, above the normal value of 0.44 mm, which could be helpful to reduce internal voids produced by overlapping the rasters [7] and compensate for filament irregularity at the same time. The flow was increased (108%) in order to compensate for filament diameter variations, the increase in flow will help maintain pressure within the nozzle and help to reduce possible void and failures due to slippage and under extrusions. The raster angle chosen was 0º, as it was shown in the literature that a raster angle of 0° is the optimum direction of depositions if high tensile strength is desired. The infill chosen was 100%; this is due to the properties of the printed parts

being associated to internal voids [8]. Slicing was performed with Ultimaker Cura® 4.12.1 and all test specimens were fabricated in a flat-edge orientation. The 0° infill direction was maintained by setting all layers as bottom layers in the specified angle. The production of 3D printed parts presents some drawbacks, especially when using noncommercial filaments, such as nozzle clogging [10]. In the present work these drawbacks were minimized by preliminary in-house tests intending to optimizing the print parameters. The filaments present little clogging, with most printing defects originating from diameter inconsistencies.

5.2.3. Tensile and flexural tests

The tensile and flexural tests were carried out in a SHIMADZU® universal testing machine (Kyoto, Japan). The tensile tests were performed with a crosshead speed of 2 mm/min using a 10 kN load cell (see Fig. 5). The specimen used for tensile tests followed the ISO 527-1:2019 size and shape. For the flexural tests a three-point bending rig with a span of 120 mm and a cross head speed of 1 mm/min and a 1 kN load cell was used, as recommended by the ASTM D790 standard.



Fig. 5. Tensile test set-up.

5.2.4. Thermal analysis

5.2.4.1. Thermogravimetric analysis (TGA)

TGA was performed in a NETZSCH TG 209 F3 Tarsus machine (Netzsch-Gerätebau GmbH, Germany). Samples of approximately 20-30 mg. were used to make the measurements. An alumina (Al_2O_3) crucible was used. Each sample was tested in the temperature range of 30 °C – 600 °C at a constant heating rate of 10 °C / min under nitrogen atmosphere (20 ml min-1).

5.2.4.2. Differential Exploratory Calorimetry (DSC)

DSC was performed in a NETZSCH DSC 200 F3 Maia equipment (Netzsch-Gerätebau GmbH, Germany). The experiments were conducted with a heating rate of 10 K min−1, in the temperature range of 30–250°C with a nitrogen flux of 20 mL min−1 according to ASTM D3418 with sample weights of approx. 8-10 mg. The glass transition temperature (T_g), crystallization temperature (T_c) and melting temperature (T_m) were determined.

5.3. RESULTS AND DISCUSSION

The representative stress-strain curves obtained from the tensile tests as a function of reinforcement can be seen in Fig. 6. The tensile data (tensile strength, Young's modulus and elongation at break) were compiled from the stress-strain curves and the average results of the calculated data can be seen in Fig.7 and Tab.4.

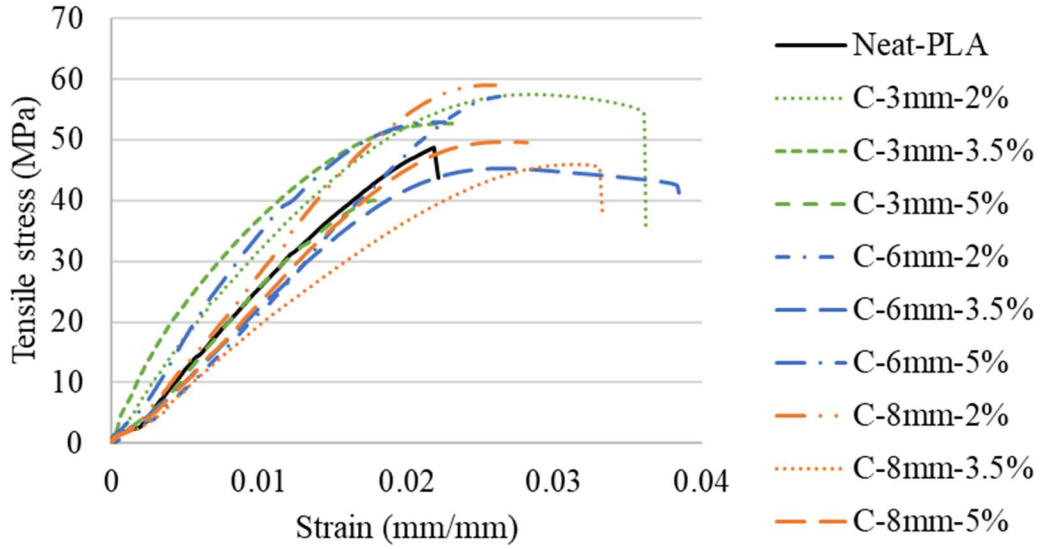
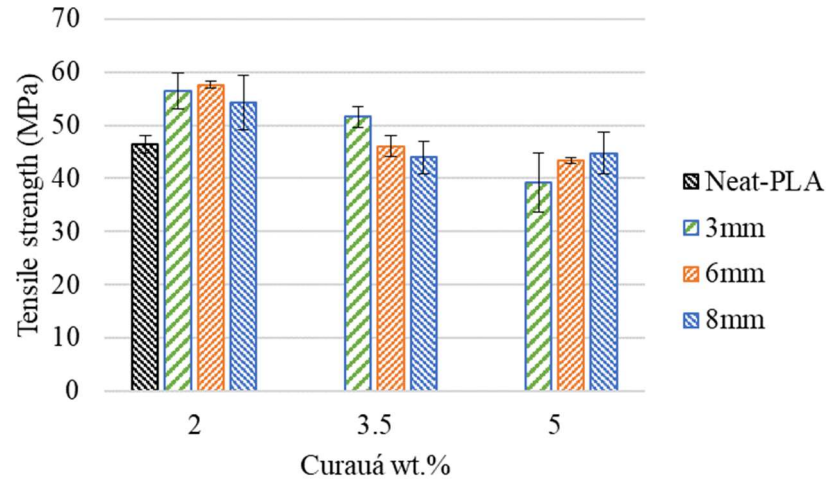
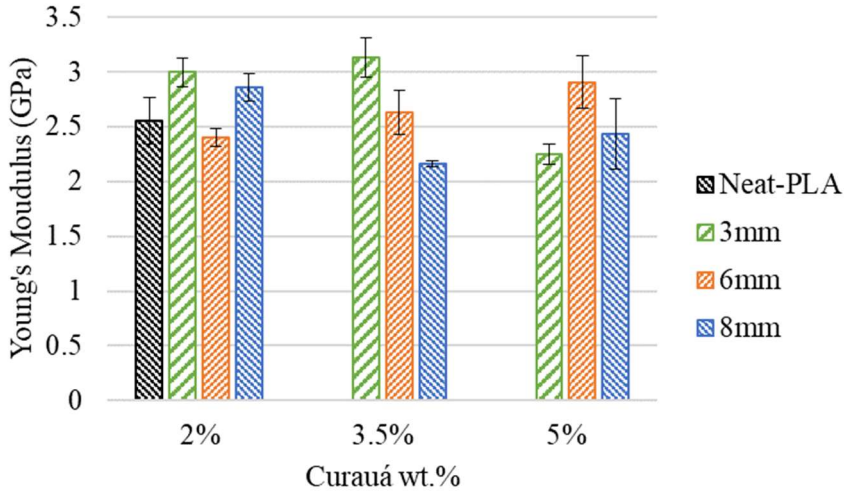


Fig. 6. Representative tensile stress-strain curves.



(a)



(b)

Fig. 7. Tensile data of all composites studied: a) Tensile strength and b) Young`s modulus.

Table 4. Tensile data of all composites studied.

Part	Tensile Strength (MPa)	Young's Modulus (GPa)	Strain (%)
Neat-PLA	46.42 ± 1.62	2.56 ± 0.21	1.94 ± 0.15
C-3mm-2%	56.45 ± 3.34	3.00 ± 0.13	2.72 ± 0.31
C-3mm-3.5%	51.58 ± 1.9	3.13 ± 0.08	2.32 ± 0.38
C-3mm-5%	39.15 ± 5.55	2.25 ± 0.12	1.81 ± 0.68
C-6mm-2%	57.56 ± 0.67	2.4 ± 0.18	2.59 ± 0.18
C-6mm-3.5%	45.98 ± 1.95	2.63 ± 0.2	2.51 ± 0.11
C-6mm-5%	43.29 ± 0.56	2.91 ± 0.02	2.21 ± 0.1
C-8mm-2%	54.25 ± 5.22	2.86 ± 0.09	2.34 ± 0.27
C-8mm-3.5%	43.91 ± 3.02	2.16 ± 0.24	3.01 ± 0.46
C-8mm-5%	44.76 ± 3.96	2.43 ± 0.32	2.62 ± 0.23

5.3.1. Effect of curauá fibre weight fraction

Fibre content had a positive effect in the 3D printed composite's tensile strength when compared to the Neat-PLA. The C-3mm-2%, C-6mm-2% and C-8mm-2% cases presented increases of approx. 22%, 24% and 17%, respectively, when compared to the Neat-PLA. Furthermore, an increase in tensile strength was also seen for the C-3mm-3.5% (approx. 11%). This is mainly due to the curauá fibre higher tensile strength when compared to the PLA (Table 1) [22]. The increase in fibre content provided limited or no increase in tensile strength, mainly due to suboptimal fibre dispersion, thus, higher concentrations can act more as fillers (i.e., reducing the polymer content, potentially reducing costs with no significant gain in mechanical properties.) than reinforcements [22,33].

The lower fibre wt.% presented the highest tensile strength. For example, the C-3mm-2% group presented an increase of approx. 9% over the C-3mm-3.5% and 44% over the C-3mm-5% case. A similar behaviour was seen for the 6mm group where the C-6mm-2% case presented an increase of approx. 25% and 33% when compared to the C-6mm-3.5% and C-6mm-5% cases in tensile strength. Furthermore, the C-8mm-2% group also presented higher tensile strength than the C-8mm-3.5% and C-8mm-5% specimens, with an increase of approx. 24% and 21%,

respectively. The results obtained reflect what is seen in the literature for natural fibre reinforced filaments, where the increase in fibre content can reduce the tensile strength of the printed material [22,33]. The saturation of fibres within the PLA during the mixing process (see Fig. 4), may result in a suboptimal mixture. Thus, the fibres begin to act more as a defect than a reinforcement. However, as seen in Berzin et al. [34], the interfacial interactions between fibre and matrix also have an important role in the specimen's strength. Being the PLA a polar matrix [35], this will exert forces onto the curauá fibres, breaking bundles and single fibres, thus reducing their size and altering their aspect ratio.

The Young's modulus presented a similar behaviour to the tensile strength, i.e. an increase in rigidity was observed for most cases, when compared to the Neat-PLA. The exceptions were the C-6mm-2%, C-6mm-3.5% and C-8mm-5% cases where no significant change was seen. Furthermore, a decrease of approx. 12% and 15% in rigidity was observed for the C-3mm-5% and C-8mm-3.5% cases, respectively, when compared to the Neat-PLA. This is likely due to the same phenomenology as previously discussed for the tensile strength.

The strain at break of the reinforced specimens presented an increase when compared to the Neat-PLA. The 3mm and 6mm groups presented a downward tendency in strain at break with the increase in fibre content, with the C-3mm-5% case presenting no significant difference from the Neat-PLA. However, no clear tendency was seen for the 8mm group. The dispersion and values found for elongation can be explained by the variation of fibre property and dispersion within the printed specimen [36].

The inclusion of fibre treatments and different fabrication methods could be beneficial to the mitigation of fibre distribution and interfacial interactions problems. However, as seen in Pawłowska et al. [37], the utilization of such methods did not present clear benefits to the mechanical properties of the natural fibre reinforced PLA. The differences in values found can be explained by the 3D printing process, which tends to better align the short fibres. Furthermore, the current work has seen similar results to the work of Jesus et al.[38], where the inclusion of fibres had a positive impact in mechanical properties but only in lower fibre wt% content (0.5 wt%). The increase in fibre wt% did not provide any significant improvement in mechanical properties due to fibre agglomerations acting as stress concentrators.

5.3.1.1. Effect of curauá fibre length

From Fig. 7 and Table 4, it can be seen that the increase in fibre length had little impact on the mechanical properties (tensile strength and, Young's modulus). The tensile strength of the C-3mm-2% case presented no significant variation from both the C-6mm-2% and C-8mm-2%

specimens. Furthermore, the C-3mm-3.5% case presented an overall higher tensile strength over both the C-6mm-3.5% and C-8mm-3.5% cases, having an increase of approx. 12% and 17%, respectively. However, the C-3mm-5% case presented a decrease in tensile strength, with a reduction of approx. 10% and 12% when compared to the C-6mm-5% and C-8mm-5% cases respectively.

Fibre length also had an impact in the stiffness properties of the materials. The C-3mm-2% group presented an increase of approx. 33% over the C-6mm-2% case, while for the C-8mm-2% case no significant change in Young's modulus was observed. The C-3mm-3.5% case presented an improvement of approx. 10% and 45% over the C-6mm-3.5% and C-8mm-3.5% cases, respectively. However, with the increase in fibre wt.%, the C-3mm-5% groups presented lower stiffness than the C-6mm-5% case, presenting a reduction of approx. 23%. The C-8mm-5% case did not present any significant statistical variation when compared to the C-3mm-5% case.

The data shows that although fibre length has an impact in the tensile properties of the 3D printed specimens, it is not as relevant as the fibre content. As seen in Fig. 7, the 2% of curauá wt.% presented overall better tensile properties than either the 3.5% or 5% curauá wt.% cases, regardless of fibre length. This is mainly due to the curauá fibre mixing process and inherent fibre characteristics. In the relevant literature, the diameter of the fibres used was much lower than of the curauá fibres used in this study [22,39,23,24]. This increase in fibre diameter can hamper the mixing of higher fibre contents. Also of note is the interaction of the fibre with the matrix, as natural fibres have notoriously lower interfacial adhesion with most thermoplastic and thermoset matrixes. However, the increase in fibre length and diameter can have a positive impact in tensile properties [22]. The combination of better fibre/matrix interfacial bond strength and a high interfacial surface area can be beneficial to the composite, presenting an increase in tensile strength, modulus and elongation.

It was observed that the best overall mechanical tensile properties were found for the C-3mm-2% case. Nonetheless, all 2% wt.% group present similar results in tensile strength, the C-3mm-2% case presented a higher Young's modulus than the C-6mm-2% case, and similar results with the C-8mm-2% case. As stated above, this is most likely due to better fibre distribution within the 3D printed specimens.

5.3.2. Flexural tests

The representative stress-strain curves obtained from the flexural tests as a function of fibre length and fibre wt.% can be seen in Fig. 8. The flexural properties (strength and modulus) were calculated from the stress-strain curves and the results are presented in Fig.9.

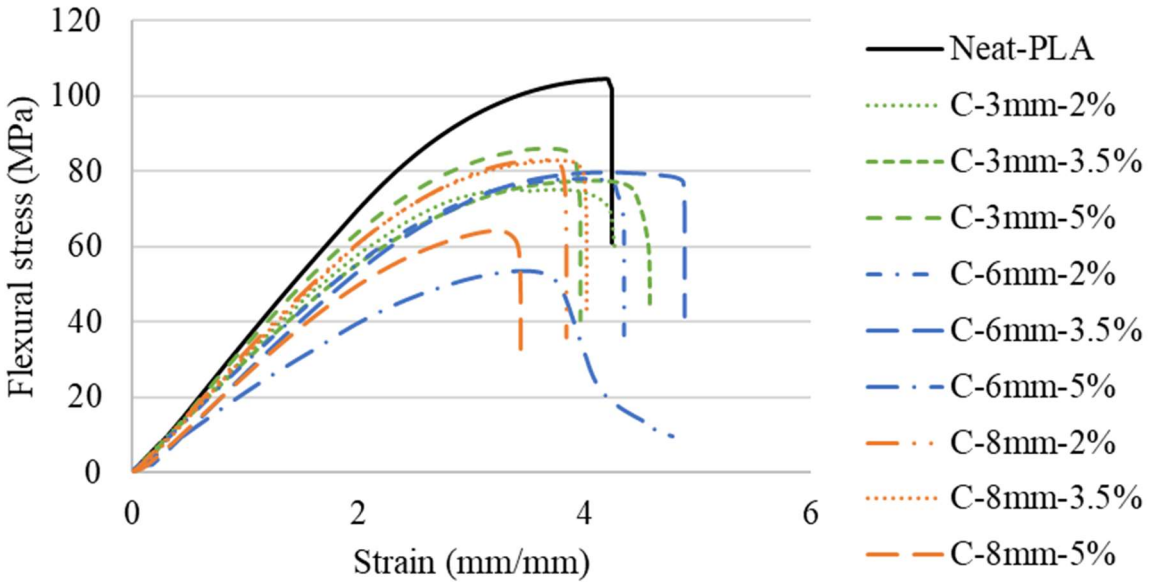


Fig. 8. Representative flexural stress-strain curves.

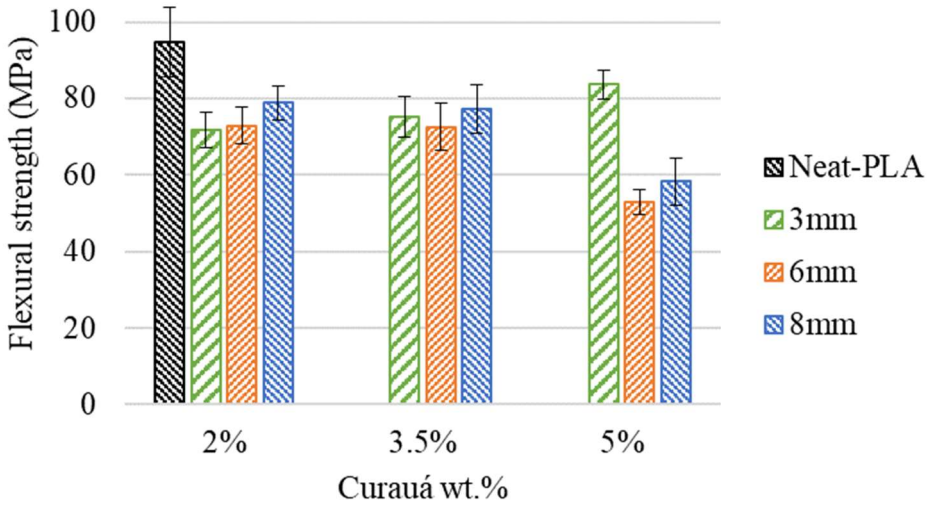
In general, the addition of the natural fibres did not present any significant improvement in flexural strength (see Fig. 9). The best result seen for the flexural strength of the fibre reinforced specimens was the C-3mm-5% group with a decrease of approx. 11% when compared to the Neat-PLA group. Within the reinforced groups it is possible to see that the C-3mm-5% case presented the best overall results, with an increase of approx. 17% and 11% over the C-3mm-2% and C-3mm-3.5% groups. The 6mm group presented a different trend, with the increase in fibre content providing a negative effect, both C-6mm-2% and C-6mm-3.5% cases presented an increase of approx. 38% when compared to the C-6mm-5% case. The C-8mm group continued the trend, present lower values with the increase of fibre wt.%. The C-8mm-5% presented approx. 35% and 32% lower flexural strength when comparing to the C-8mm-2% and C-8mm-3.5%, respectively. No significant variation between both C-8mm-2% and C-8mm-3.5% was seen.

The flexural modulus followed a similar trend with the flexural strength. The flexural modulus presented no significant variation between the C-3mm-2% and C-3mm-3.5% cases. Additionally, the C-3mm-5% case presented an increase of approx. 43% when compared to the

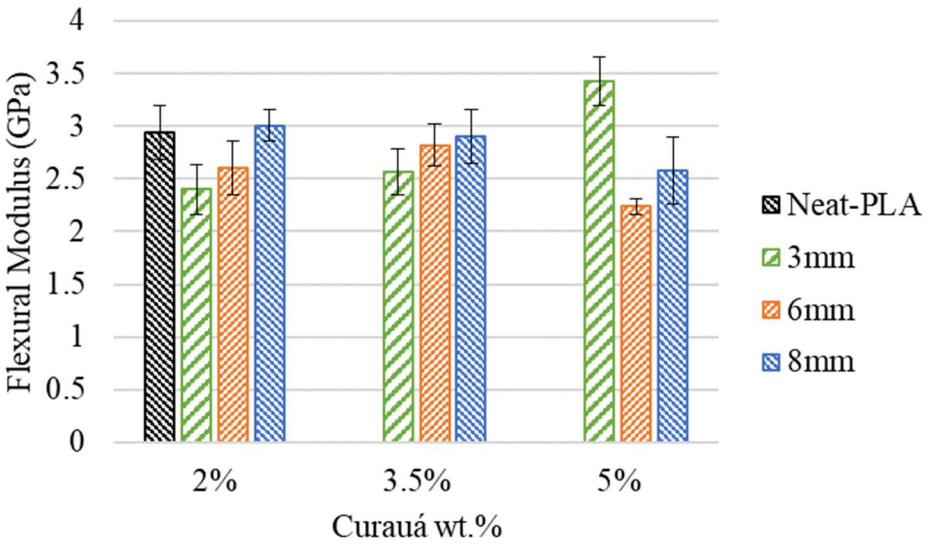
C-3mm-2%. As seen in the flexural strength the C-6mm-2% and C-6mm-3.5% also did not present a significant change in stiffness. Following a similar behaviour to the flexural strength, the lowest value was seen for the C-6mm-5%, having a reduction of approx. 14% and 21% when compared to the C-6mm-2% and C-6mm-3.5%, respectively. The 8mm cases presented similar trends to the C-6mm cases. The C-8mm-2% and C-8mm-3.5% presented higher values than the C-8mm-5% (approx. 14% and 11%, respectively), whilst showing no significant variation between them.

As seen in the tensile tests, the fibre weight fraction had a higher impact in flexural strength than the fibre length. This is evident by the insignificant variation between the C-3mm-2%, C-6mm-2% and C-8mm-2% groups. Furthermore, the C-3mm-3.5%, C-6mm-3.5% and C-8mm-3.5% presented similar behaviour, with no significant variation between them. However, the C-3mm-5%, C-6mm-5% and C-8mm-5% groups presented significant variation between them, in which the C-3mm-5% group presented approx. 58% and 44% increase in flexural strength.

The flexural properties of the materials did not follow the trends set by the tensile tests. The flexural strength and modulus were affected negatively by the introduction of the fibres, apart from the C-3mm-5% case, which presented an increase in stiffness of approx. 17% over the Neat-PLA.



(a)



(b)

Fig. 9. Flexural data of all composites as a function of fibre length and wt.%: a) Flexural strength and b) Flexural modulus.

It was shown in the literature that the addition of natural fibres as reinforcements for additive manufactured parts does not translate in an increase in flexural properties. Data presented a general trend of flexural strength reduction [22]. The present work follows this trend for most cases, with a reduction in flexural strength and modulus, with the only exception being the C-3mm-5% group.

5.3.3. Fracture analysis

The fractured specimens were visually examined after the tensile and flexural tests. The representative failure modes can be seen in Fig. 10, and Fig. 11. The 3D printed composites presented a similar failure behaviour. As seen in Fig. 10 the tensile specimen's failure was predominantly fragile with a clear stock break. The voids seen in the image are related to the separation between rasters. Although good interlayer adhesion can be seen, the failure tended to propagate between rasters as seen in Fig. 10 for the C-3mm-5%, C-6mm-5% and C-8mm-3.5% cases. These defects can be attributed to the filament diameter variations, leading to a reduction in flow and resulting in a smaller raster width, thus hampering the interfacial interaction between them [40].

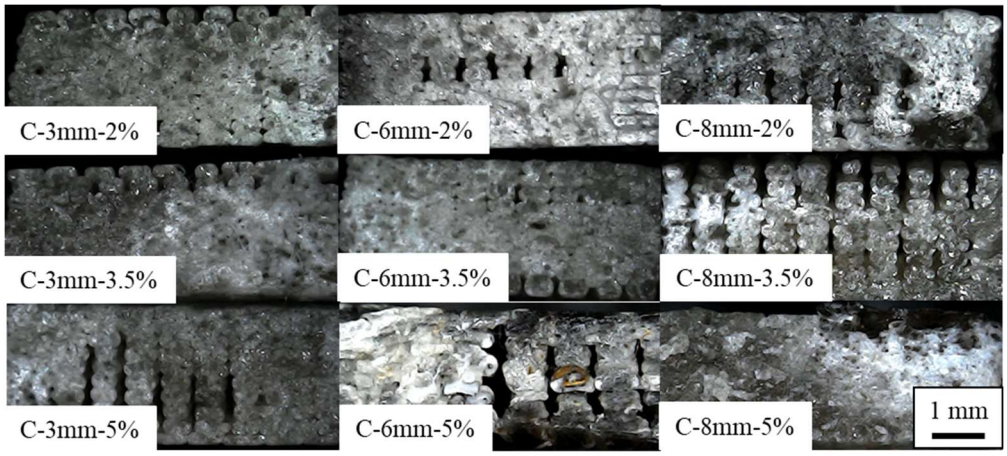


Fig. 10. Representative failure modes of the 3D printed tensile specimens.

The representative flexural failure modes cross sections can be seen in Fig. 11. All failures presented a similar behaviour with complete break, therefore only the 5% group was shown. The failure surface presented two distinct areas separated approximately in the middle (neutral line). The bottom side (Submitted to tensile loads) presented a rougher surface with less flat surfaces, this is likely due to deformation during the flexural tests. The top side (compressive side) presented a clearer failure, this is in line with a catastrophic failure with little to no deformation resulting in a pure fragile failure mode.

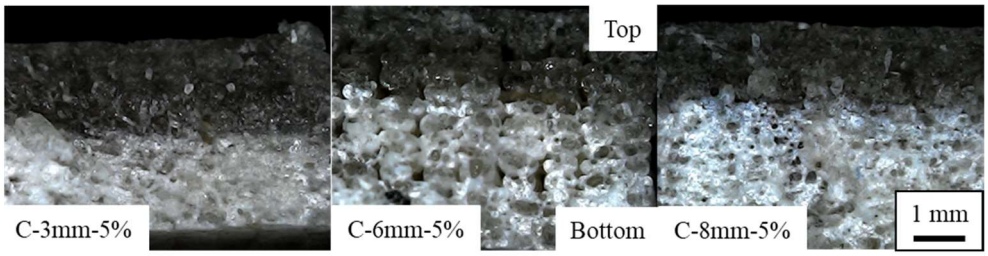


Fig. 11. Representative failure modes of the 3D printed flexural specimens.

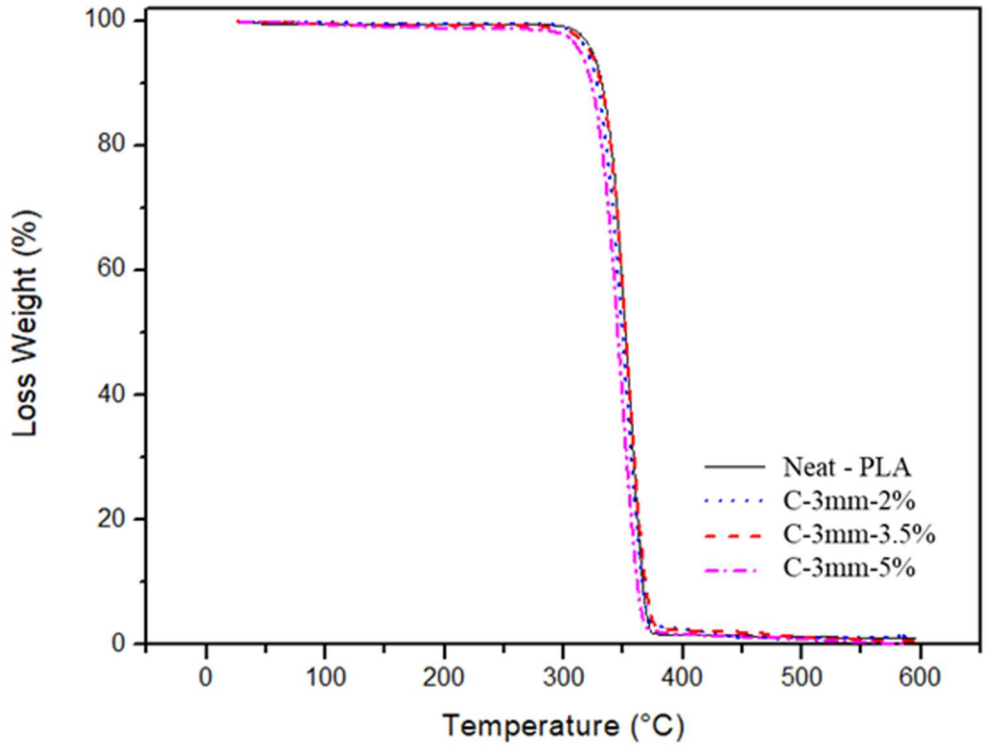
5.4. THERMAL PROPERTIES

5.4.1. TGA analysis

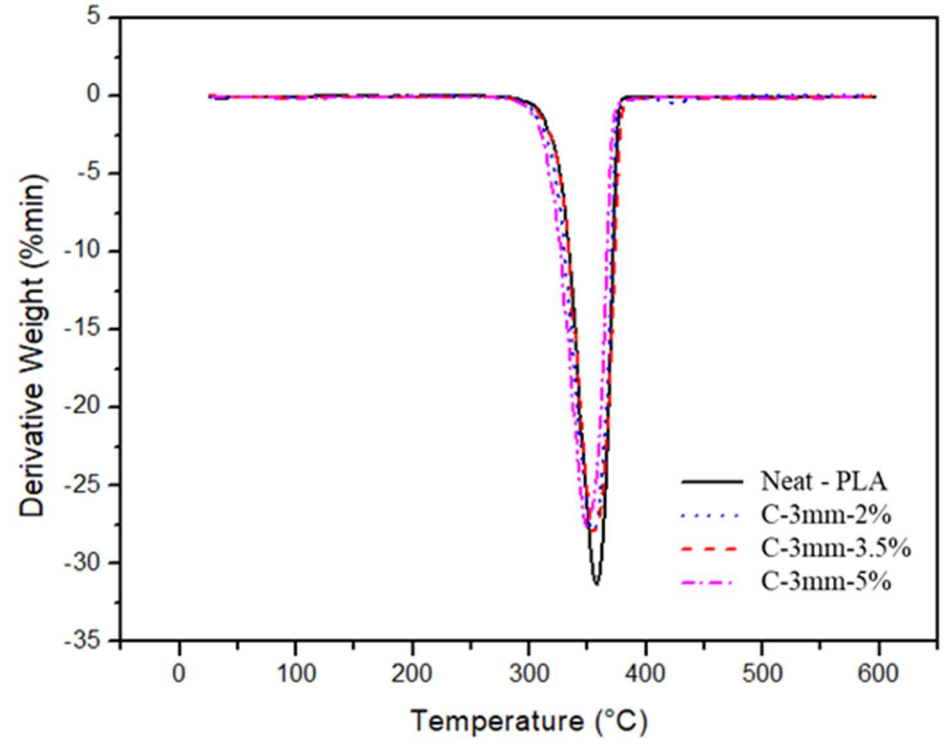
The thermal stability of curauá fibre reinforced composite was investigated for two fibre (3 mm and 6 mm) length specimens and Neat-PLA. The weight loss and derivative weight are shown in Figure 12 and 13. The Neat-PLA presented a temperature onset of 329.7°C, during the whole heating process only one degradation step was seen. The incorporation of the short fibres, as well as their size and concentration had an impact in the composite's thermal properties. The

C-3mm-2% case did not show significant changes in thermal properties (330°C). The C-3mm-3.5% case presented an increase in the onset temperature of 334°C. However, the increase in fibre concentration for the C-3mm-5% presented a reduction in temperature onset when compared to the Neat-PLA. The increase in fibre concentration reduces the thermal stability of the composites, mainly due to the inclusion of materials with lower thermal stability, such as such as hemicellulose and lignin [39]. An important factor in improving the thermal stability of natural fibres is the removal of these low stability components thought the use of chemical treatments [26,41]. Furthermore, the C-3mm-5% DTG (349°C) presents a decay when compared to the Neat-PLA (357°C), as seen in Fig. 13(b).

From Table 5 it can be seen that the C-6mm-2% and C-6mm-5% specimens did not present any significant onset temperature variation, when compared to the Neat-PLA specimens. However, for the C-6mm-3.5% specimens a deterioration of onset temperature (326°C) when compared to the Neat-PLA was observed. As stated by Silva et al. [39], the incorporation of natural fibres has a tendency of reducing the thermal stability of composites in general, since these reinforcing natural fibres present lower thermal stability than the matrices.

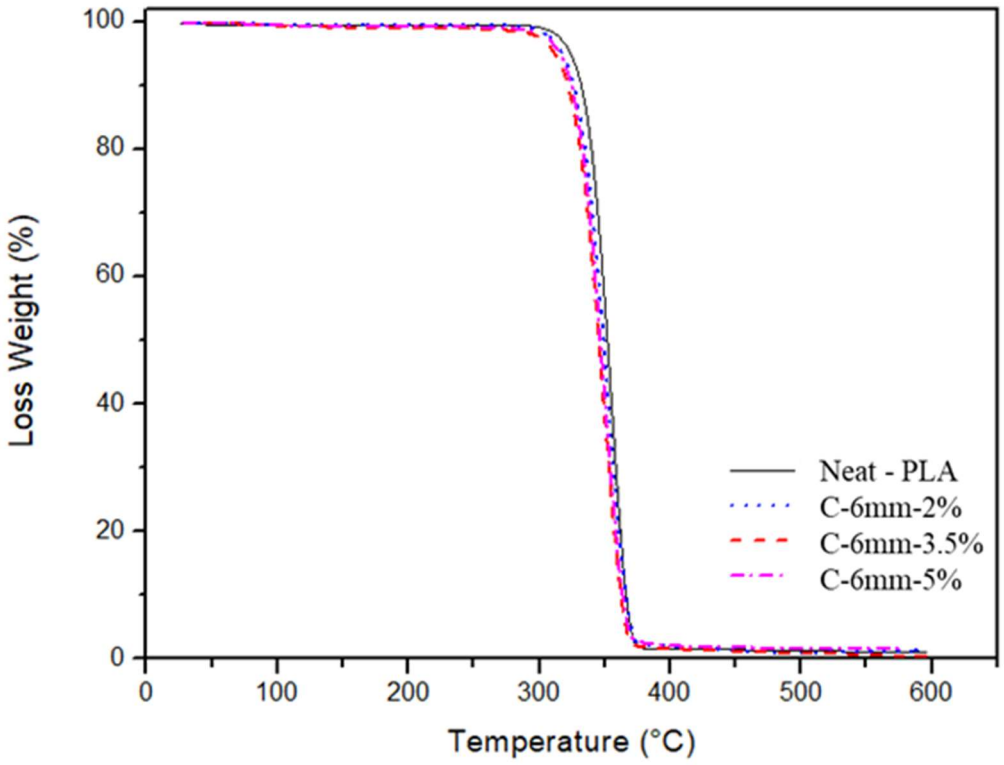


(a)

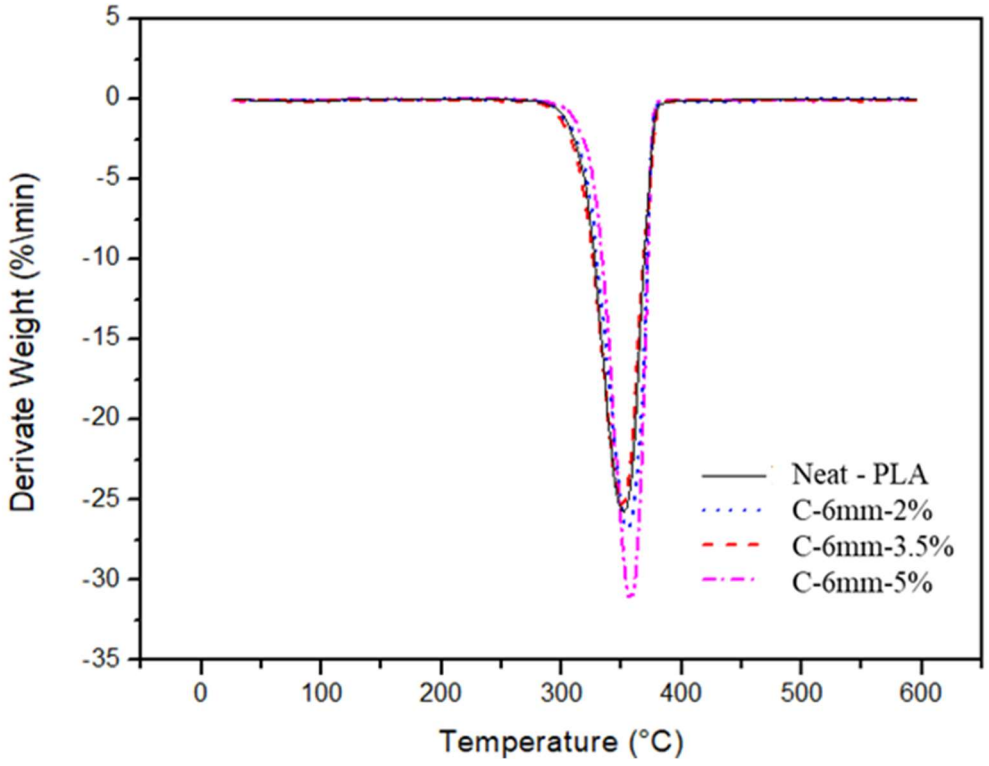


(b)

Fig. 12. TGA analysis data: (a) TG curves; (b) DTG curves.



(a)



(b)

Fig. 13. TGA analysis data: (a) TG curves; (b) DTG curves.

Table 5. TGA analysis data.

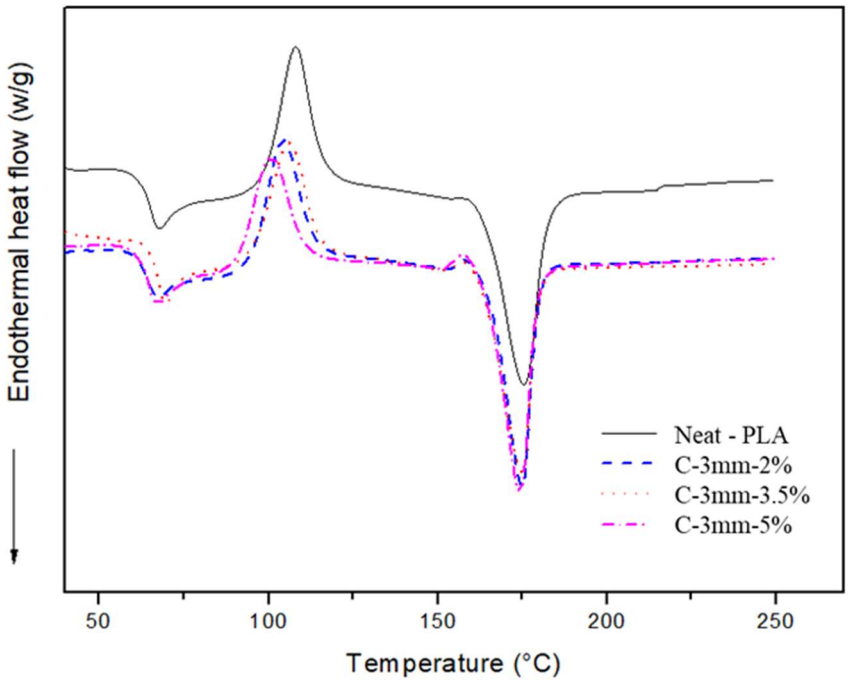
Specimen type	Onset temperature (°C)	Maximum temperature (°C)	Residual mass (%)
Neat-PLA	330	357.5	1
C-3mm-2%	330.0	355.0	1.4
C-3mm-3.5%	334.0	354.5	0.7
C-3mm-5%	327.8	349.0	0.2
C-6mm-2%	329.6	355.0	1.4
C-6mm-3.5%	326.3	350.0	0.4
C-6mm-5%	328.0	351.5	1.6

5.4.2. DSC analysis

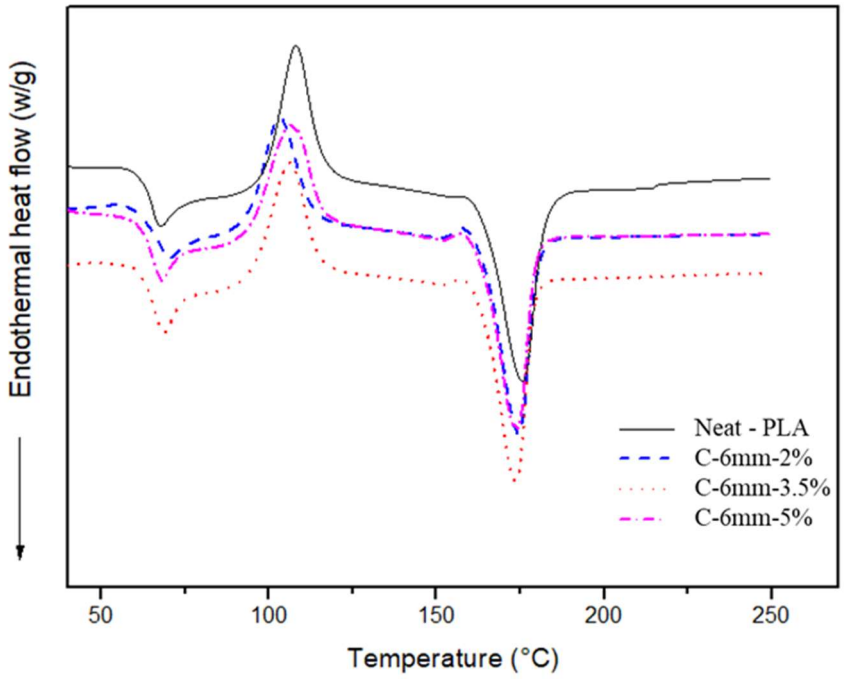
DSC analysis was used to determine the following parameters: glass transition (T_g), crystallization temperature (T_c) and melting temperature (T_m) of the specimens studied. The DSC curves produced are shown in Figures 14a and b. During the heating cycle the materials

showed three transition zones: glass transitions 60 to 68°C [42], cold crystallization at 100 to 110°C [43], and melting at 170 to 176°C [44]. The Neat-PLA presented a value of Tg of 64.5°C (see Table 6). The value found is in accordance with the literature [45,46]. For the reinforced (2%, 3.5% and 5%) composites a change in the thermal properties with the insertion of the curauá fibre in the composite was observed (a small increase in Tg for the 2% e 3.5 wt.% when compared to Neat-PLA was observed. However, for the case of C-3mm-5% showed no significant change in the Tg of the material. For the case of composite C-6mm-2% showed an increase in T_g (1.6°C) when compared to Neat-PLA. However, the C-6mm-3.5% and C-6mm-5% showed no significant change in Tg. For the reinforced (2%, 3.5% and 5%) composites a change in the thermal properties with the insertion of the curauá fibre in the composite was observed (a small increase in Tg for the 2% e 3.5 wt.% when compared to Neat-PLA was observed.

The 6mm fibre length specimens presented a decrease in T_c compared to Neat-PLA, exhibiting the same behaviour as the 3mm fibre length reinforced composites. For the two cases C-3mm-(3.5 and 5wt.%) and 6mm fibre length specimens (2, 3.5 and 5wt.%) a small decrease in Tm was observed when compared to Neat-PLA. Akonda et al. [48], showed that the flax/PLA composite presents a decrease in Tm at the beginning of the melting temperature of the composites. However, the C-3mm-2% specimens showed no significant change in Tm. These results are in accordance with results found in the literature [49].



(a)



(b)

Fig. 14. DSC analysis data: a) 3 mm fibre length group; b) 6 mm group and Neat-PLA.

Table 6. DSC analysis data.

Specimen type	Glass transition Temperatures (T_g)	Crystallization Temperatures (T_c)	Melting Temperature (T_m)
Neat-PLA	64.0	108.1	175.5
C-3mm-2%	65.1	104.1	175.0
C-3mm-3.5%	67.5	106.4	174.7
C-3mm-5%	64.3	100.9	174.2
C-6mm-2%	66.1	103.4	174.3
C-6mm-3.5%	64.0	106.3	173.5
C-6mm-5%	64.4	106.5	174.2

5.5. CONCLUSIONS

In this work, short curauá fibre- reinforced PLA composites made via fused deposition modelling was investigated. Three different fibre lengths (3, 6 and 8 mm), and three concentration in fibre weight percentage (2, 3.5 and 5 wt.%) were used to fabricate the PLA

filaments. Tensile and flexural tests in accordance with their respective ASTM standards were performed. A thermal analysis was also carried out in order to investigate the thermal stability of the new materials. The following conclusions can be drawn: In general, the addition of the short fibres increased the tensile properties of the 3D printed specimens, both tensile strength and Young's modulus benefited from the reinforcements.

The fibre weight fraction dominates the tensile properties of the 3D printed parts, with lower content (2 wt.%) presenting a significant improvement in tensile properties. Fibre length also affect the tensile properties; however, a downward trend was seen with the increase in length, with the C-3mm-2% (56.45 MPa and 3 GPa) group presenting the best results.

For flexural properties, the best condition was the C-3mm-5% case, with values of 83.71 MPa and 3.42 GPa for flexural strength and modulus, respectively. Unlike the tensile properties the addition of the fibres did not provide an increase in flexural strength, with the best case presenting a reduction of 12% when compared to the Neat-PLA. However, the reinforcements did have a positive impact in flexural modulus (the C-3mm-5% specimens presented an increase of approx. 17% over the Neat-PLA).

The incorporation of natural fibre presented, in some cases, changes in the composite's thermal stability. The C-3mm-3.5% specimens presented the best condition with values of Tonset of 334°C and 67.5°C for the T_g .

Adding curauá short fibres to PLA filaments for 3D printed materials may be a promising innovation to improve their mechanical and thermal properties while maintaining their biodegradable characteristics. The present work adds to the ever-growing green-friendly industry, with possible applications in biomedical, food packing, disposable single use components, eco-friendly moulds, and lightweight customizable parts for the transport industry. Further studies on the use of this type of fibre are necessary to prove that natural fibres are a good substitute to more commonly used synthetic fibres.

REFERENCES

1. Ngo TD, Kashani A, Imbalzano G, Nguyen KTQ, Hui D (2018) Additive manufacturing (3D printing): A review of materials, methods, applications and challenges. Composites Part B: Engineering 143:172-196. doi:https://doi.org/10.1016/j.compositesb.2018.02.012

2. Singh S, Ramakrishna S, Singh R (2017) Material issues in additive manufacturing: A review. Journal of Manufacturing Processes 25:185-200. doi:https://doi.org/10.1016/j.jmapro.2016.11.006

3. Tofail SAM, Koumoulos EP, Bandyopadhyay A, Bose S, O'Donoghue L, Charitidis C (2018) Additive manufacturing: scientific and technological challenges, market uptake and opportunities. Materials Today 21 (1):22-37. doi:https://doi.org/10.1016/j.mattod.2017.07.001

4. Cavalcanti D, Banea M, Queiroz H (2019) Mechanical Characterization of Bonded Joints Made of Additive Manufactured Adherends. Annals of" Dunarea de Jos" University of Galati Fascicle XII, Welding Equipment and Technology 30:27-33

5. Harris M, Potgieter J, Archer R, Arif KM (2019) Effect of Material and Process Specific Factors on the Strength of Printed Parts in Fused Filament Fabrication: A Review of Recent Developments. Materials 12 (10):1664

6. Jiang C, Wang K, Jiang X, Zhang C, Wang B (2020) Quantitative Investigation of the Process Parameters of Electrohydrodynamic Direct-Writing and Their Effects on Fiber Surface Roughness and Cell Adhesion. Polymers 12 (11):2475

7. Borg G, Kiss S, Rochman A (2021) Filament Development for Laser Assisted FFF 3D Printing. Journal of Manufacturing and Materials Processing 5 (4):115

8. Ahmadifar M, Benfriha K, Shirinbayan M, Tcharkhtchi A (2021) Additive Manufacturing of Polymer-Based Composites Using Fused Filament Fabrication (FFF): a Review. Applied Composite Materials 28 (5):1335-1380. doi:10.1007/s10443-021-09933-8

9. Oktavianty O, Haruyama S, Ishii Y (2022) Enhancing Droplet Quality of Edible Ink in Single and Multi-Drop Methods by Optimization the Waveform Design of DoD Inkjet Printer. Processes 10 (1):91

10. Gutiérrez E, Barreto JdJ, Garcia-Hernandez S, Morales R, González-Solorzano MG (2020) Decrease of Nozzle Clogging through Fluid Flow Control. Metals 10 (11):1420

11. Lalehpour A, Janeteas C, Barari A (2018) Surface roughness of FDM parts after post-processing with acetone vapor bath smoothing process. The International Journal of Advanced Manufacturing Technology 95 (1):1505-1520. doi:10.1007/s00170-017-1165-5

12. Wu H, Fahy WP, Kim S, Kim H, Zhao N, Pilato L, Kafi A, Bateman S, Koo JH (2020) Recent developments in polymers/polymer nanocomposites for additive manufacturing. Progress in Materials Science 111:100638. doi:https://doi.org/10.1016/j.pmatsci.2020.100638

13. Parandoush P, Lin D (2017) A review on additive manufacturing of polymer-fiber composites. Composite Structures 182:36-53. doi:https://doi.org/10.1016/j.compstruct.2017.08.088

14. Ning F, Cong W, Hu Y, Wang H (2017) Additive manufacturing of carbon fiber-reinforced plastic composites using fused deposition modeling: Effects of process parameters on tensile properties. Journal of Composite Materials 51 (4):451-462. doi:10.1177/0021998316646169

15. McIlroy C, Olmsted PD (2017) Disentanglement effects on welding behaviour of polymer melts during the fused-filament-fabrication method for additive manufacturing. Polymer 123:376-391. doi:https://doi.org/10.1016/j.polymer.2017.06.051

16. Weng Z, Wang J, Senthil T, Wu L (2016) Mechanical and thermal properties of ABS/montmorillonite nanocomposites for fused deposition modeling 3D printing. Materials & Design 102:276-283. doi:https://doi.org/10.1016/j.matdes.2016.04.045

17. Afrose MF, Masood SH, Nikzad M, Iovenitti P (2014) Effects of Build Orientations on Tensile Properties of PLA Material Processed by FDM. Advanced Materials Research 1044-1045:31-34. doi:10.4028/www.scientific.net/AMR.1044-1045.31

18. Carrasco F, Pagès P, Gámez-Pérez J, Santana OO, Maspoch ML (2010) Processing of poly(lactic acid): Characterization of chemical structure, thermal stability and mechanical properties. Polymer Degradation and Stability 95 (2):116-125. doi:https://doi.org/10.1016/j.polymdegradstab.2009.11.045

19. Cavalcanti DKK, Banea MD, de Queiroz HFM (2020) Effect of material on the mechanical properties of additive manufactured thermoplastic parts. Annals of "Dunarea de Jos" University of Galati, Fascicle XII, Welding Equipment and Technology 31:5-12. doi:10.35219/awet.2020.01

20. Gomes TEP, Cadete MS, Dias-de-Oliveira J, Neto V (2022) Controlling the properties of parts 3D printed from recycled thermoplastics: A review of current practices. Polymer Degradation and Stability 196:109850. doi:https://doi.org/10.1016/j.polymdegradstab.2022.109850

21. Justo J, Távara L, García-Guzmán L, París F (2018) Characterization of 3D printed long fibre reinforced composites. Composite Structures 185:537-548. doi:https://doi.org/10.1016/j.compstruct.2017.11.052

22. Le Duigou A, Correa D, Ueda M, Matsuzaki R, Castro M (2020) A review of 3D and 4D printing of natural fibre biocomposites. Materials & Design 194:108911. doi:https://doi.org/10.1016/j.matdes.2020.108911

23. Yan J, Demirci E, Ganesan A, Gleadall A (2022) Extrusion width critically affects fibre orientation in short fibre reinforced material extrusion additive manufacturing. Additive Manufacturing 49:102496. doi:https://doi.org/10.1016/j.addma.2021.102496

24. Yu T, Jiang N, Li Y (2014) Study on short ramie fiber/poly(lactic acid) composites compatibilized by maleic anhydride. Composites Part A: Applied Science and Manufacturing 64:139-146. doi:https://doi.org/10.1016/j.compositesa.2014.05.008

25. Taborda-Ríos JA, López-Botello O, Zambrano-Robledo P, Reyes-Osorio LA, Garza C (2020) Mechanical characterisation of a bamboo fibre/polylactic acid composite produced by fused deposition modelling. Journal of Reinforced Plastics and Composites 39 (23-24):932-944. doi:10.1177/0731684420938434

26. Neto JSS, Lima RAA, Cavalcanti DKK, Souza JPB, Aguiar RAA, Banea MD (2019) Effect of chemical treatment on the thermal properties of hybrid natural fiber-reinforced composites. Journal of Applied Polymer Science 136 (10):47154. doi:https://doi.org/10.1002/app.47154

27. Neto J, Queiroz H, Aguiar R, Lima R, Cavalcanti D, Banea MD (2022) A review of recent advances in hybrid natural fiber reinforced polymer composites. Journal of Renewable Materials 10 (3):561-589. doi:10.32604/jrm.2022.017434

28. Souza SF, Leão AL, Cai JH, Wu C, Sain M, Cherian BM (2010) Nanocellulose from Curava Fibers and their Nanocomposites. Molecular Crystals and Liquid Crystals 522 (1):42/[342]-352/[352]. doi:10.1080/15421401003722955

29. Schindelin J, Arganda-Carreras I, Frise E, Kaynig V, Longair M, Pietzsch T, Preibisch S, Rueden C, Saalfeld S, Schmid B, Tinevez J-Y, White DJ, Hartenstein V, Eliceiri K, Tomancak P, Cardona A (2012) Fiji: an open-source platform for biological-image analysis. Nature Methods 9 (7):676-682. doi:10.1038/nmeth.2019

30. Coppola B, Cappetti N, Di Maio L, Scarfato P, Incarnato L (2018) 3D Printing of PLA/clay Nanocomposites: Influence of Printing Temperature on Printed Samples Properties. Materials 11 (10):1947

31. de Araujo Alves Lima R, Kawasaki Cavalcanti D, de Souza e Silva Neto J, Meneses da Costa H, Banea MD (2020) Effect of surface treatments on interfacial properties of natural intralaminar hybrid composites. Polymer Composites 41 (1):314-325

32. Correia C, Gomes TEP, Gonçalves I, Neto V (2022) Reprocessability of PLA through Chain Extension for Fused Filament Fabrication. Journal of Manufacturing and Materials Processing 6 (1):26

33. Yu T, Li Y, Ren J (2009) Preparation and properties of short natural fiber reinforced poly(lactic acid) composites. Transactions of Nonferrous Metals Society of China 19:s651-s655. doi:https://doi.org/10.1016/S1003-6326(10)60126-4

34. Berzin F, Lemkhanter L, Marcuello C, Chabbert B, Aguié-Béghin V, Molinari M, Castellani R, Vergnes B (2020) Influence of the polarity of the matrix on the breakage mechanisms of lignocellulosic fibers during twin-screw extrusion. Polymer Composites 41 (3):1106-1117. doi:https://doi.org/10.1002/pc.25442

35. Graupner N, Rößler J, Ziegmann G, Müssig J (2014) Fibre/matrix adhesion of cellulose fibres in PLA, PP and MAPP: A critical review of pull-out test, microbond test and single fibre fragmentation test results. Composites Part A: Applied Science and Manufacturing 63:133-148. doi:https://doi.org/10.1016/j.compositesa.2014.04.011

36. Guessasma S, Belhabib S, Nouri H (2019) Understanding the microstructural role of bio-sourced 3D printed structures on the tensile performance. Polymer Testing 77:105924. doi:https://doi.org/10.1016/j.polymertesting.2019.105924

37. Pawłowska A, Stepczyńska M, Walczak M (2022) Flax fibres modified with a natural plant agent used as a reinforcement for the polylactide-based biocomposites. Industrial Crops and Products 184:115061. doi:https://doi.org/10.1016/j.indcrop.2022.115061

38. Jesus LCC, Oliveira JM, Leão RM, Beltrami LR, Zattera AJ, Anflor CTM, Doca TCR, Luz SM (2022) Tensile behavior analysis combined with digital image correlation and mechanical and thermal properties of microfibrillated cellulose fiber/ polylactic acid composites. Polymer Testing 113:107665. doi:https://doi.org/10.1016/j.polymertesting.2022.107665

39. Silva CG, Campini PAL, Rocha DB, Rosa DS (2019) The influence of treated eucalyptus microfibers on the properties of PLA biocomposites. Composites Science and Technology 179:54-62. doi:https://doi.org/10.1016/j.compscitech.2019.04.010

40. Butt J, Bhaskar R, Mohaghegh V (2021) Investigating the effects of extrusion temperatures and material extrusion rates on FFF-printed thermoplastics. The International Journal of Advanced Manufacturing Technology 117 (9):2679-2699. doi:10.1007/s00170-021-07850-5

41. Neto JSS, de Queiroz HFM, Aguiar RAA, Banea MD (2021) A Review on the Thermal Characterisation of Natural and Hybrid Fiber Composites. Polymers 13 (24). doi:10.3390/polym13244425

42. Azlin MNM, Sapuan SM, Zuhri MYM, Zainudin ES, Ilyas RA (2022) Thermal Stability, Dynamic Mechanical Analysis and Flammability Properties of Woven Kenaf/Polyester-Reinforced Polylactic Acid Hybrid Laminated Composites. Polymers 14 (13):2690

43. Iannace S, Sorrentino L, Di Maio E (2014) 6 - Biodegradable biomedical foam scaffolds. In: Netti PA (ed) Biomedical Foams for Tissue Engineering Applications. Woodhead Publishing, pp 163-187. doi:https://doi.org/10.1533/9780857097033.1.163

44. Na H, Huang J, Xu H, Bao X, Xie L, Liu F, Zhu B, Wang J, Zhu J (2022) Effect of high content filling jute fiber with large aspect ratio on structure and properties of PLA composite. Polymer Composites 43 (3):1429-1437. doi:https://doi.org/10.1002/pc.26463

45. Mofokeng JP, Luyt AS, Tábi T, Kovács J (2012) Comparison of injection moulded, natural fibre-reinforced composites with PP and PLA as matrices. Journal of Thermoplastic Composite Materials 25 (8):927-948. doi:10.1177/0892705711423291

46. Ye C, Ma G, Fu W, Wu H (2015) Effect of fiber treatment on thermal properties and crystallization of sisal fiber reinforced polylactide composites. Journal of Reinforced Plastics and Composites 34 (9):718-730. doi:10.1177/0731684415579090

47. Xia X, Shi X, Liu W, Zhao H, Li H, Zhang Y (2017) Effect of flax fiber content on polylactic acid (PLA) crystallization in PLA/flax fiber composites. Iranian Polymer Journal 26 (9):693-702. doi:10.1007/s13726-017-0554-9

48. Akonda M, Alimuzzaman S, Shah DU, Rahman ANMM (2018) Physico-Mechanical, Thermal and Biodegradation Performance of Random Flax/Polylactic Acid and Unidirectional Flax/Polylactic Acid Biocomposites. Fibers 6 (4):98

49. Zhang K, Chen Z, Smith LM, Hong G, Song W, Zhang S (2021) Polypyrrole-modified bamboo fiber/polylactic acid with enhanced mechanical, the antistatic properties and thermal stability. Industrial Crops and Products 162:113227. doi:https://doi.org/10.1016/j.indcrop.2020.113227

CHAPTER 6

6. CONCLUSION

This thesis focused on the development, mechanical characterization, and joining of new polymeric materials using additive manufacturing techniques. Several manufacturing methodologies were developed and tested, and the results demonstrated an improvement in mechanical properties to varying degrees. The impact of material type, printing parameters, and fiber reinforcement on the mechanical performance of 3D printed parts emphasizes the advantages and limitations of these approaches, particularly in relation to interfacial strength and their potential for wider applications. Notably, the addition of fiber reinforcements was found to markedly improve the mechanical properties of 3D printed parts.

The first study on additive manufactured polymeric parts demonstrated that the type of filaments, such as PLA, ABS, and Tritan, played a crucial role in determining the mechanical performance, with variations observed in tensile strength, stiffness, and deformation capacity. This was also true for the printing parameters, where a good balance between printing time and mechanical properties was found.

The addition of fiber reinforcements, as seen in the second paper included natural fibres such as curauá and synthetic fibres like glass. The reinforced parts presented improved mechanical properties compared to neat polymers. Notably, curauá fiber-reinforced composites exhibited notable enhancements in both tensile and flexural strength, highlighting the potential of these sustainable reinforcements.

Furthermore, the thesis investigated the joining behaviour of fiber-reinforced 3D printed parts through adhesively bonded joints. The results indicated that the choice of material for the 3D printed cores, such as PLA or ABS, influenced the mechanical properties of the bonded joints. PLA-reinforced specimens exhibited superior interface adhesion and higher failure loads compared to ABS-reinforced specimens. The failure modes observed varied depending on the adherend material, emphasizing the importance of interfacial bonding strength in determining joint performance.

This thesis also contributed to the field of natural fiber-reinforced 3D composites, offering a sustainable alternative to synthetic reinforcements commonly used in additive manufacturing. The investigation of short curauá fiber-reinforced PLA composites demonstrated the positive effects of fiber addition on tensile properties, while flexural properties showed variations depending on fiber length and weight fraction. Moreover, thermal stability was assessed, revealing changes in the composite's thermal behaviour due to the incorporation of natural fibres.

In conclusion, this thesis represents a significant advancement in the development and characterization of polymeric materials using additive manufacturing techniques. The incorporation of fiber reinforcements, particularly natural fibres, has shown great potential for enhancing the mechanical properties of 3D printed parts. This not only expands the application range of commercial low-cost FDM 3D printers but also contributes to the growing demand for sustainable and environmentally friendly materials in the field. The findings and methodologies presented in this thesis lay the foundation for further research on natural fiber utilization in 3D printing, offering valuable insights for the materials science community and facilitating the development of more efficient and sustainable manufacturing techniques.

6.1 FUTURE WORKS

The field of 3D printing remains ripe with unexplored topics, several of which are proposed herein. The author intends to expand this research further by studying other forms and methodologies of reinforcements.

- The use of different types of short natural fibres such as linen, hemp, and bamboo could provide different mechanical and thermal properties to the filaments.
- The mixing and extrusion process can also be further developed. The use of a double helix extruder and larger or modified nozzles could prove useful in mitigating many of the problems found within the presented research.
- The use of functionalizing agents and methodologies, such as chemical, mechanical and the use of nano particles could also provide better interfacial adhesion between fibre and matrix.

Moreover, the utilization of other types of filaments and fibre dimensions provide an interesting new area of research. Of these, the most interesting are:

- The use of biomass as a filament. While biomass filaments are already in current study and productions, the use of short and long fibres could mitigate many of the shortcomings and printing complications of the biomass filaments. The manufacture of highly biodegradable and natural filament should be very interesting.
- The use of long natural fibres, especially those native from Brazil, is another interesting topic. The expected gains in both strength/weight ratio and recyclability, when compared to their synthetic counterparts, cannot be understated.

Given the wide range of underdeveloped topics within this sector of material science, the author proposes future studies aimed at providing quality research that serves as a linchpin or starting point for the expansion and future adoption of more sustainable 3D printing resources.